ELECTRICAL CONDUCTION IN NYLON FIBRE

AND CELLULOSIC CAPACITOR TISSUE

A Thesis Presented in Partial Fulfillment of the
Requirements for the Degree of Master of Science
at Lakehead University

By

J. E. Hanneson, B.Sc.

Lakehead University

1970

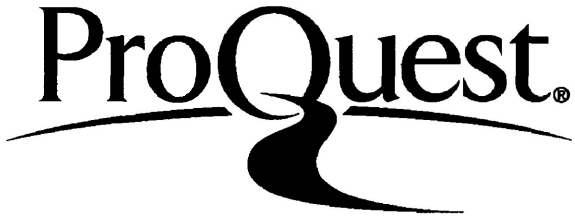

ProQuest LLC.
789 East Eisenhower Parkway
P.O. Box 1346
Ann Arbor, MI 48106 - 1346

ABSTRACT

The experiments described in this work are divided into two main parts. The first is concerned with electrical properties of a single filament of nylon held between two tungsten hook-electrodes. Currents were observed in atmospheres of different relative himidities and attempts were made to determine the voltage distribution along the filament. The voltage measurements were made using a high-impedence electrostatic null detector with a potentiometer system for balancing. The results were not highly reproducible and no definite conclusions could be made.

The second part deals with currents through capacitor tissue in a metal- insulation- metal sandwich arrangement. A time-dependent polarization was observed and is discussed along with methods for determining an acceptable value for the steady-state current. Some attempts are made to apply Poole-Frenkel theory since there is a certain quantitative agreement with experiment. Current-temperature observations indicated that the activation energy is about 1 ev. Conclusions concerning the mechanism of conduction are suggested on the basis of available theory.

ACKNOWLEDGMENTS

I wish to express my gratitude to Dr. J. Hart for his guidance and supervision throughout the project. I would also like to convey my appreciation to Dr. R. Raman for his constant interest, his many helpful suggestions and for his assistance in the preparation of the text. Furthermore, it is a pleasure to acknowledge enlightening discussions with Dr. V. V. Paranjape. I am also grateful to J. R. Butler, K. Sumpter and G. Anderson for valuable technical assistance, to Mr. R. Lightfoot of the Dryden Paper Company who generously supplied samples of capacitor tissue, and to D. Cadieu and J. Parnell for typing the manuscript. Financial assistance was received from NRC and Lakehead University.

TABLE OF CONTENTS

LIST OF FIGURES

LIST OF TABLES

CHAPTER I

INTRODUCTION

The electrical properties of insulating materials have considerable importance in relation to their applications to the electronics and electrical industry. Two such materials of great relevance to the work to be described are nylon and cellulosic fibre. In particular, we deal here with nylon in the form of a thin filament or thread, and the cellulosic fibre in the form of capacitor tissue. Nylon fibres are often applied as armature twines etc., whereas the application of tissue paper is as insulation in capacitors, transformers, motors and cables. The nylon material is any long chain synthetic polymeric amide in which, when formed into a filament, the structural elements are oriented in the direction of the axis. On the other hand, capacitor tissue is manufactured from sulphate pulps of select grade made from certain species of soft woods. These pulps are chosen for their long thin fibres and high degree of purity.

The quality control of the electrical specifications is fundamentally relevant to any a.c. or d.c. applications. For instance, a.c. capacitors need low power factor, long a.c. life and high a.c. dielectric strength, while d.c. capacitors need long d.c. life and high d.c. dielectric strength. Such applications of twines to the banding of armatures and commutators require high dielectric strengths.

In the industry, quality control is normally achieved by routine tests on the materials and some of these tests include electrical conductivity, dielectric strength, power factor, moisture content etc. While a great deal of technical data is available in this regard, the amount of fundamental studies which have been carried out is rather limited; the main reasons for this being:

(i) the inherent difficulties in making measurements of extremely small currents,

(ii) the problems associated with the separation of surface, bulk and electrode effects,

(iii) complexity of the system, especially with regard to the capacitor tissue.

The work discussed herein is an attempt to understand some of the salient features in question with special reference to the d.c. conductivity. For sake of convenience, the discussion is divided into two sections; section one dealing with polarization effects in a nylon filament, and section two dealing with polarization effects as well as some aspects of the mechanism of conduction in capacitor tissue.

The experiments with the nylon filament were conducted using a null detecting method in which an attempt was made to determine the voltage distribution along the string having several electrodes. In this method, the measurement technique is very similar to the so-called probe methods which are normally used to investigate internal polarization -- electret effects -- in a variety of organic materials. To determine the potential distribution within the polarized sample, two probes were attached to the filament at different distances from the cathode and the voltage of each probe was monitored by a potentiometer system with a null detector. The null detector is essentially a string electrometer of a sturdy construction and can easily be assembed to produce an instrument with extremely low leakage currents. It must be pointed out that under these circumstances it is difficult to separate the surface effects from bulk effects, so much so in fact that even to a first approximation one is restricted to a purely qualitative analysis of the parameters measured.

Compared to this, the experiments with capacitor tissue offer the possibility of obtaining better quantitative data because one can easily study the system as a metal-insulator-metal sandwich arrangement, thereby eliminating to a considerable extent, the surface current effects. With such an arrangement, one can study the d.c. conductivity in the insulator under a variety of conditions, and in past years, the conduction

phenomena in a large number of insulating films and layers have been investigated. Of special interest are conductivity studies in silicon dioxide,[13] silicon nitride,[15, 30] polyethyleneterephthalate (mylar)[1, 19, 20] polytetraflourcethylene (teflon),[20] alkali halides,[2, 29] and tantalum oxide.[22] In all these investigations, the following characteristics have been noted and recognized:

(i) when a constant electric field is applied to the dielectric, the current density per unit field decreases with time from an initial conductivity to a final steady-state value. This arises from the fact that the polarization is often a slow process.

(ii) when the field is removed, current flows for a time in the opposite direction.

(iii) the steady-state current increases roughly exponentially with the voltage especially for high field values.

(iv) the logarithm of the steady-state current is roughly proportional to the reciprocal of the absolute temperature.

It is significant that the interpretation of these results is complicated not only by conflicting theoretical models but also by ambiguities owing to peculiarities in any one particular system. These pecu-

liarities relate to the complexity in structure of the material, physical dimensions of the sample, electrode effects, physical environment etc. While some materials have been found to be easily amenable to theoretical treatment others seem to be particularly difficult.

With reference to the fundamental studies of any one system it is relevant to consider the following two aspects:

(a) the time dependent polarization in the insulator.

(b) the mechanism of charge transport.

We now wish to consider these points in greater detail.

(a) THE TIME DEPENDENT POLARIZATION

An insulating material under the actions of an electric field becomes polarized due either to the relative displacement of positive and negative charges within it or to the rotation of permanent dipoles. As pointed out by Sutter and Nowick[29] such polarization is not always instantaneous. This effect is manifested by a decrease in current with time which approximately follows the empirical relation

$$i = Kt^{-n} \qquad \text{Eq. (1.1)}$$

where i is the current, t is the time and K and n are constants. This polarization is a reversible process so that complementary to the decreasing current in the presence of a constant applied field, there follows, upon removal of the field, a reverse current which indicates a transient state of depolarization. The effect is described by the Superposition Principle which states[29] that if the charging current, i (t), is allowed to reach its final steady-state value, i_∞, then the discharge current, i_d (t), which flows in the opposite direction is related in magnitude to i (t) by

$$i(t) - i_\infty = i_d(t) \qquad \text{Eq. 1.2}$$

This is best illustrated by Fig. 1.1. Eq. 1.2 often found to be valid although in some cases it only approximates reality. The decreasing current normally is of the form of i (t) in Fig. 1.1. It is significant that the shaded area under i (t) represents the amount of charge displaced from equilibrium position during the polarizing process and according to the Superposition Principle it should equal the area above the i_d (t) curve. The magnitude of this quantity is defined as the Polarization.

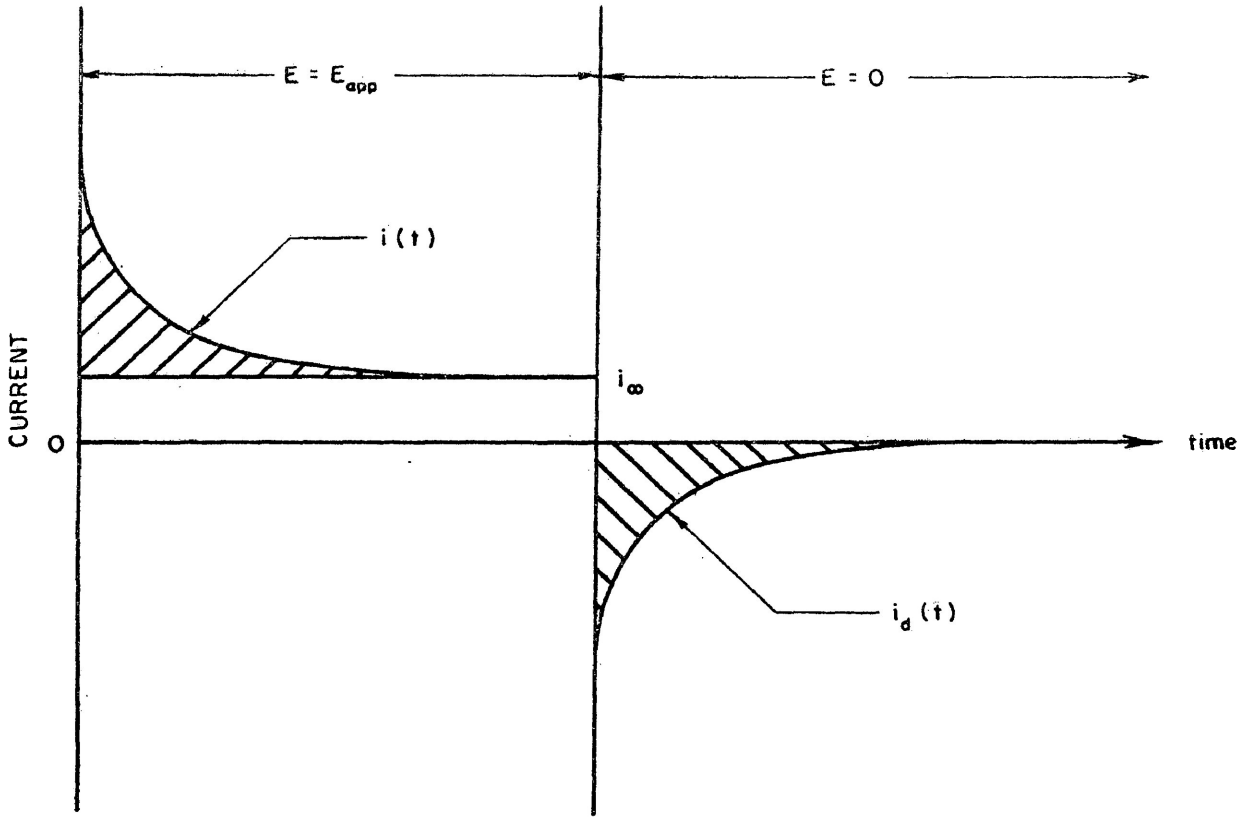

Fig. 1·1

CHARGE and DISCHARGE CURRENTS

As shown by Sutter and Nowick[29] the empirical relationship given by Eq. 1.1 cannot hold while t becomes indefinitely large since otherwise the polarization

$$P = \int_0^\infty [i(t) - i_\infty]\, dt \qquad \text{Eq. 1.3}$$

or, using Eq. 1.2

$$P = K \int_0^\infty t^{-n}\, dt \qquad \text{Eq. 1.4}$$

would become infinite. It is also pointed out that since the initial current i(o) is infinite the equation cannot be taken too seriously for short times either.

From a formal point of view two diverse theories for the time dependent polarization have been proposed. According to the first theory which has been expounded by A. Joffé,[12] the build-up of space charge occurs at one or both of the electrodes due to the fact that charge carriers are not discharged at the electrodes. Thus the potential distribution with reference to a given electrode is not linearly dependent on the distance

from that electrode. In the second theory the time dependent polarization represents a change in the macroscopic dielectric constant of the material with time. This is a true relaxation process and the potential distribution varies linearly across the bulk.

(b) MECHANISM OF CHARGE TRANSPORT

It has been pointed out that the logarithms of the observed steady-state currents are roughly proportional to the voltage for a fixed temperature and to the reciprocal of the absolute temperature when the voltage is constant. As indicated by Mead[22] mechanisms which might explain one or more of the observed charateristics are: ionic flow, space-charge-limited currents with distributed traps and Schottky or Poole-Frenkel effects. Although it is possible to arrive at definite conclusions regarding the conduction mechanisms (as well as electrode effects) on the basis of the current behaviour under diverse conditions, it has been found difficult to determine unequivocally the exact mechanism in materials such as those under study. According to Hickmott[7] all of these processes probably contribute to the leakage currents in such systems and which one predominates will depend on the particular conditions of study.

In order to have a significant ionic flow in any system, there must be a possibility for the production of protons or some other ions in the bulk. This is followed by actual electrolysis due to the discharge of the migrating ions, however, direct diagnosis of this phenomenon would be difficult due to the small currents involved. It is also known[10] that a slow relaxation process is observed in the case of ionic conduction before steady-state is reached.

A second process which may play a prominant role in determining the electrical properties of insulation is the build-up of space charge which is facilitated by direct charge injection from an ohmic contact. The character and magnitude of these effects are largely due to the presence of localized states which can trap and store charge in equilibrium with the free mobile charge. The theories and models for space-charge-limited currents are well developed and extensive descriptions are available from Rose[25], Lampert[18], and others.[3]

However, the most important and most extensively applied models are based on the Schottky and Poole-Frenkel effect.

The theories associated with these two effects both predict current-voltage characteristics of the form

$$i = i_o \exp \left[- \frac{bV^{\frac{1}{2}}}{kT} \right] \qquad \text{Eq. 1.5}$$

where T is the absolute temperature and for all practical intents and purposes i_o, b and k, are constants, and this relationship is very often observed in thin films and layers. These models differ in that in one, the movement of charges (we consider these charges to be electrons) is restricted by forces at the electrode - insulator contact while in the other the conduction is limited by forces within the bulk of the dielectric.

The first of these models, which describes an electrode limited process, is based on the Richardson-Schottky law for the emission of electrons from a metal into a vacuum. The precise relationship relevant to the metal - dielectric interface is, as shown in Appendix A, given by

$$j = j_o \exp \left[- \frac{\phi_s - \Delta\phi_s}{kT} \right] \qquad \text{Eq. 1.6}$$

where j is the current and for practical purposes j_o is a constant. We also have

$$\Delta\phi_s = \tfrac{1}{2}\left[\frac{e^3}{\pi\,\varepsilon_o\varepsilon}\right]^{\frac{1}{2}} F^{\frac{1}{2}} \qquad \text{Eq. 1.7}$$

with T the absolute temperature, F the applied field, k Boltzmann's constant, e the electronic charge, and ϕ_s the work function of the metal-dielectric interface. The permittivity of free space and the relative dielectric constant are given by ε_o and ε respectively. The second term in the numerator of Eq. 1.6 gives the field-reduction of the barrier height from the zero-field barrier or work function, associated with the metal-dielectric interface. Thus $\phi_s - \Delta\phi_s$ is the barrier height in the presence of a field and is referred to as the motional activation energy or simply the activation energy in experiments which are concerned with current as a function of temperature.

The second model which qualitatively predicts the observed current-voltage relationship arises from the consideration of fixed positive charges throughout the bulk of the dielectric and in the presence of an external electric field. The mechanism which now restricts the motion of electrons

is a series of coulombic barriers distributed throughout the physical dimensions of the insulator. The detailed analysis given in Appendix B describes the field-dependent barrier which is manifested by the current-voltage characteristics. The barrier height is connected mathematically to the current-voltage characteristic by the expression for the number of electrons in the conduction band of the insulator and thus the number which are free to contribute to the current through the dielectric. The expression for the number of free electrons is found to be

$$n_c = n_o' \exp\left[-\frac{\phi}{2kT}\right] \qquad \text{Eq. 1.8}$$

when donor impurities and only donor impurities are present in the dielectric. If the donors are partially compensated by acceptor impurities then

$$n_c = n_o'' \exp\left[-\frac{\phi}{kT}\right] \qquad \text{Eq. 1.9}$$

where n_o' and n_o'' are constants which depend on the impurity concentrations. ϕ is the energy gap between the emission sites and the conduction band and is given by

$$\phi \equiv \phi_{PF} - \Delta\phi_{PF} \equiv \phi_{PF} - 2\left[\frac{e^3}{4\pi\epsilon_o\epsilon}\right]^{\frac{1}{2}} F^{\frac{1}{2}} \qquad \text{Eq. 1.10}$$

Use is then made of the relation

$$j = n_c e\mu F, \qquad \text{Eq. 1.11}$$

where μ is the carrier mobility, to determine the expressions for current density, j, as a function of the applied voltage. The equation arising for each of the two cases based on impurity concentrations can be combined to give

$$j = e\mu n_o F \exp\left[-\frac{\phi_{PF} - \Delta\phi_{PF}}{r k T}\right] \qquad \text{Eq. 1.12}$$

where r is a factor which varies between unity for the case of partial carrier compensation and two in the absence of the compensation of donor impurities. If r is known, the slope of an empirical ln j - vs - $V^{\frac{1}{2}}$ plot can be used in comparison with the theoretical slopes to determine which mechanism, bulk- or electrode- limited is operating. That r is known, however, is seldom the case and the usual procedure (see for instance Yeargan and Taylor[31]) is to determine whether the current is bulk- or-electrode- limited by some other means and thence the degree of compensation.

Frenkel's original 1938 publication[4] gives Eq. 1.12 in the case where r = 2 but has been misquoted by several

authors[22, 32], as the case where r = 1. The situation, however, is clarified by such workers as Hu, Kerr and Gregor[9], and Lilly and McDowell[20], who, in agreement with the above development state that when only donor impurities are present (Fermi level is above the donor level) the Richardson-Schottky and Poole-Frenkel equations are indistinguishable. This is because the r = 2 cancels with the two factor in $\Delta\phi_{PF}$ (recall from Appendix B that $\Delta\phi_{PF} = 2\Delta\phi_S$) to give the same field dependence predicted by Schottky theory. On the other hand, when impurity compensation is taking place, the two mechanisms can be distinguished since different slopes for the ln i - vs - $V^{\frac{1}{2}}$ curves are predicted.

Unfortunately, there are many insulators[19, 20, 23], for which the high-field slopes of the Schottky plots (ln i - vs - $V^{\frac{1}{2}}$) do not lie within the theoretical limits of

$$\frac{1}{kT}\left[\frac{e^3}{4\pi\varepsilon_o\varepsilon d}\right]^{\frac{1}{2}} \text{ and } \frac{2}{kT}\left[\frac{e^3}{4\pi\varepsilon_o\varepsilon d}\right]^{\frac{1}{2}}$$

where d is the dielectric thickness, and when this occurs most workers[19,20,23], claim that the presence of space charge

causes the effective field within the dielectric to differ from the applied field. It has already been stated that current absorption through dipole re-orientation exhibits a linear voltage distribution throughout the insulator while space charge effects lead to local variations in the electric field but this latter point should be expanded.

It is readily seen from Poisson's equation

$$\underset{\sim}{\nabla} \cdot \underset{\sim}{F} = \frac{dF}{dx} = \frac{4\pi}{\varepsilon} e (p - n) \qquad \text{Eq. 1.13}$$

where p and n are the positive and negative carrier densities respectively, that the gradient of the field is affected by the carrier densities. If (p - n) = 0, i.e. no space charge, then the field, F, is constant and using

$$F = \frac{-dV}{dx} \qquad \text{Eq. 1.14}$$

the voltage V is seen to be linearly dependent on the distance from a given electrode. This is illustrated by Fig. 1.2a. However, when (p - n) is non-zero and position dependent, space charge is present and the field and voltage within the material vary with position. Fig. 1.2b illustrates this point when there is

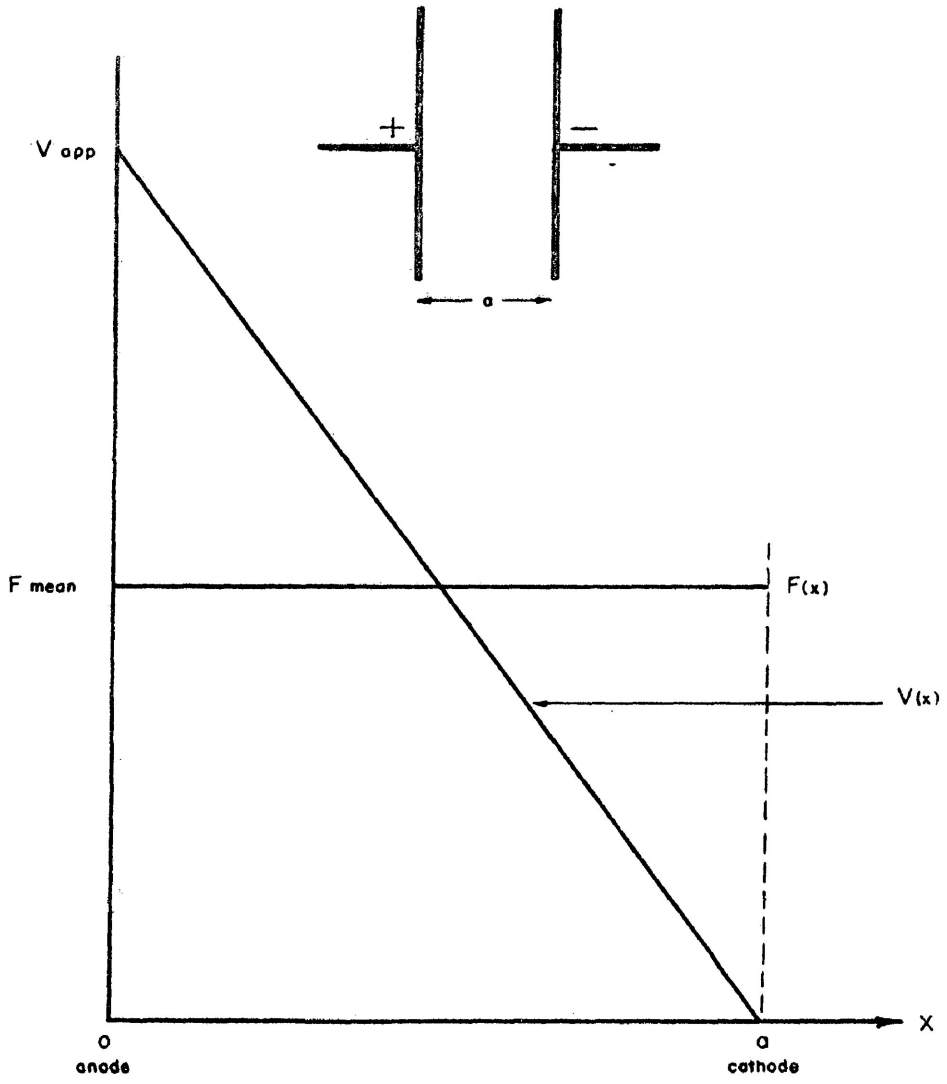

Fig. 1·2a

FIELD and VOLTAGE DISTRIBUTION

NO SPACE CHARGE

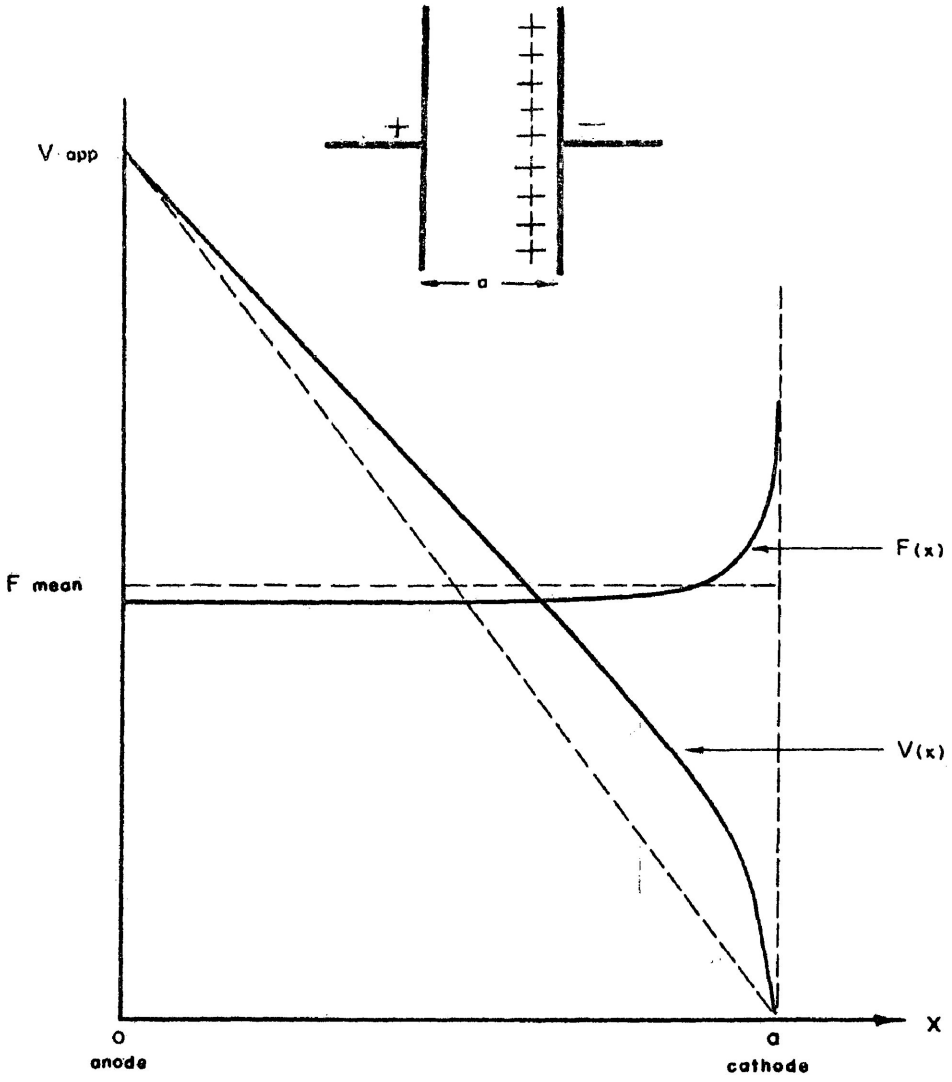

Fig. 1·2b

FIELD and VOLTAGE DISTRIBUTION

HETEROCHARGE AT CATHODE

a heterocharge at the cathode while Fig. 1.2c applies to the case with heterocharges at both electrodes. Clearly the development of space charge leads to an increase in the field near the electrodes while deep within the bulk of the insulator the field is decreased. Croiteru[3] discusses further details concerning space charge although they are not given here.

To deal with this idea that space charge causes the effective and applied fields to differ, several investigators[19, 20, 23] write for the effective field

$$F_{eff} = \frac{\gamma V}{d}. \qquad \text{Eq. 1.15}$$

Studying cadmium sulphide with gold contacts, Muller[23] treats γ as a geometrical factor equal to unity for plane parallel electrodes and greater when irregularities occur in the electrode surfaces. Working with nylon and teflon, Lilly and McDowell[20] attribute values of γ differing from unity solely to the buildup of space charge near the electrodes and give values of 0.86 to 25.6 depending on thickness. These workers[20] base their calculations on the theoretical value of $\Delta\phi_s$ but indicate that there is some reason to doubt the choice of an electrode - limited process over

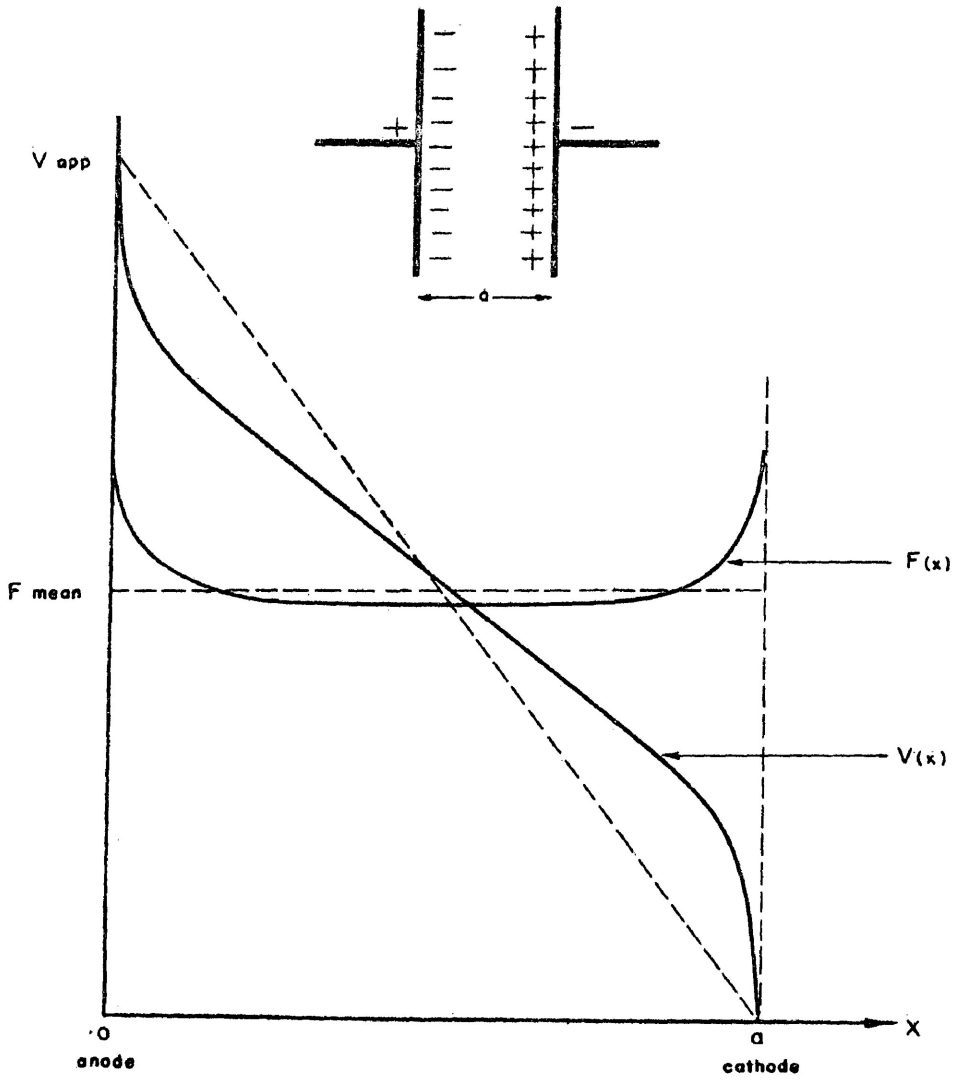

Fig. 1-2c

FIELD and VOLTAGE DISTRIBUTION

HETEROCHARGE at BOTH ELECTRODES

a bulk- limited one. In an earlier work, Lengyel[19] also invokes the γ factor to bring the theoretical slopes for mylar into line with those observed*, and assumes that the steady-state current was limited by charge injection.

It must be re-emphasized that the interpretation of the results is quite complicated. The limitations of the experiments as well as the validity of the various models is implied by the above discussion. In view of this, it is needless to say that the scope of the present work is severely restricted. However, an attempt is made to determine some of the important electrical parameters associated with nylon and cellulosic fibre.

---

* Lengyel determines a value of 1.35 for γ where, for similar temperatures, Lilly and McDowell give 0.86. However, the data of the latter workers indicate that Lengyel's fields were below those required for Schottky emission at the electrodes.

CHAPTER II

RESULTS AND DISCUSSIONS OF STUDIES ON NYLON FILAMENT

In the measurement of insulation resistance high accuracy is seldom required and hence simple circuits are usually adequate. The experimental arrangement used herein to study the electrical properties of nylon filament is no exception. The current was measured with a Victoreen Model 475B dynamic capacitor electrometer while the voltage was applied with a Hewlett-Packard Model 712C power supply. The nylon samples were cut from spools of monofilament fibre from the Horrocks-Ibbotson Company, Utica, N. Y. and were about 3 inches long with a 17 mil diameter. For support, small loops were tied in the ends of the filament and held by tungsten hooks, also acting as electrodes, which were fused into the ends of a cylindrical glass tube. The filament holder is illustrated in Fig. 2.1. One of the difficulties associated with measuring insulation resistance is that the currents are invariably small. Thus leakage currents may be comparable to the currents to be measured and suitable precautions must be taken to eliminate them from the measurement. In this case a grounded guard ring was used so that the currents passing along the walls of the glass tube would bypass the meter, and the network is shown schematically in Fig. 2.2.

The first measurements were directed toward determining the resistivity of the filament from the currents produced by various voltages. It is apparent from Fig. 2.3 that Ohm's law is valid at least up to 600 v. with some sample to sample variation. The resistances calcu-

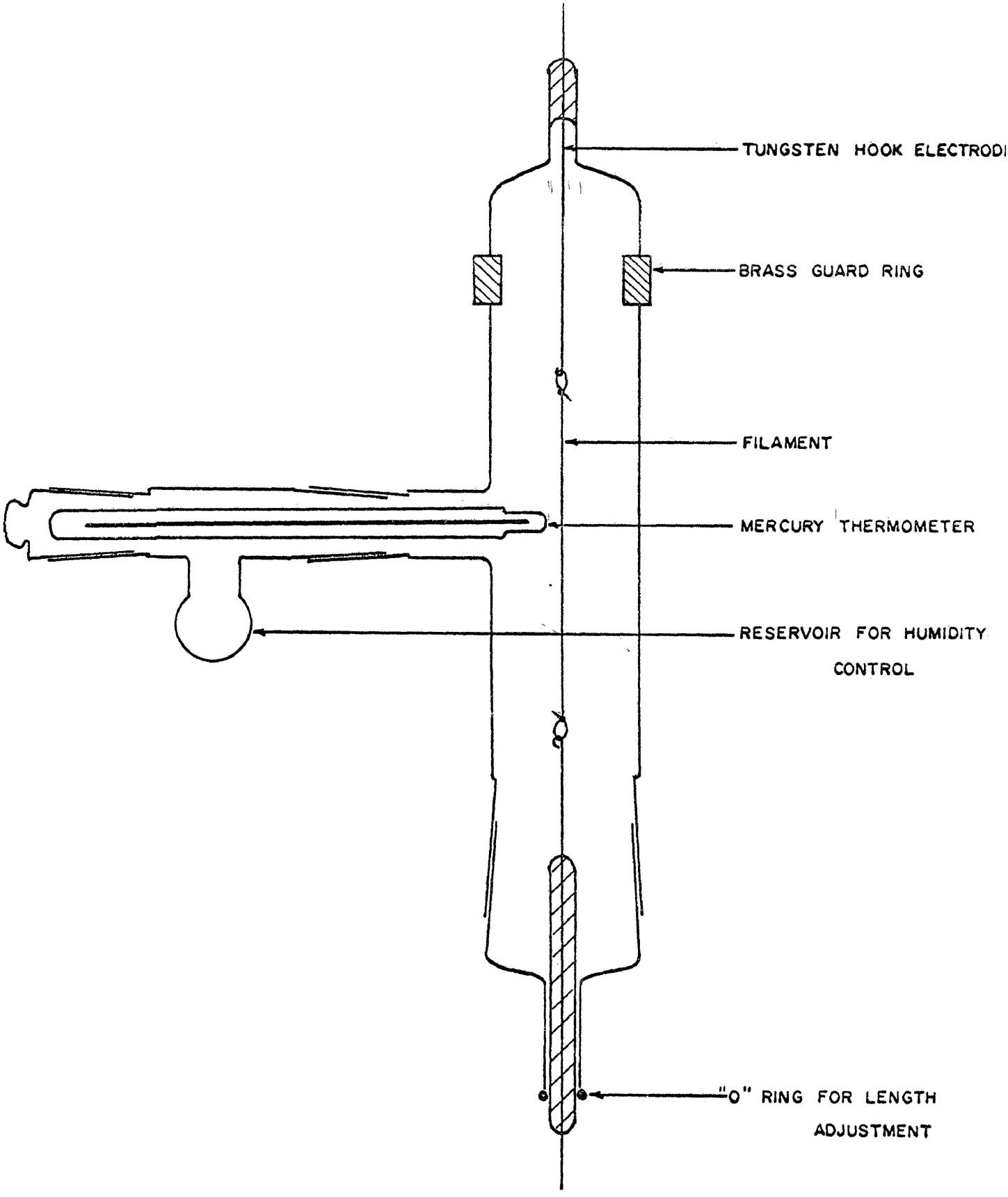

Fig. 2·1

GLASS FILAMENT HOLDER

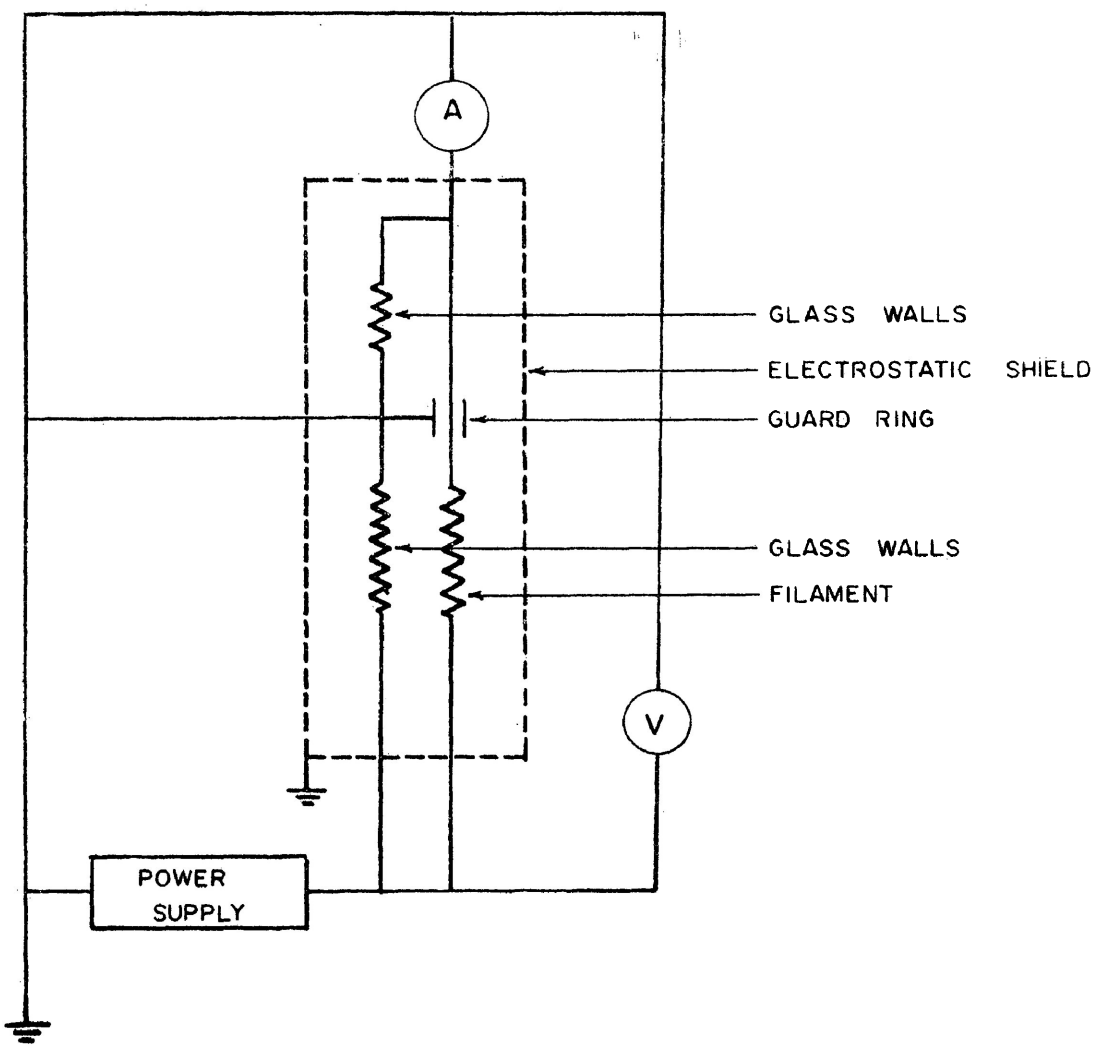

Fig. 2·2

SCHEMATIC DIAGRAM of MEASURING NETWORK

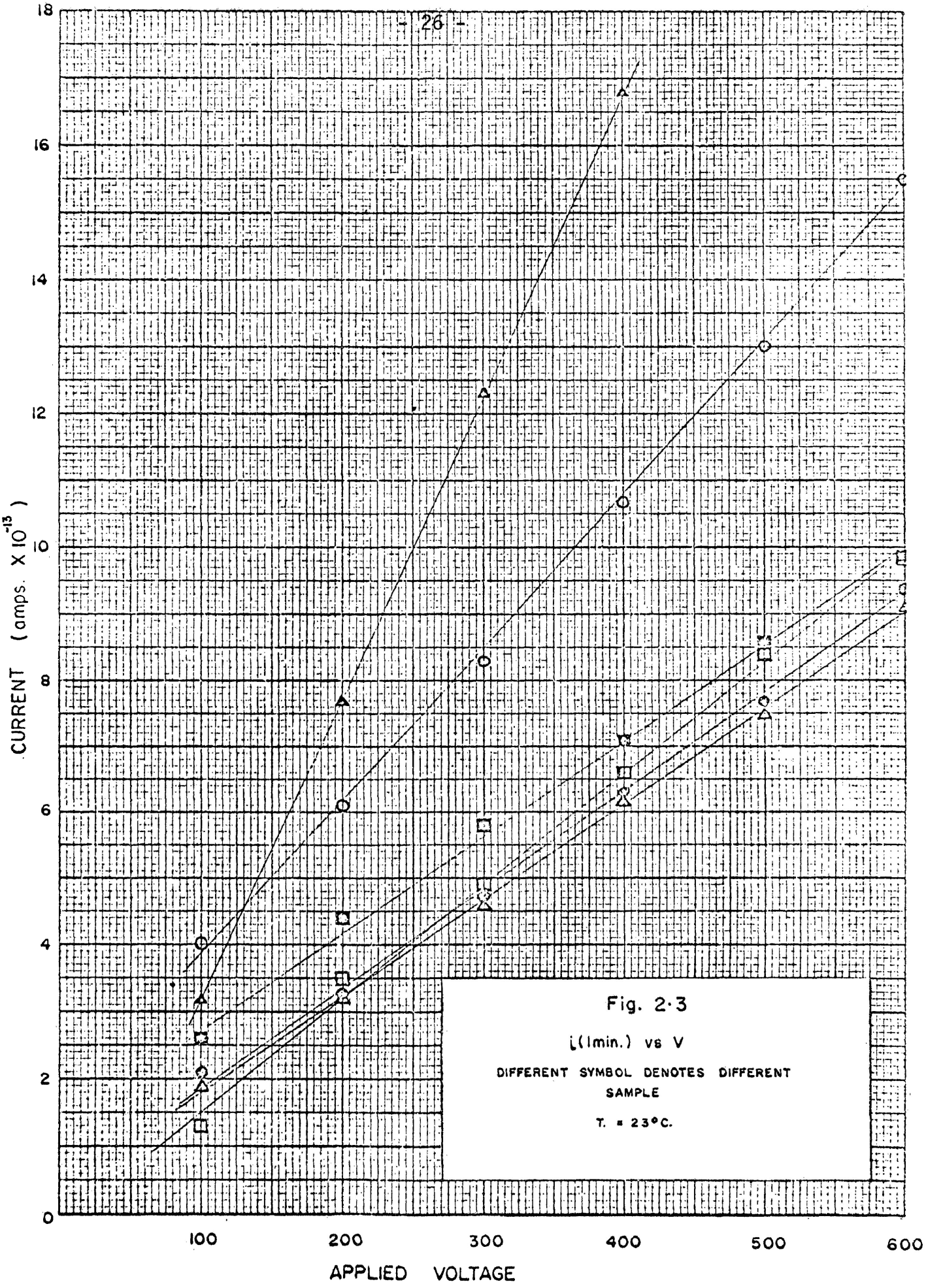

Fig. 2·3

i(1min.) vs V

DIFFERENT SYMBOL DENOTES DIFFERENT SAMPLE

T. = 23°C.

lated from the slopes of the curves are given in Table 2.1 along with the resistivity values obtained when the physical dimensions are taken into account. The current values used in the preceding figure are the initial values and they appeared steady for the few

STRING NO.	RESISTANCE	RESISTIVITY
1	$2.21 \times 10^{+14}$ Ω	1.103×10^{11} Ωcm.
2	4.27	.465
3	7.13	.850
4	6.03	.745
5	6.07	.975
6	7.07×10^{14}	$.951 \times 10^{11}$

TABLE 2.1
RESISTANCE AND RESISTIVITY BASED ON INITIAL CURRENTS.

minutes in which they were observed. However, more lengthy observations indicated that the current was decreasing with time thus casting some doubt on the validity of using the initial currents to determine the resistivity. The long term observations showed that the current was dependent on temperature variations in the room as well as the humidity. The temperature was regulated by installing a fan and a heating element, regulated with a bimetal strip, into the box which acted as an electrostatic shield. 36° C was chosen as a standard for many of the subsequent experiments. The humidity was regulated by placing in the reservoir, saturated aqueous solutions of various salts and which contained a few grams of the

solid phase. The salts used were lithium chloride (LiCl), potasium nitrite (KNO_2), and sodium nitrite ($NaNO_2$), producing relative humidities of 15%, 45% and 66% respectively in the surrounding atmospheres. The two humidity extremes were obtained by placing phosphorous pentoxide (0%) and water (100%) in the reservoir.

It was found that the magnitude of the current, as well as the rate of decrease was affected by the relative humidity of the atmosphere about the string. The current as a function of time roughly obeyed the hyperbolic

$$i = Kt^{-n}$$

relation discussed in Chapter I and reported by other investigators working with thin films and layers. The best fit of the experimental data to this relation occured in the driest atmospheres while the fit became poorer and poorer as the relative humidity increased. Fig. 2.4 shows the current-time curves for a single sample at the indicated humidities. The observations were made in order of increasing humidity and the initial atmosphere was assumed to be completely dry after phosphorous pentoxide had been in the reservoir for two days. Following the application of 500 v. the current was observed for about eleven hours. The subsequent current observations for the greater humidities were made when the appropriate salt solution had been in the reservoir for not less than twenty-four hours.

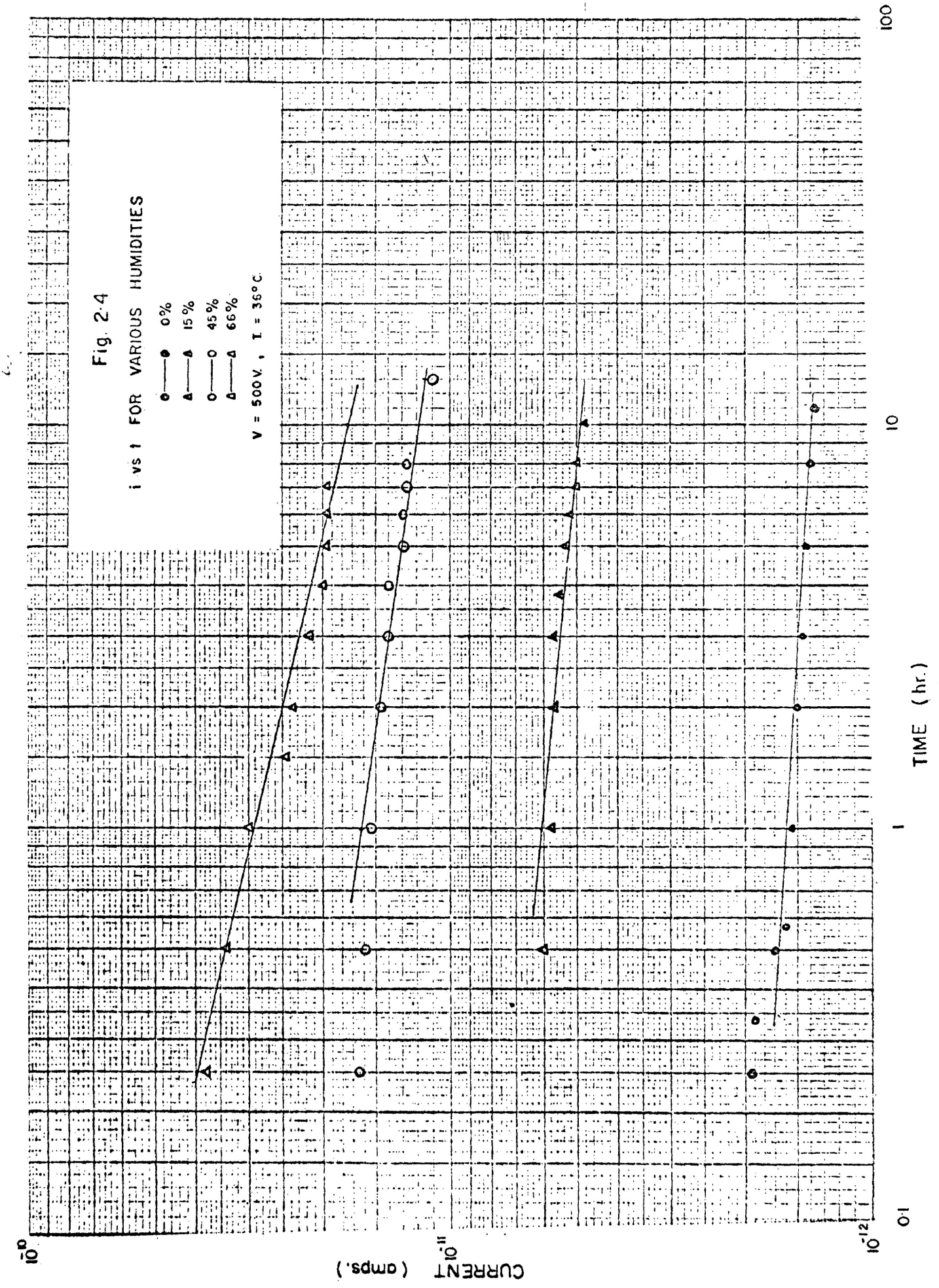
Fig. 2·4
i vs t FOR VARIOUS HUMIDITIES
0%
15%
45%
66%
V = 500 V. , T = 36°C.
CURRENT (amps.)
10^{-10}
10^{-11}
10^{-12}
0·1
1
10
100
TIME (hr.)

During these periods of time when the moisture content of the atmosphere was changing, the sample ends were shorted and it is assumed that any polarization effects which remained in the filament after these twenty-four hour periods, were negligible in comparison to the processes occuring when the voltage was reapplied. The calculated values of the decay constant, n, are tabulated in Table 2.2.

R.H. %	n
0	.06
15	.09
45	.13
66	.22

TABLE 2.2

SINGLE DETERMINATION OF DECAY CONSTANT AT VARIOUS HUMIDITIES

In moist atmospheres (R.H. = 100%) the correlation of the experimental results with the hyperbolic relation was poor although it was clear that these conditions produced a dramatic increase in the value of n; this indicates that the state of polarization develops most rapidly in the highest humidities. The currents observed in three different samples at R.H. = 100% are given in Fig. 2.5. There is a certain amount of sample to sample variation indicated by the values of n given in Table 2.3 as well as by the differences in the current magnitudes

SAMPLE	n	LENGTH
1	0.9	8.1
2	1.3	7.9
3	1.2	7.4

TABLE 2.3

DECAY CONSTANT AT R.H. = 100%

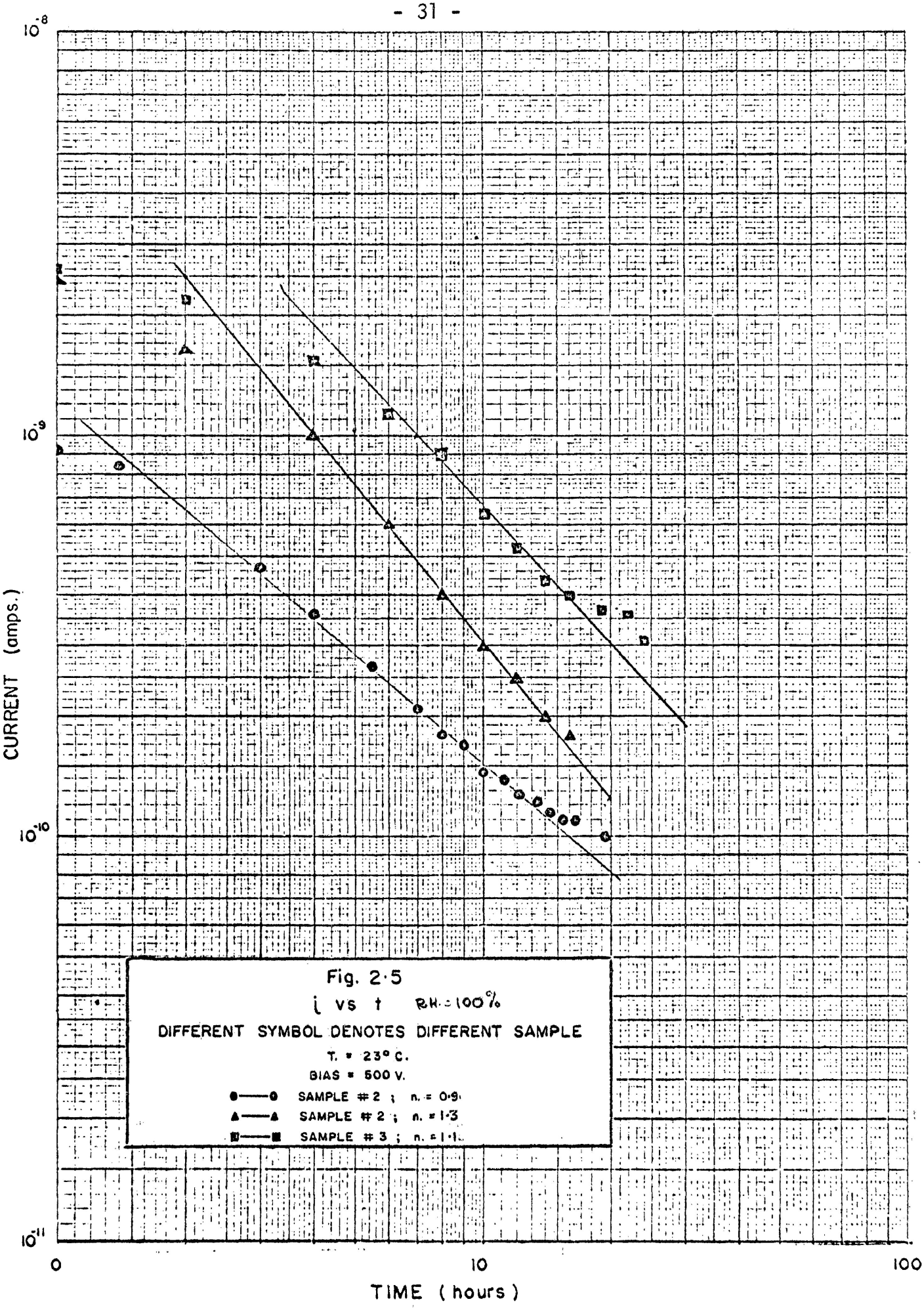

Fig. 2·5

i vs t R.H. = 100%

DIFFERENT SYMBOL DENOTES DIFFERENT SAMPLE

T. = 23° C.

BIAS = 500 V.

●——● SAMPLE # 2 ; n. = 0·9

▲——▲ SAMPLE # 2 ; n. = 1·3

■——■ SAMPLE # 3 ; n. = 1·1

which cannot be attributed solely to variations in the string length.

The decrease in current, or the current absorption, is due to the decrease in the effective field within the insulator. As pointed out in Chapter I, this can be due either to dipole orientation or to the build-up of space charge, and which is the operating mechanism can be determined by examination of the voltage distribution throughout the dielectric. It was with this purpose in mind that considerable effort was put forth in the measurement of voltage since the filament is especially amenable to this type of study. These measurements however, are complicated by the fact that the voltages to be determined occur across resistances of the order of 10^{12} ohms and any voltage measuring device drawing more than about 10^{-14} amps. from the filament could be expected to disturb the potential. This is far beyond the capabilities of conventional meters which seldom have input impedences greater than 10^{8} ohms.

In this case an attempt was made to solve the problem by developing a high impedence electrostatic null detector of the type originally described by Hart and Mungall[5]. The instrument as first constructed (Fig. 2.6) was nearly identical to the original[5]. It consists essentially of two fixed plates A and B, and one movable plate C, all of which are supported inside a hollow teflon block. The central

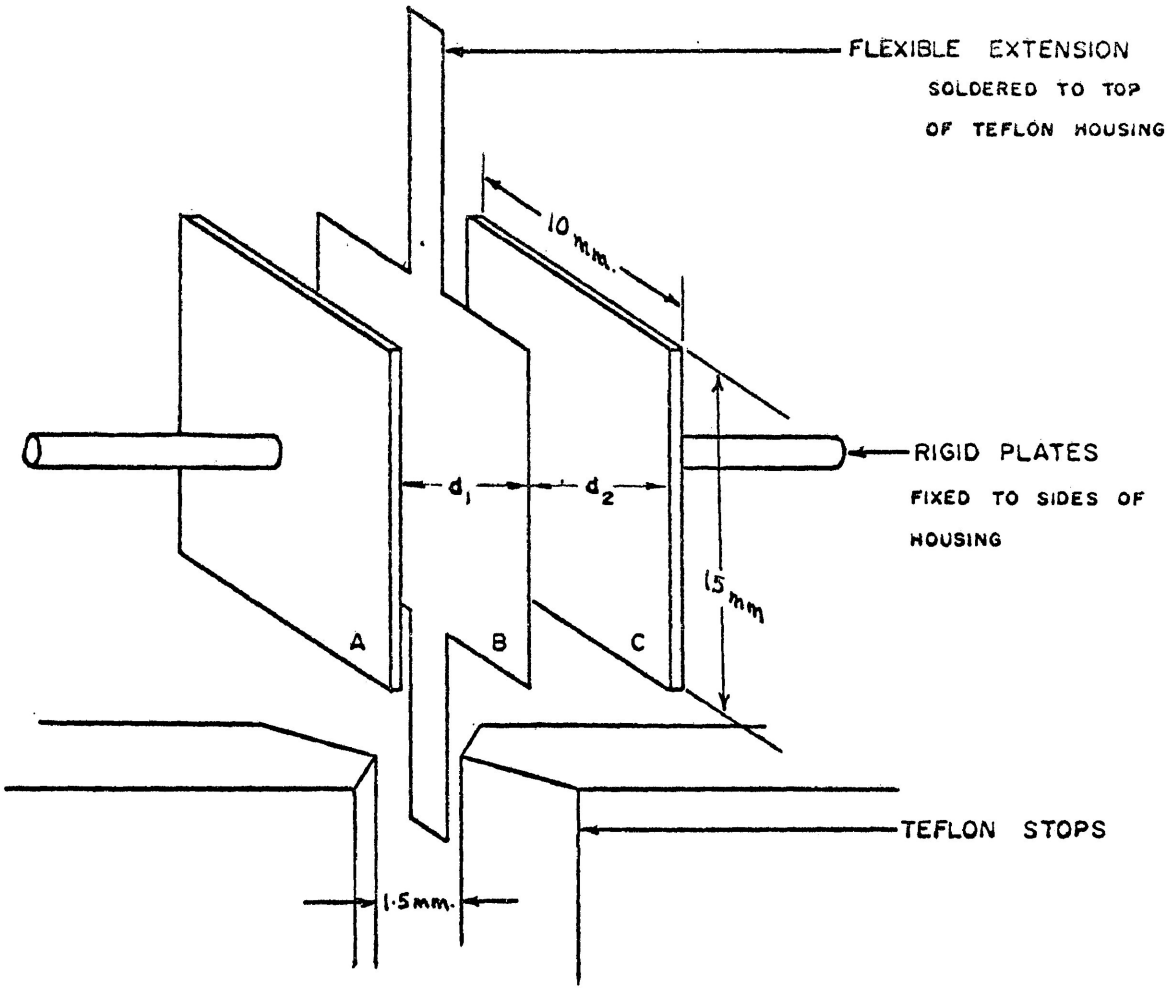

Fig. 2·6

ESSENTIAL FEATURES of the ELECTROSCOPE

plate was made from a flexible 1 mil sheet of brass with extensions at the top and bottom. The top extension, when soldered to a copper shaft provided the mechanical support while the bottom extension hanged between two teflon edges which acted as stops to the suspension and to prevent shorting against plates A and B. As a further insurance against shorting, thin teflon sheets were fixed to the insides of the rigid plates.

A brief explanation of the principle of operation is now presented. If a field is applied between plates A and B, and plate C is maintained at a voltage V_1 with respect to A and V_2 with respect to B, then the electrical force which acts on C,

$$F = \frac{A}{2}\left[\frac{V_1^2}{d_1^2} - \frac{V_2^2}{d_2^2}\right]$$

where d_1 and d_2 are the respective distances of C from A and B, deflects the vane from the zero position. There is however, a mechanical restoring force which brings the central plate back to the zero position when the electrical forces have been balanced out. Fig. 2.7 is a schematic diagram of the circuitry involved, and the procedure for making a voltage determination is as follows: with the switch, s, in position 1 the electroscope vane can be moved

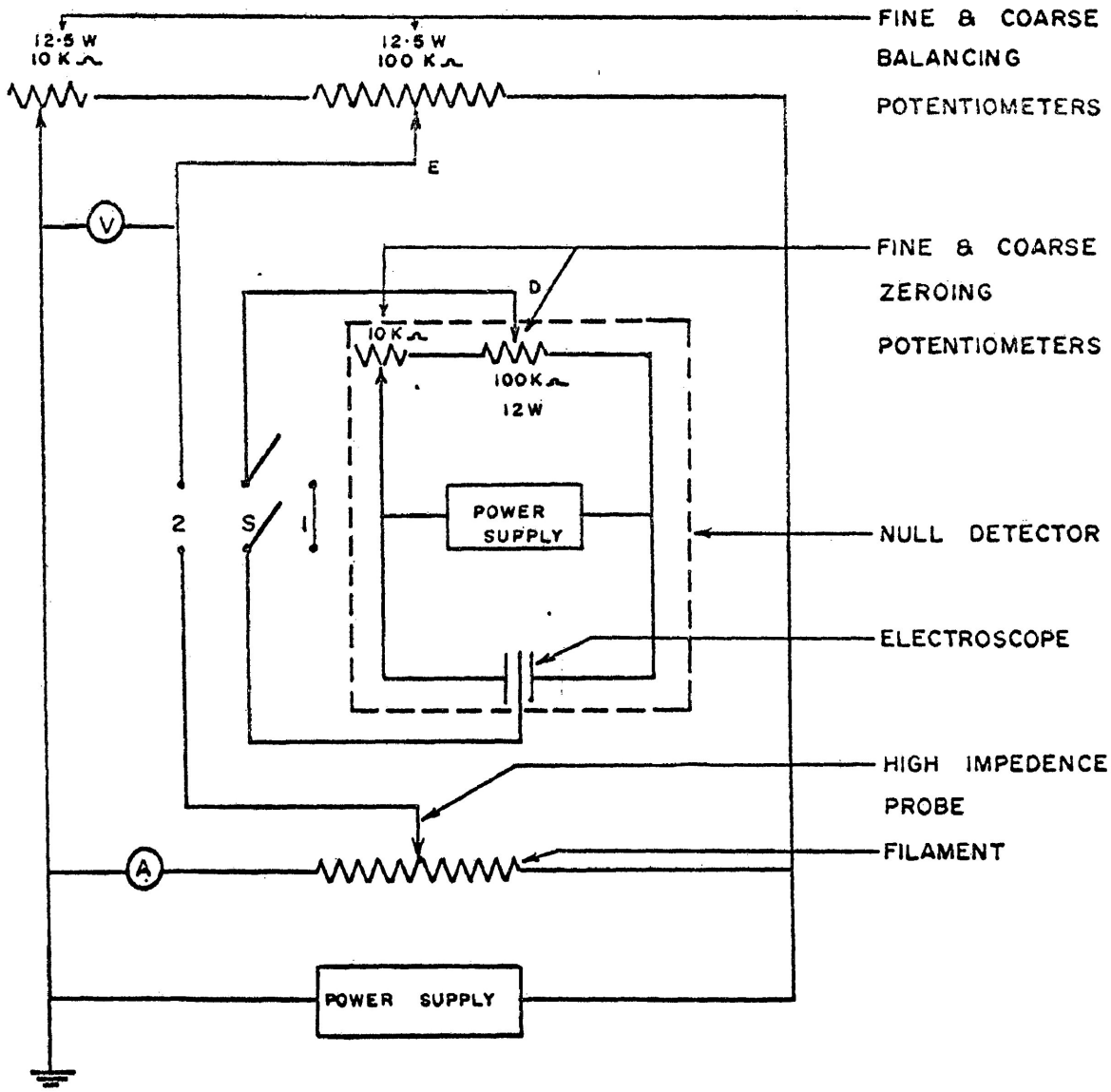

Fig. 2·7

NULL DETECTOR and ASSOCIATED CIRCUITRY

anywhere between the plates by adjustment of the zeroing potentiometer. This serves to fix a zero position for the leaf since there is no potential difference between it and the centre tap of this potentiometer (point D in Fig. 2.7) and gives a precise method of lining up the vane with the cross hairs of a microscope (in this case a 20X microscope) or some other optical sighting system. When the switch is in position 2 the electroscope vane is no longer at the same potential as D and is deflected from the arbitrary zero position by the field between the plates. A zero voltage between the vane and point D can be re-established by adjusting the balancing potentiometer until the vane returns to the original null position. The voltage at point E, which can be measured with a standard meter, is now at the same voltage as the vane and thus the potential of the high impedence probe is established.

The initial test of the system was made with the electroscope as well as switches and potentiometers enclosed in a rack-mounted module and was found to work well when the test voltages were generated across 1.0 megohm resistors. However, difficulties pertaining mainly to zero drift and to erratic and unreasonably low balancing voltages, were apparent when the high impedence probe was attached to the more highly resistive filament. This suggested that the probe was drawing relatively high currents

due to leakage to ground even though the best insulation available was being utilized.

To combat the problem of leakage it was decided that the electroscope vane should hang directly from a horizontally disposed filament which would mean that the probe (i.e. the vane) touched nothing as it hanged between the rigid plates of the electrometer. Several modifications were obviously necessary to incorporate the new concept into the apparatus and it was felt that two probes could be handled as easily as one. The vanes were attached to the string by soldering them to a brass connecting boss which could be fastened directly to the filament. The rigid plates were held by a mounted teflon housing which was now open at the top to allow the vanes to hang freely. The electrical contact to the movable plates was made by touching the connecting boss with a fine copper wire. This however, caused the failure of the particular design since touching the boss upset the delicate mechanical zero position of the leaf and it was clear that an electrical but not a mechanical contact was necessary.

The design of the null detector which eventually was used to obtain values of voltage along the string involved the use of a brine solution to contact the electroscope vane and the essential features of the detector and filament holder are illustrated in Fig. 2.8. The

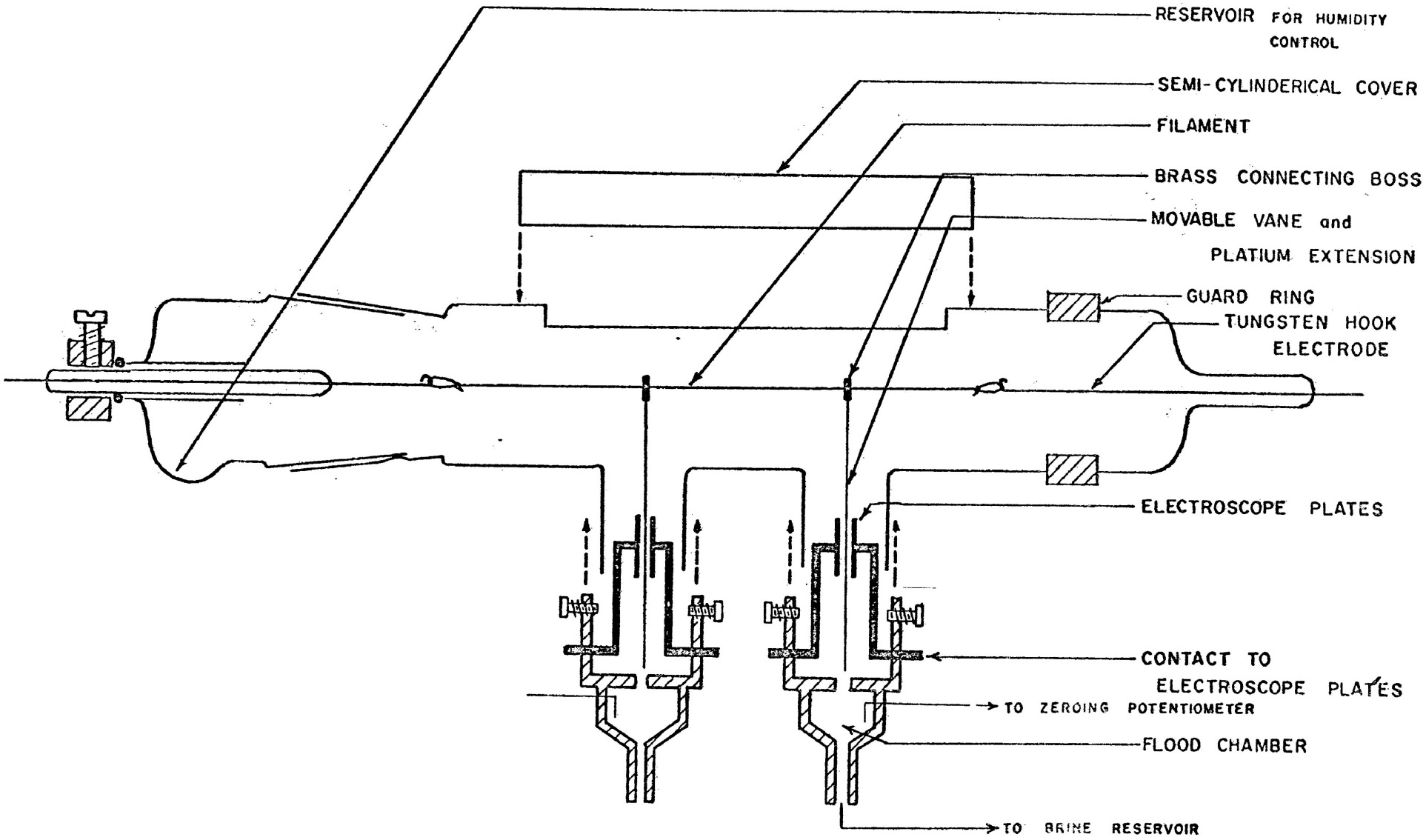

Fig. 2·8

ESSENTIAL FEATURES of NULL DETECTOR and FILAMENT HOLDER

upper extension of the vane was again attached to the string with a brass boss while the lower extension was soldered to a short length of 10 mil platinum wire which extended into a chamber that could be flooded with salt water. The brine, when it filled the flood chamber, was electrically connected to the centre tap of the respective zeroing potentiometer (see Fig. 2.9) and presented a negligible resistance when the leaf of the electroscope was discharged for purposes of zeroing. When the brine in the flood chamber was drained off the voltage probe was suspended freely presenting a resistance to leakage currents which approached infinity.

When attempts were made to determine voltages along the string it was found that due to the small currents (about 10^{-11} amps) and the capacitance of the electroscope which was about 10pf., the charging time of the null detector was many minutes. Reasonable results however, could be obtained and a typical set of observed balancing voltages is illustrated by Fig. 2.10. These data suggest the true probe voltage is somewhat above 460 v. while the assumption that the voltage distribution is linear predicts a value of 494 v. for this probe setting. The balancing voltages with the switch, s, in the balance position were low until the brine-filled flood chamber was evacuated indicating high leakage currents from the probe to ground through the standard insulation.

It is seen from Fig. 2.10 that some fifty minutes were required

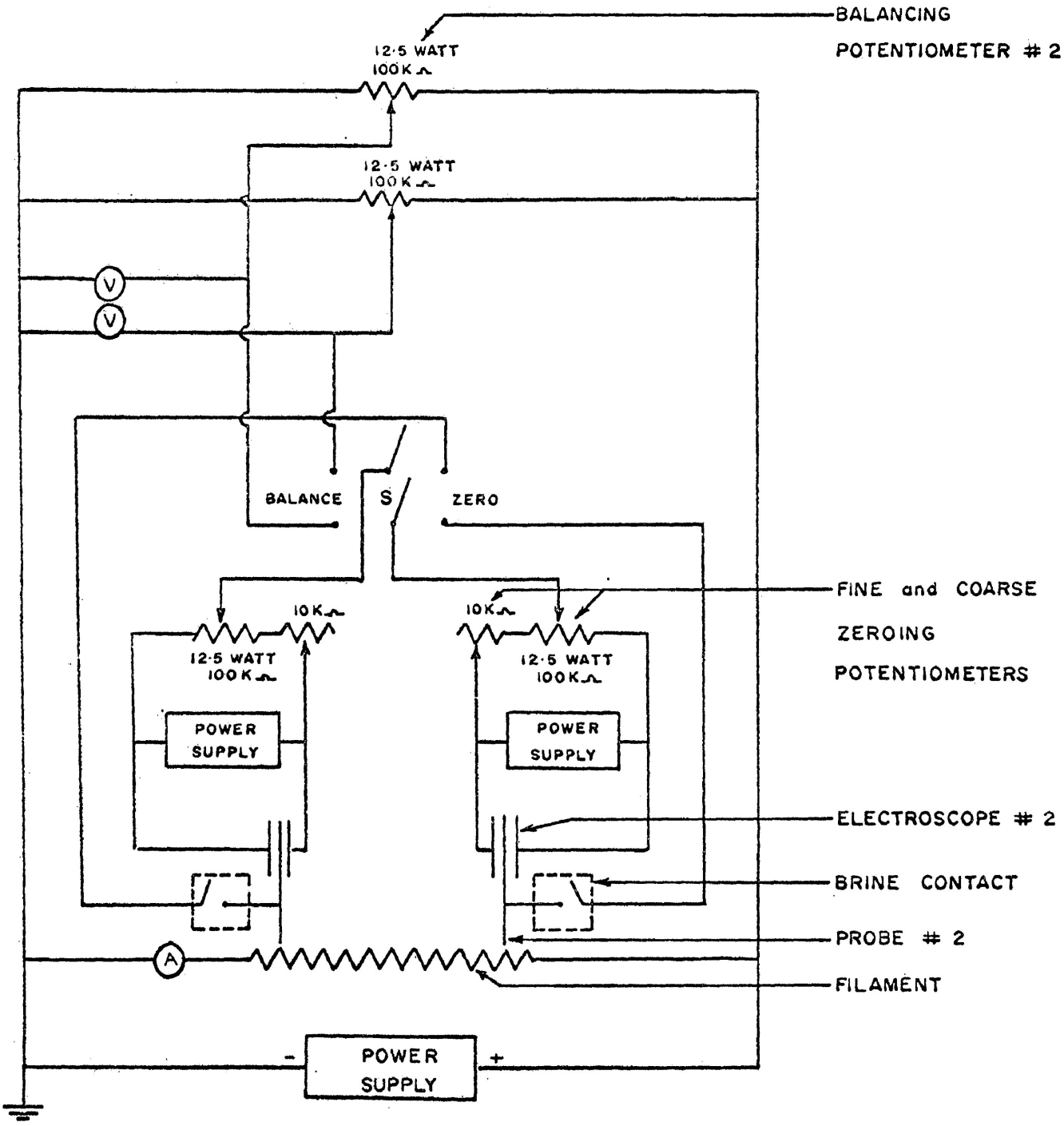

Fig. 2·9

CIRCUITRY FOR MULTI-PROBE MEASURING SYSTEM

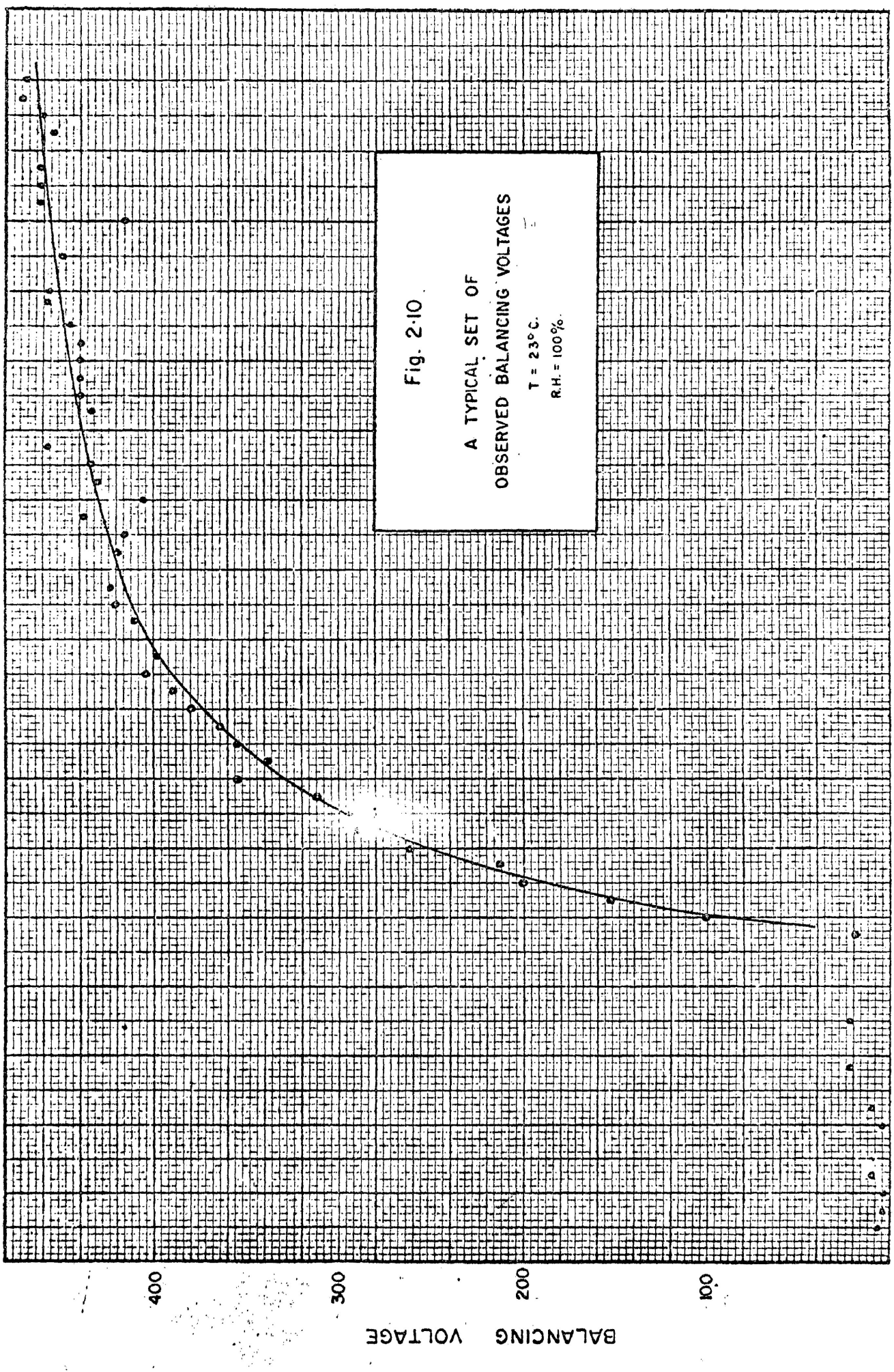
Fig. 2·10
A TYPICAL SET OF
OBSERVED BALANCING VOLTAGES
T = 23°C.
R.H. = 100%
BALANCING VOLTAGE
400
300
200
100
0
8
16
24
32
40
48
56
64
72
TIME (min.)

before reasonably steady balancing voltages were obtained and this rather long response time was confirmed in several other voltage determinations. To combat this effect the capacitance of the null detector was decreased by lowering the rigid plates with respect to the suspended vane. Comparison of voltage measurements for the detector at maximum and half-maximum capacitance is illustrated in Figs. 2.11 to 2.14. Clearly the response is greatly improved but it is at the expense of the sensitivity of the detector as is shown by the rather wide variations in readings in Fig. 2.12 and 2.14 as compared to the close grouping in Figs. 2.11 and 2.13. These two voltage determinations of each probe suggest that the results are indeed indicative of the true voltage on the string but the reproducibility was not good and was generally poorer than is indicated by these figures. The results of further voltage measurements which were made with the capacitance at a maximum showed a similar increase in balancing voltage with time. In two diffferent cases the positions of the two probes were arbitrarily set and the potentials determined several times. The voltage observations one hour after the vane was allowed to charge are tabulated in Tabs. 2.4 and 2.5. In the former set of experiments the two probe voltages were observed separately while in the latter they were read simultaneously.

It is evident that the observed values are often lower than the values for a linear voltage distribution which suggests the presence of a small amount of positive space charge. However, in view of the wide

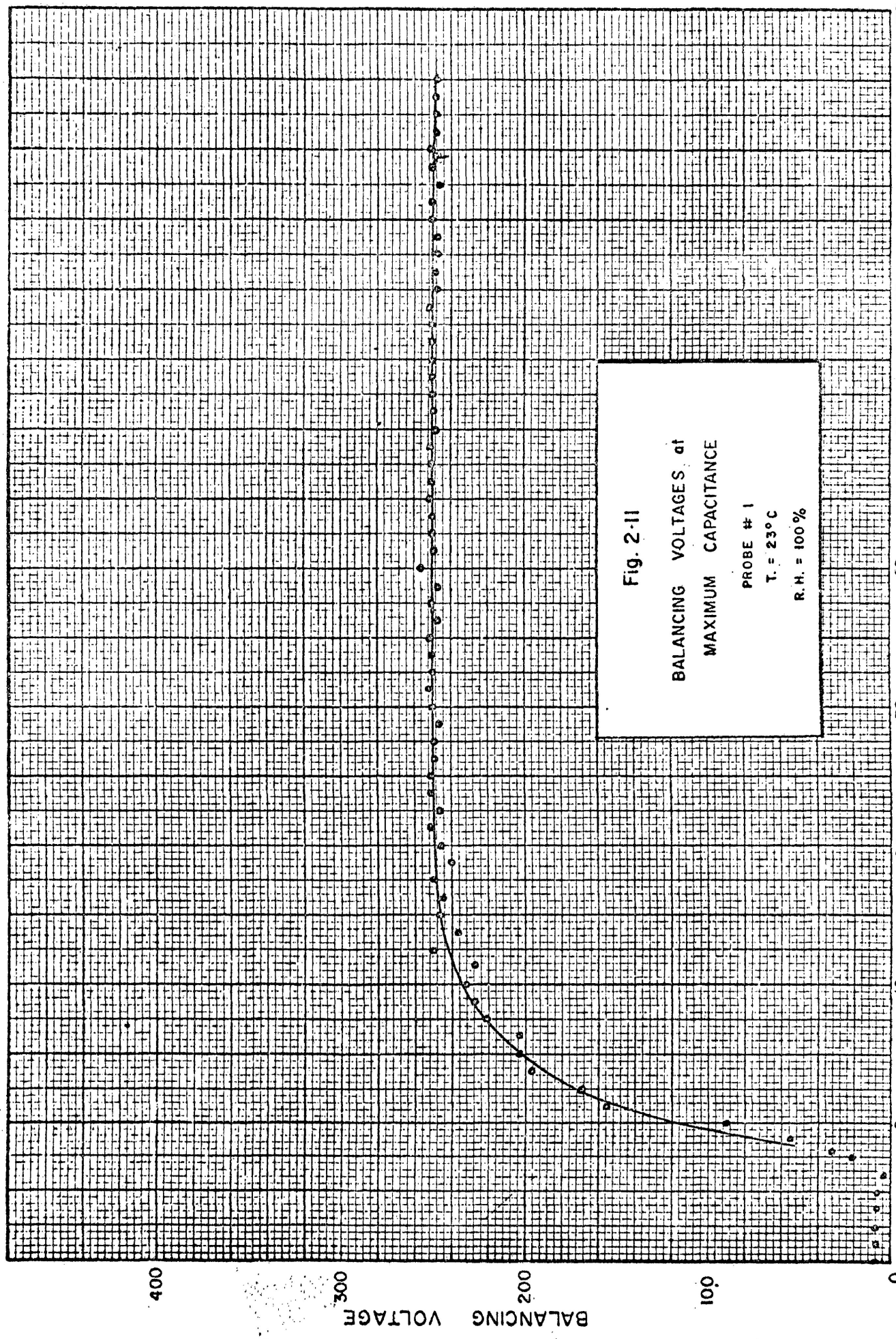
BALANCING VOLTAGE
400
300
200
100
0
8
16
24
32
40
48
56
64
72
TIME (min.)
Fig. 2-11
BALANCING VOLTAGES at
MAXIMUM CAPACITANCE
PROBE # 1
T. = 23°C
R.H. = 100%

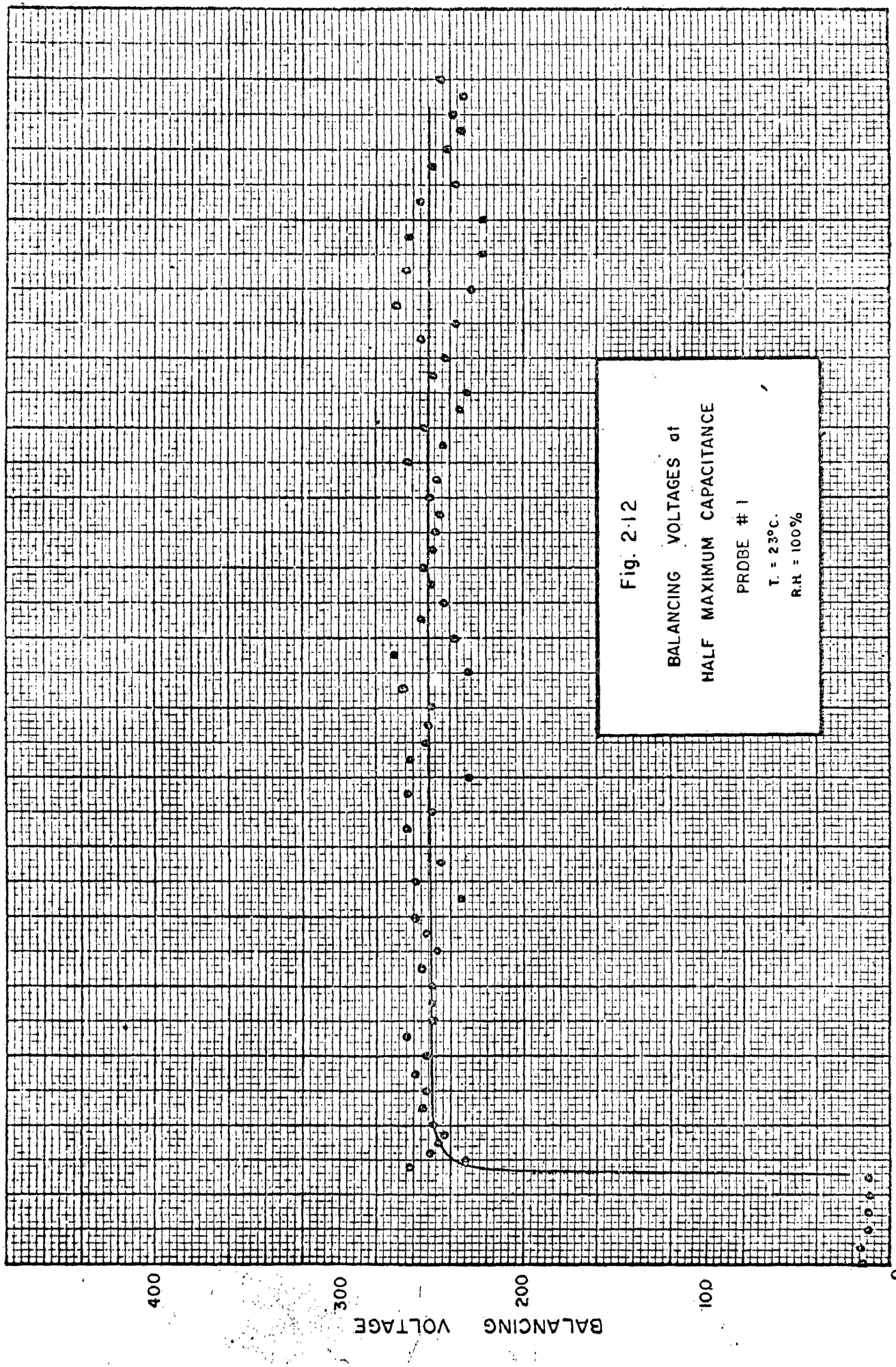
BALANCING VOLTAGE
400
300
200
100
0
8
16
24
32
40
48
56
64
72
TIME (min.)
Fig. 2·12
BALANCING VOLTAGES at
HALF MAXIMUM CAPACITANCE
PROBE # 1
T. = 23°C.
R.H. = 100%

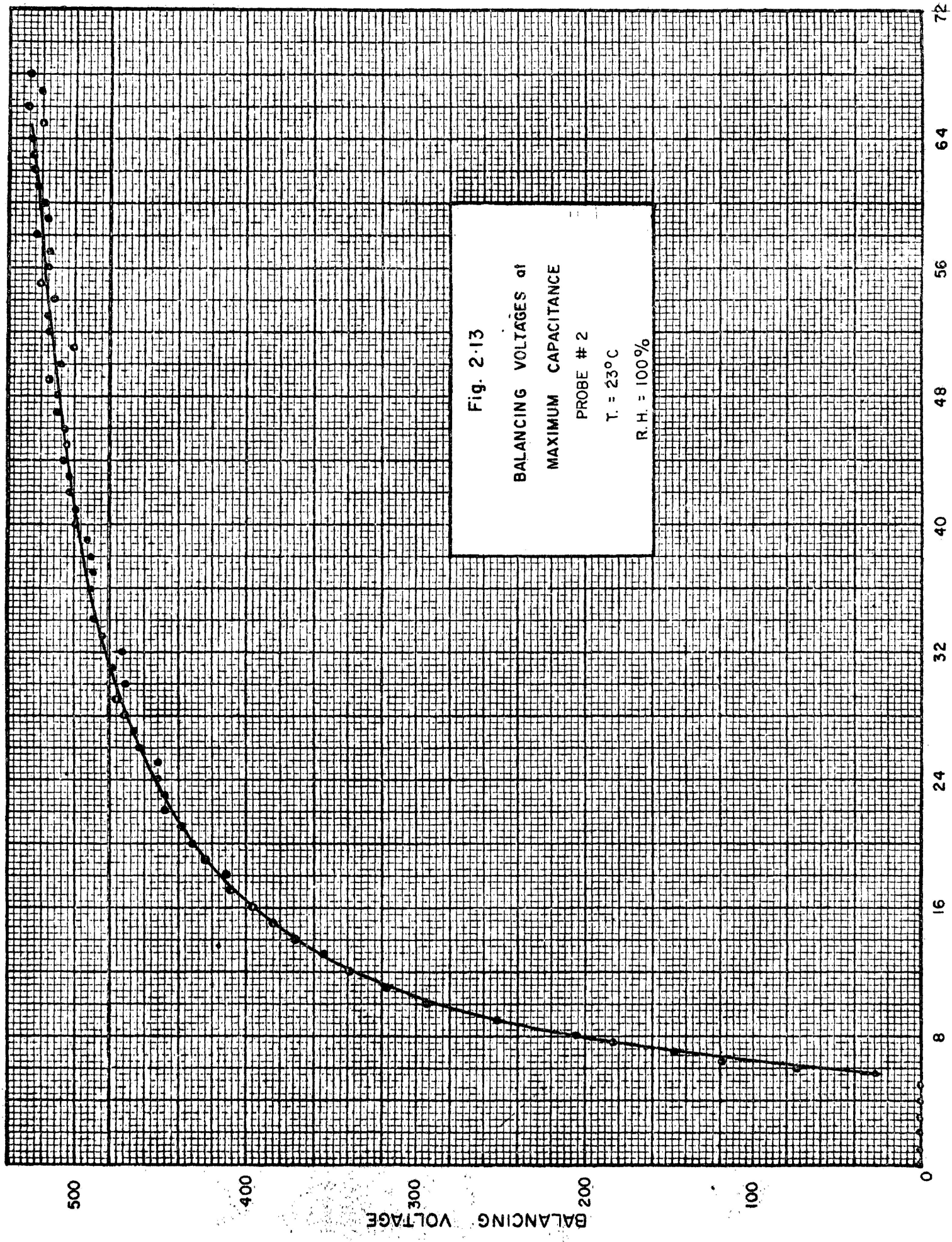
Fig. 2·13
BALANCING VOLTAGES at
MAXIMUM CAPACITANCE
PROBE # 2
T. = 23°C
R.H. = 100%
BALANCING VOLTAGE
500
400
300
200
100
0
8
16
24
32
40
48
56
64
72
TIME (min.)

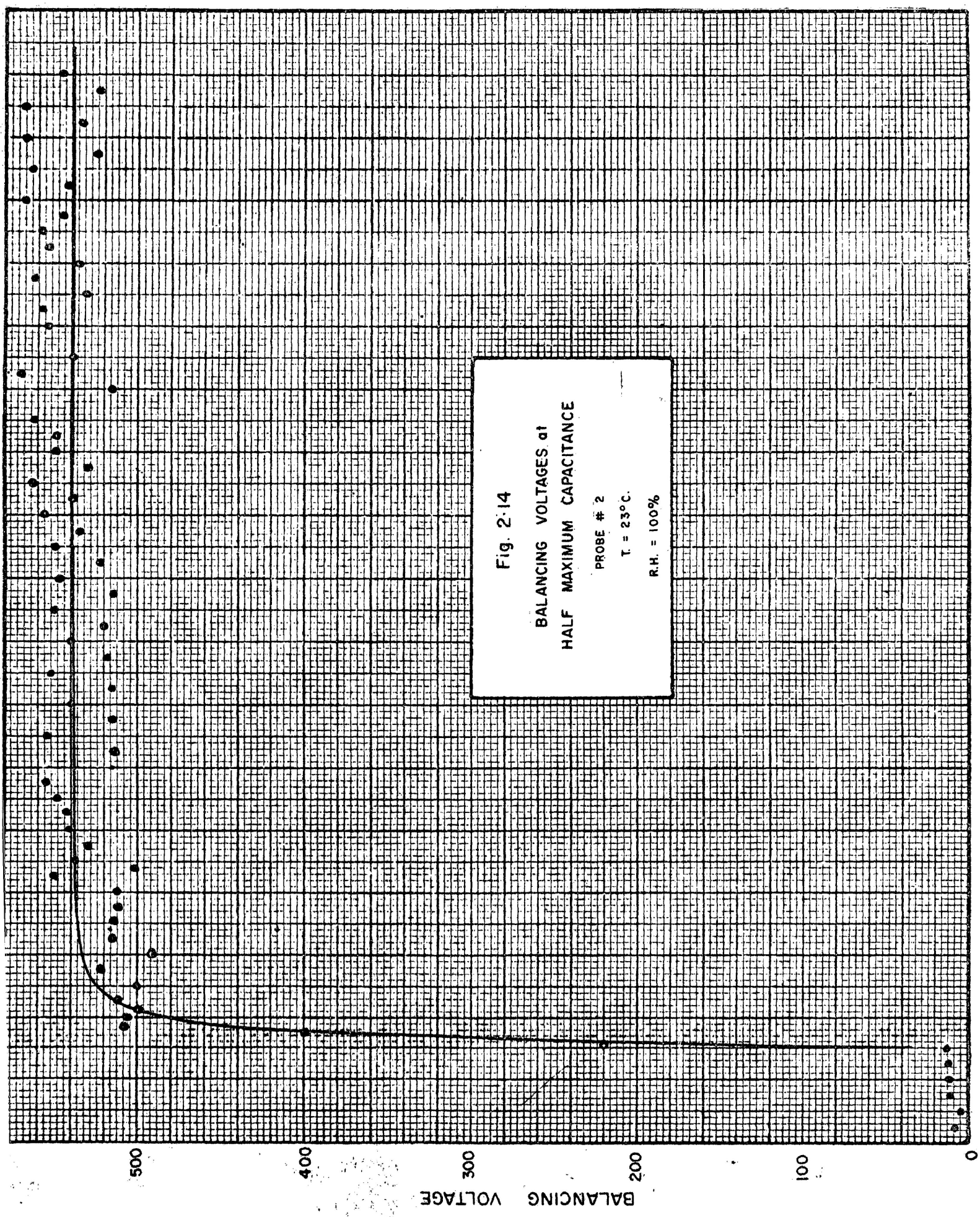

Fig. 2·14

BALANCING VOLTAGES at
HALF MAXIMUM CAPACITANCE

PROBE # 2
T. = 23°C.
R.H. = 100%

spread in the data the evidence is not conclusive.

EXPERIMENT NUMBER	VOLTAGE OF PROBE #1 AFTER 1 HOUR	VOLTAGE OF PROBE #2 AFTER 1 HOUR
1	242	470
2	300	470
3	250	500
4	250	530
5	230	530
6	230	520
7	250	510
8	-	490
AVERAGE	250	502
EXPECTED VALUE BASED ON LINEAR VOLTAGE DISTRIBUTION	271	509

TABLE 2.4

INDIVIDUAL DETERMINATIONS OF PROBE VOLTAGE

It should be noted that for these measurements 700 v. were invariably applied to the ends of the string which was kept in an atmosphere of 100% relative humidity. The voltage measurements were usually made when the field had been applied to the string for not more than four hours and typical current time curves (see Fig. 2.5) indicate that the polarization process has barely begun; thus a deviation from a linear voltage distribution may in any event be small. It would seem a simple matter to wait

longer before beginning the voltage measurements, however, difficulties are invariably experienced not only in setting up the rather delicate null detector but also in keeping it

EXPERIMENT NUMBER	VOLTAGE OF PROBE #1 AFTER 1 HOUR	VOLTAGE OF PROBE #2 AFTER 1 HOUR
1	285	670
2	305	670
3	270	630
4	260	610
5	250	540
6	220	530
AVERAGE	265	606
EXPECTED VALUE BASED ON LINEAR VOLTAGE DISTRIBUTION	309	618

TABLE 2.5

SIMULTANEOUS DETERMINATIONS OF PROBE VOLTAGE

operational for the extended periods of time required for the slow polarization process.

It is clear that due to the extremely high resistance to leakage currents, the method which has been described herein has a great scope for applications to insulation testing; however, further refinements are obviously necessary before highly reproducible results and conclusive evidence can be obtained.

CHAPTER III

RESULTS AND DISCUSSION OF STUDIES ON CAPACITOR TISSUE

(i) INTRODUCTION

In view of the difficulties which were experienced in obtaining meaningful data from the measurements on nylon filament, it is a logical development to use a system which is more amenable to quantitative interpretation. Such a system is naturally provided by a metal- insulator- metal (MIM) sandwich arrangement, reference to which has already been given in Chapter I. The basic advantages of this system are:

(i) a more satisfactory experimental arrangement wherein the physical dimensions of the sample permit the application of a wide range of fields across the specimens with relatively low voltages.

(ii) most theoretical models have been developed with reference to systems in the MIM sandwich form. It can be hoped that this arrangement will facilitate better description of the observed parameters.

This method of investigation of electrical properties has been extensively used to study a variety of organic materials especially polymers; for example polyamides (McColl and Anderson[21]) polyethyleneterephthalate (Lengyel[19], Lilly and McDowell[20], Amborski[1], Inuishi and Powers[11]), polytetraflouroethylene (Lilly and McDowell[20]) polyvinylformal (Lengyel[19]). Despite the availability of a considerable amount

of data on these materials, the interpretation has been rather conflicting. In the present work to be described, electrical measurements have been made on condenser tissue paper, which is, essentially, a polymer containing ring shaped glucose molecules, in the hope of understanding some of the basic mechanisms.

(ii) EXPERIMENTAL

Samples were cut from rolls of capacitor tissue obtained from the Peter J. Schweitzer Division of the Kimberly Clark Company with thicknesses varying from 0.2 mil to 1 mil. A few supplementary experiments were conducted on 0.17 mil samples from the Weyerhanser Company. The general experimental arrangement, a schematic of which is given in Fig. 3.1, was similar to the set-up used by Lilly and McDowell[20]. Although some preliminary tests were done using 2cm square brass plates as electrodes, the major part of the work was carried out using brass as well as stainless steel discs. These electrodes which were 2 inches in diameter were enclosed with the sample between in a copper canister which acted as a good electrostatic shield. Temperature measurements were done in an oven manufactured by Associated Testing Laboratories Inc., (Wayne, N.J.). A set of brass rings were placed over the upper electrode to provide a uniform pressure on the sample. The temperature was monitored using a copper-constantan thermocouple placed between the brass rings coupled with a potentiometer and an electronic reference zero unit of Consolidated Ohmic Devices Inc. Well regulated voltages

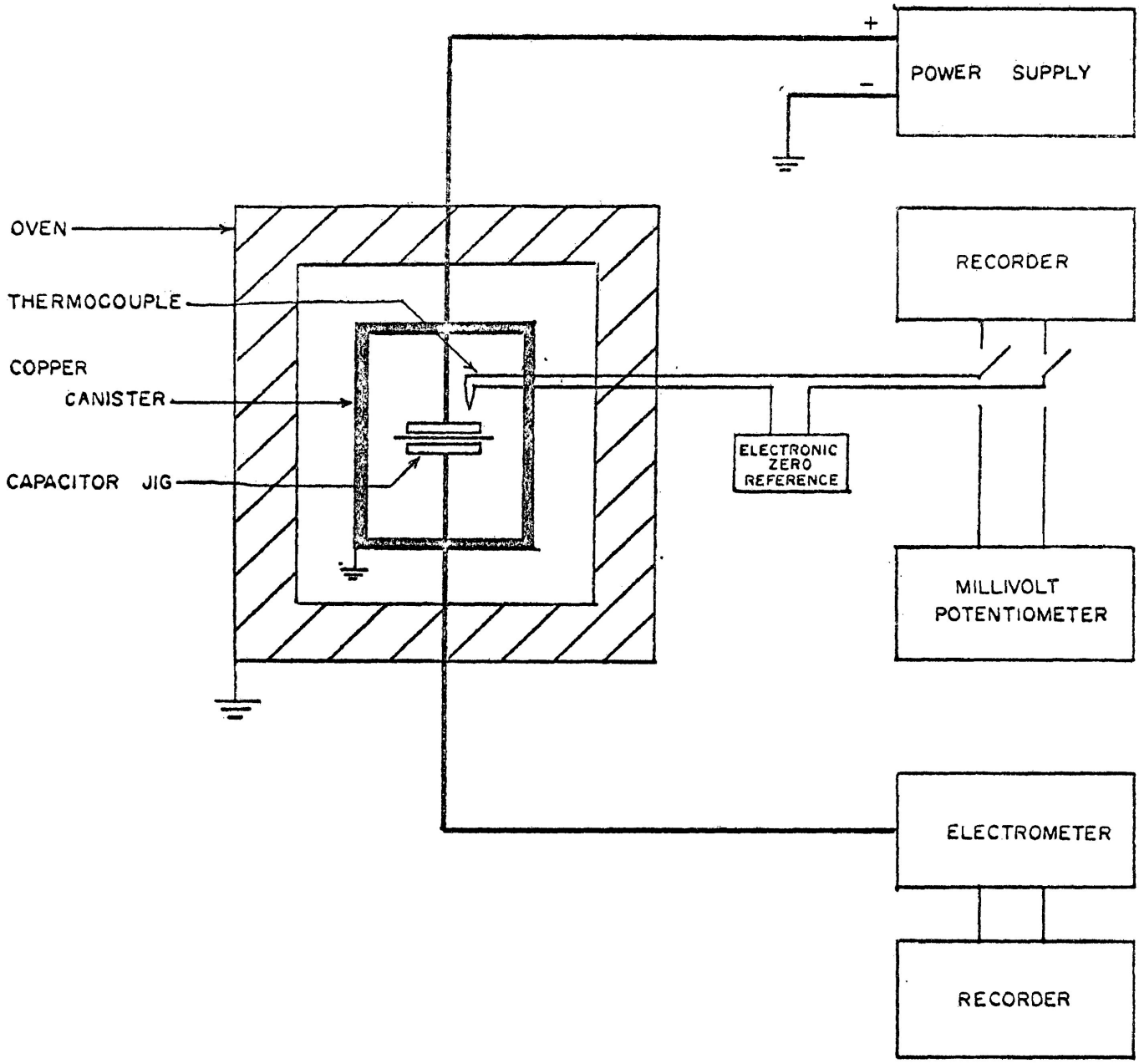

Fig. 3·1

SCHEMATIC DIAGRAM of APPARATUS

were applied with a Hewlett-Packard 6516A d.c. power supply while the current was determined using a Victoreen, Model 475B dynamic capacitor electrometer as well as a Keithley Model 610B electrometer. Currents over extended periods of time were observed using suitable recorders. Special precautions were taken to see that all electrical connections and lead cables were well shielded and resistant to temperatures up to 200°C.

When a voltage step function is applied to an insulating material, a long term absorption current decays approximately according to

$$i = Kt^{-n}$$

as has been pointed out earlier. One also finds that at low temperatures and low voltages a considerable wait may be necessary before steady-state conditions are reached. In order to obtain reproducible results, one must expect that extensive standardization procedures need be followed, and to ascertain what procedures were necessary, some preliminary tests were undertaken.

Many dozens of samples were studied under a variety of conditions and in each case, the effects of time as well as the applied voltage were examined carefully. This was done with a view to not only establishing standardization conditions, but also to confirm that consistent and reasonable values, in keeping with what is known about similar systems, could be obtained. A typical example of such a set of pre-

liminary experiments is given in Table 3.1, while some highlights of the results for .35 mil tissue are given in Figs. 3.2 to 3.8

EXPERIMENTAL SPECIFICATION	PARAMETERS TESTED	VARIABLES
1) Arbitrary electrode pressure.	a) time constant (i) short time (ii) long time	Voltage
2) Sample as received	b) Dependence of steady-state current on applied voltage	Temperature
3) No electrical or Thermal history 4) No pre-treatment or conditioning	c) dependence of steady current on temperature	Voltage

TABLE 3.1

PRELIMINARY TESTS

In all these experiments the steady-state values of the current are the values which are observed from fifteen to twenty minutes after the application of the voltage.

In order to improve the reproducibility of the results, the effect of the history of the sample on the decay of the current with a constant

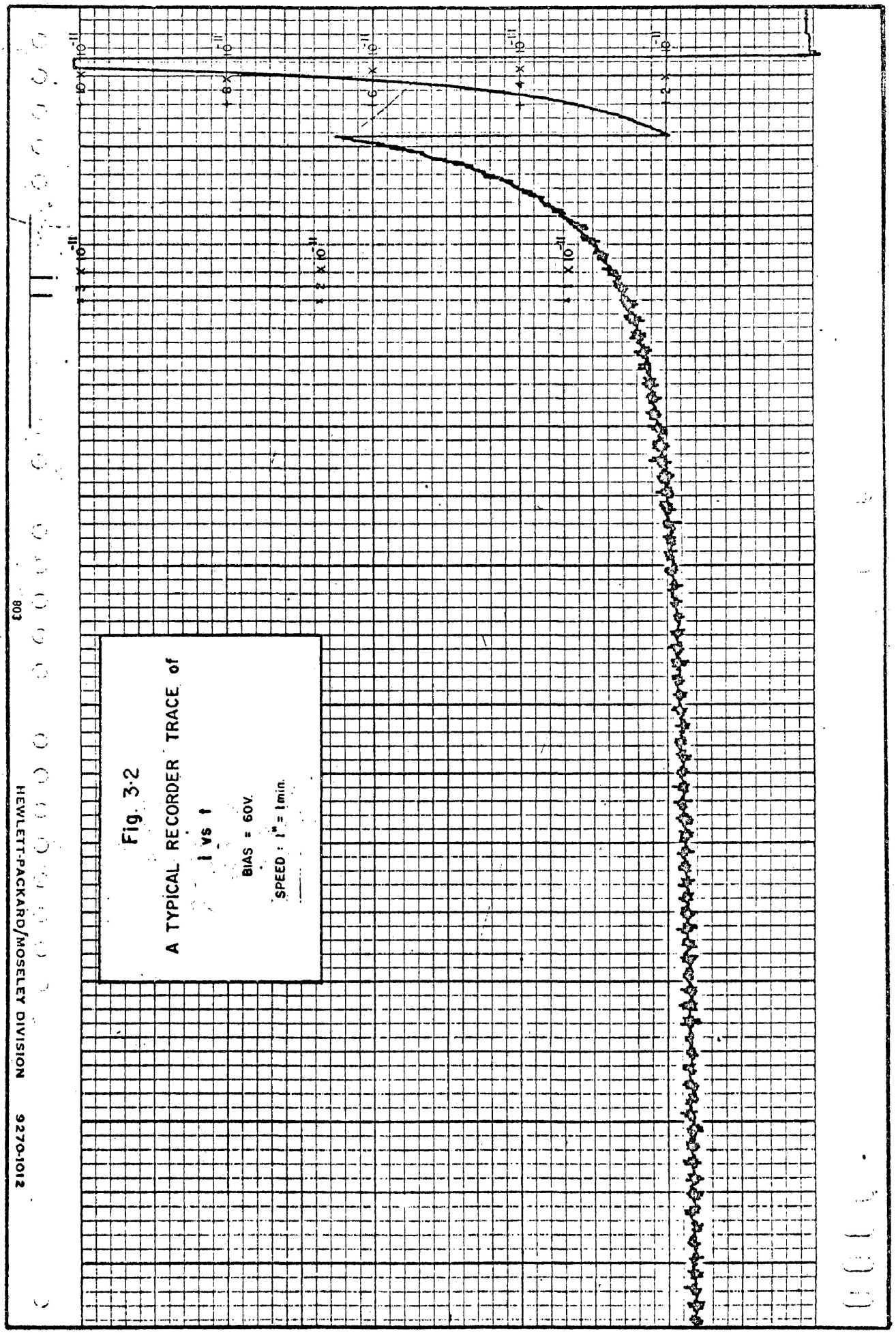
Fig. 3·2
A TYPICAL RECORDER TRACE of
I vs t
BIAS = 60V.
SPEED : 1" = 1 min.
HEWLETT-PACKARD/MOSELEY DIVISION
6270-1012

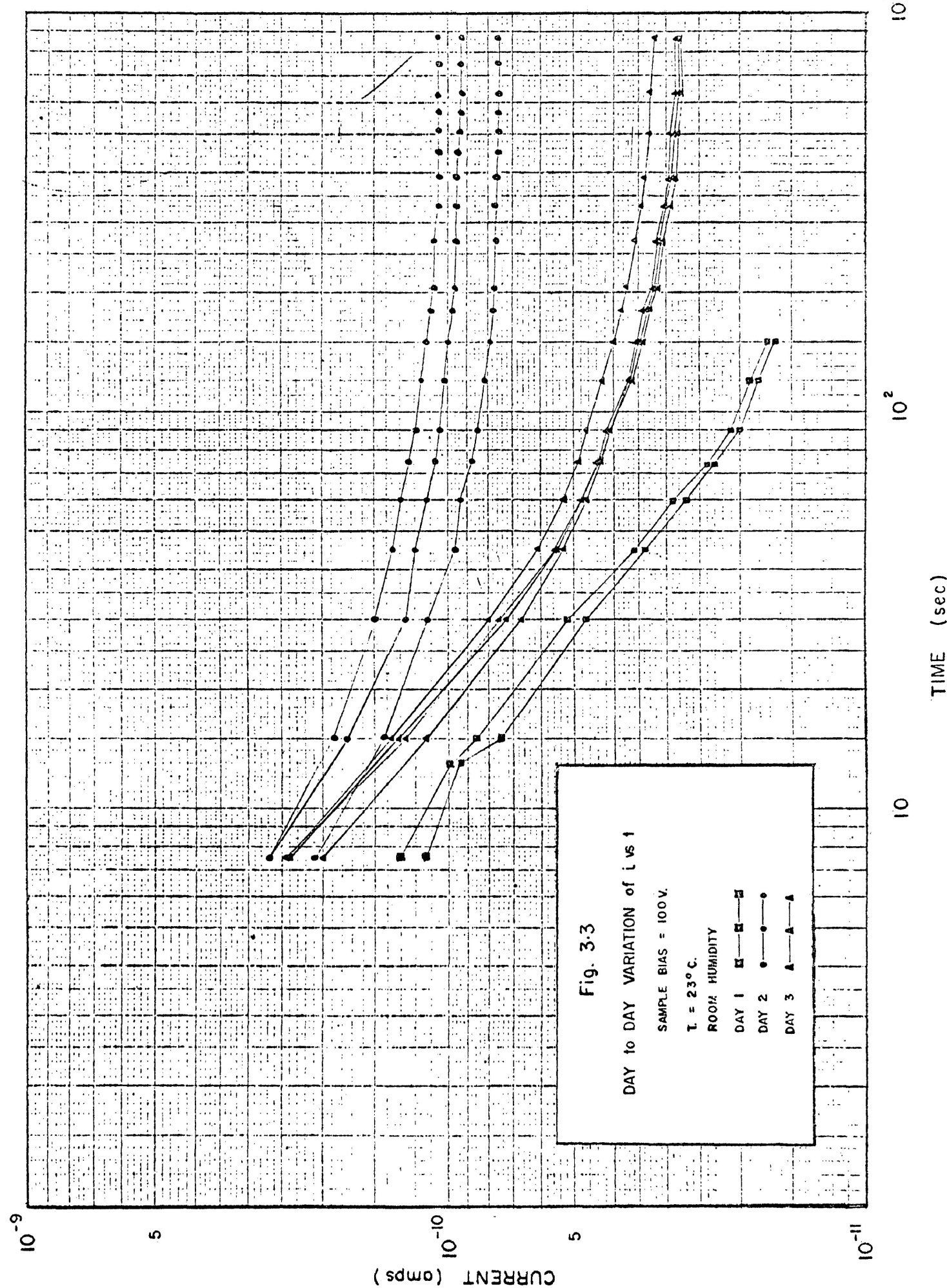
CURRENT (amps)
10^{-9}
5
10^{-10}
5
10^{-11}
10
10^{2}
10^{3}
TIME (sec)
Fig. 3.3
DAY to DAY VARIATION of i vs t
SAMPLE BIAS = 100 V.
T. = 23° C.
ROOM HUMIDITY
DAY 1
DAY 2
DAY 3

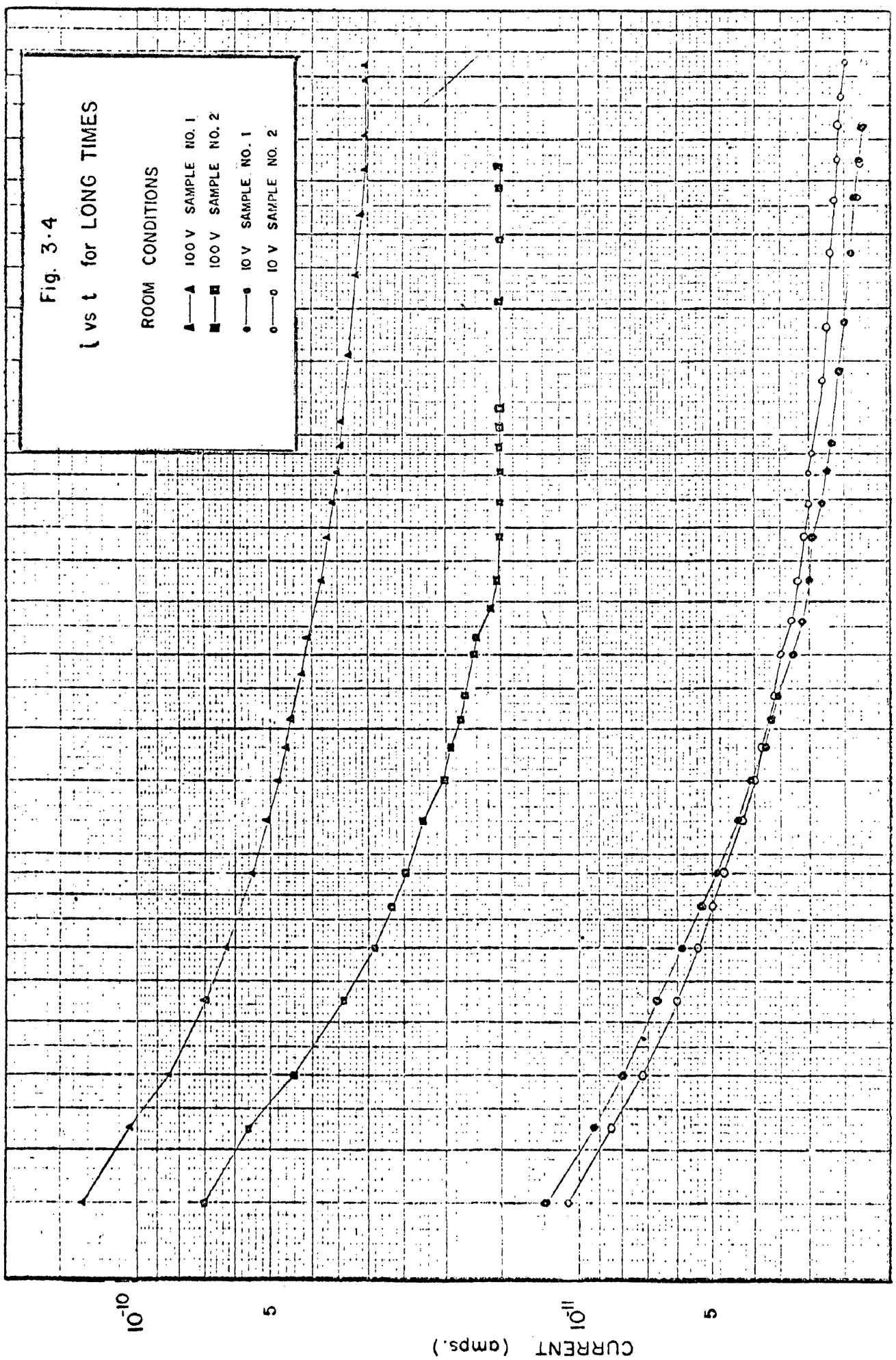
Fig. 3·4
i vs t for LONG TIMES
ROOM CONDITIONS
100 V SAMPLE NO. 1
100 V SAMPLE NO. 2
10 V SAMPLE NO. 1
10 V SAMPLE NO. 2
CURRENT (amps.)
10^{-10}
5
10^{-11}
5
10^{2}
10^{3}
10^{4}
TIME (sec.)

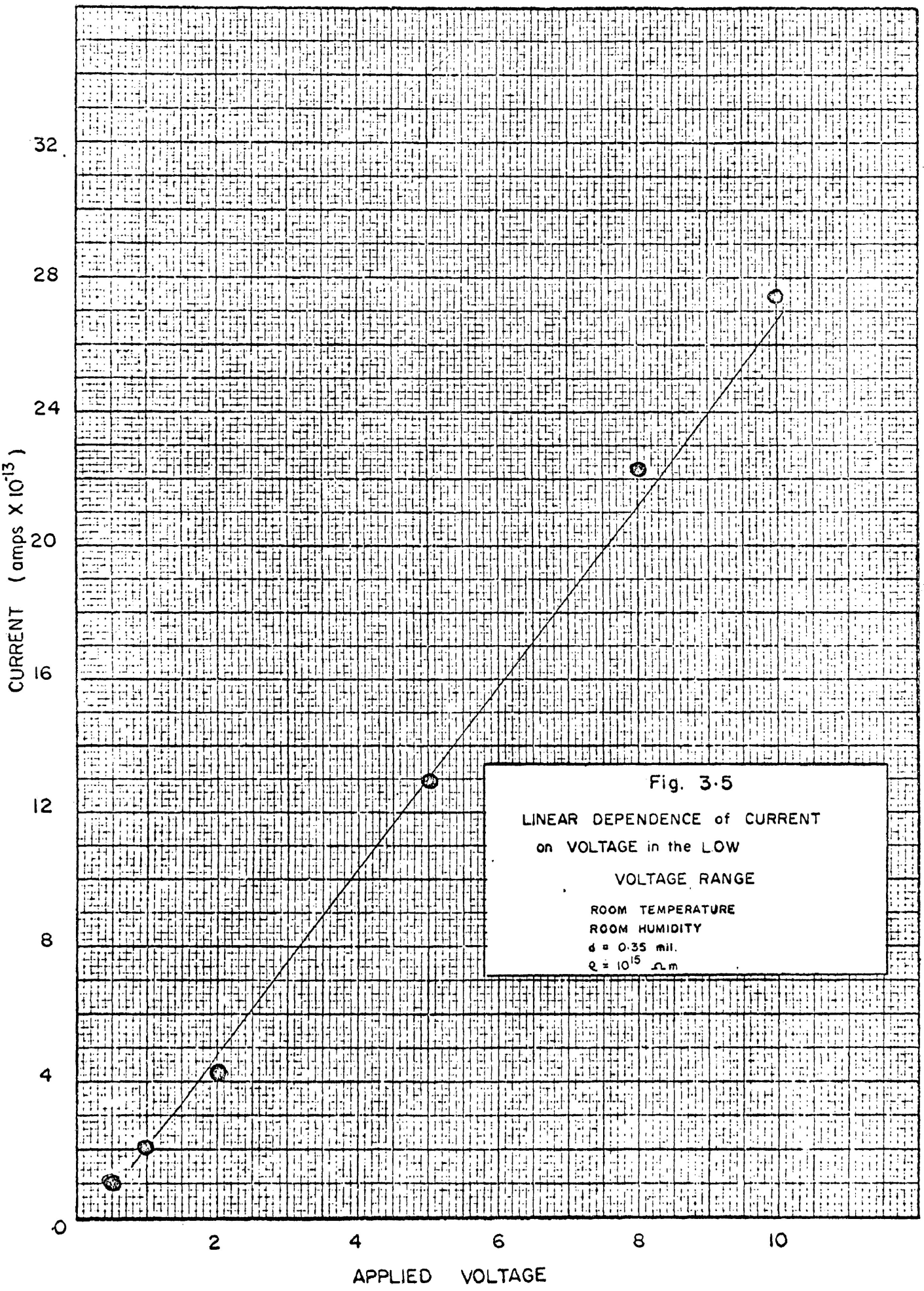

Fig. 3·5

LINEAR DEPENDENCE of CURRENT on VOLTAGE in the LOW VOLTAGE RANGE

ROOM TEMPERATURE
ROOM HUMIDITY
d = 0.35 mil.
$\varrho = 10^{15}$ Ω m

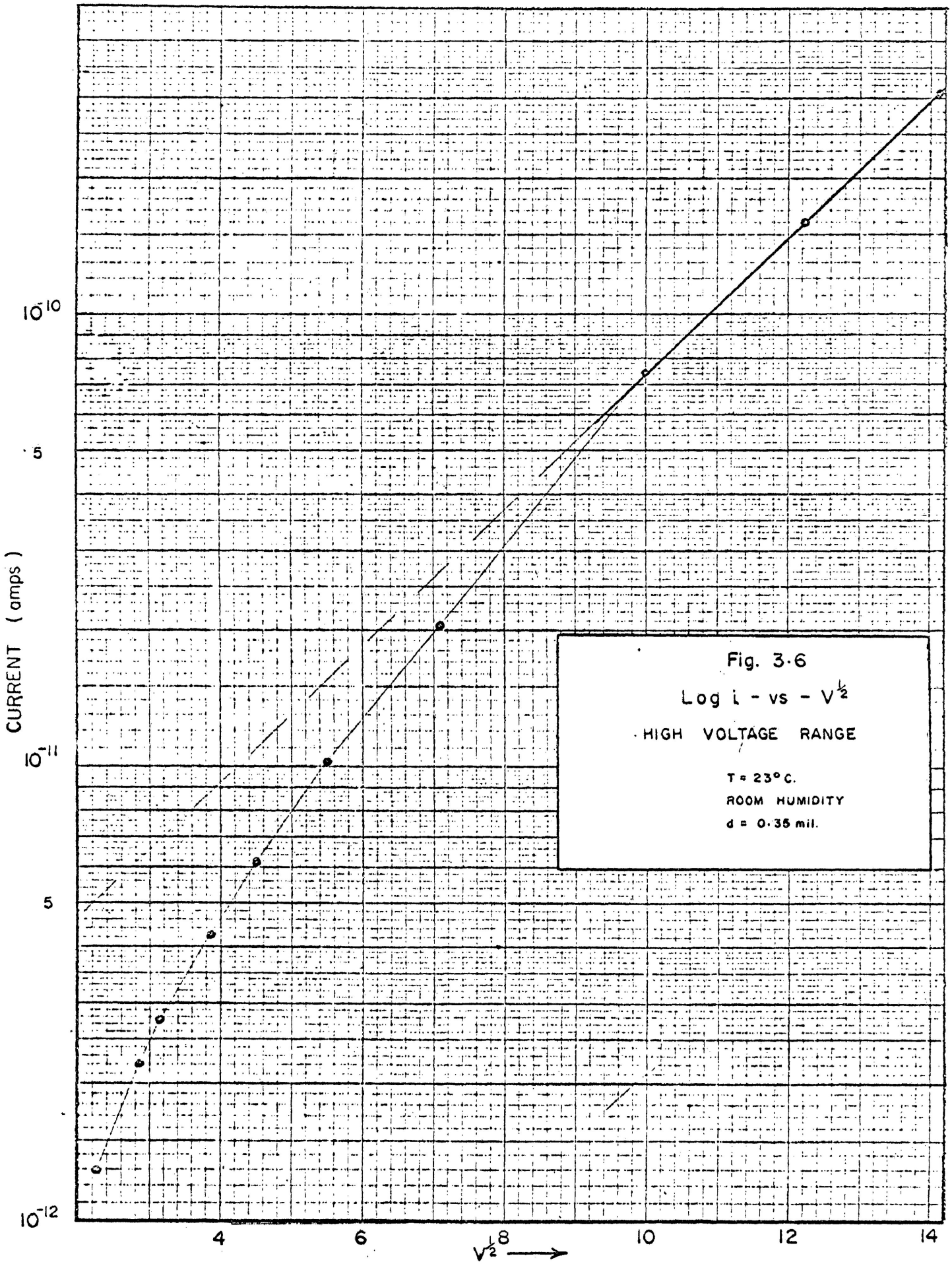

Fig. 3·6

Log i - vs - $V^{\frac{1}{2}}$

HIGH VOLTAGE RANGE

T = 23° C.

ROOM HUMIDITY

d = 0·35 mil.

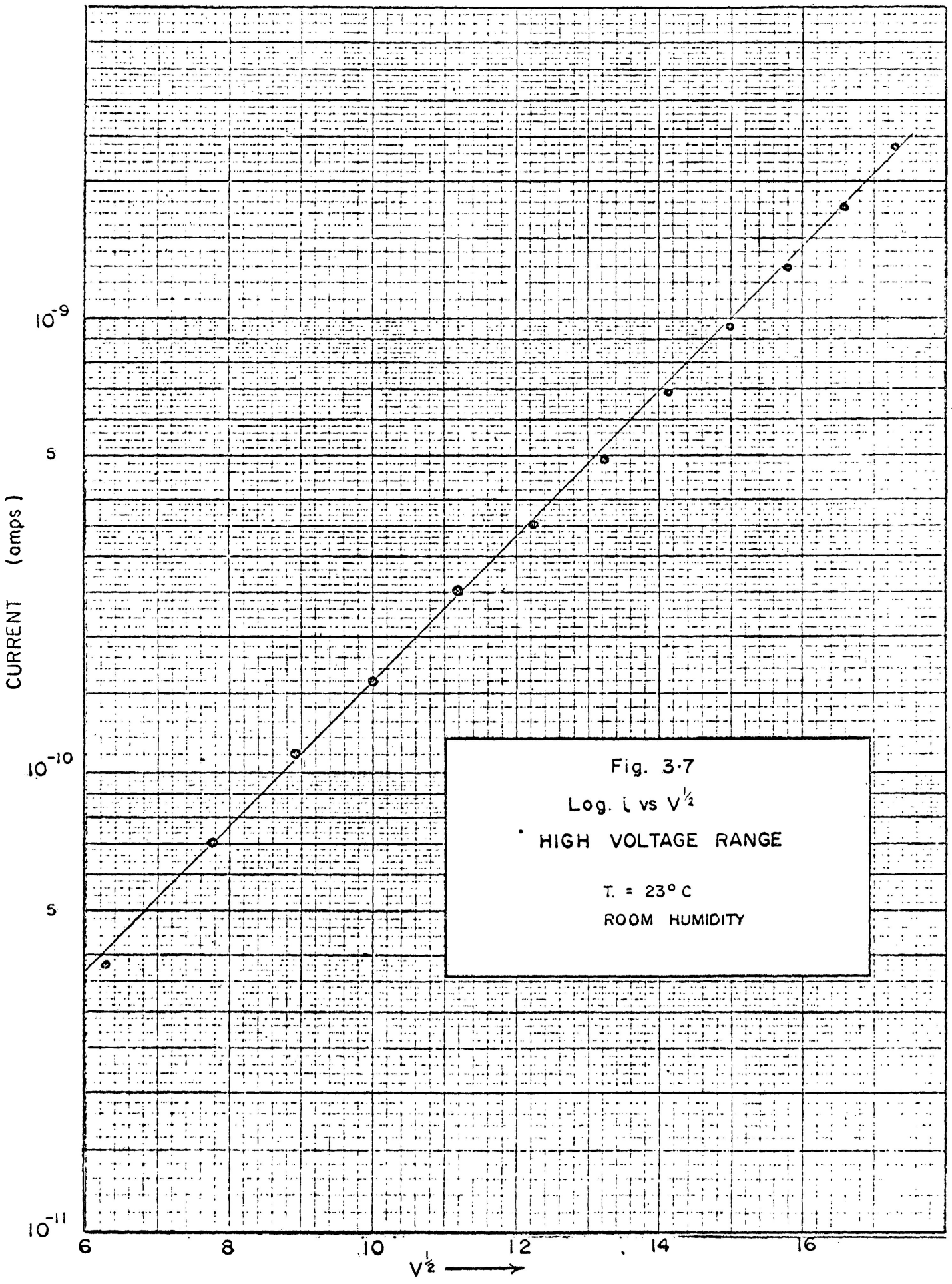

Fig. 3·7

Log. i vs $V^{1/2}$

HIGH VOLTAGE RANGE

T. = 23° C

ROOM HUMIDITY

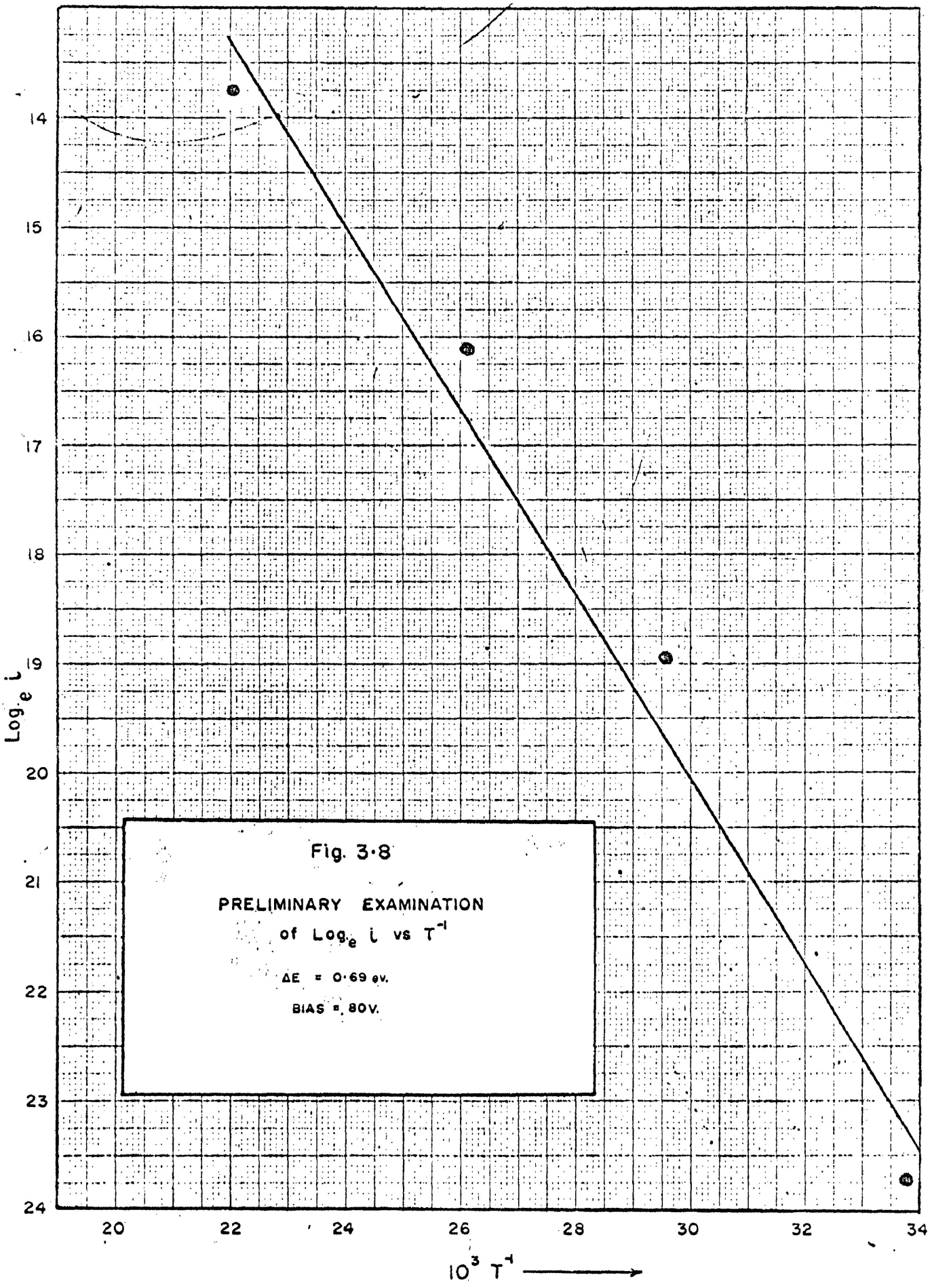

Fig. 3·8

PRELIMINARY EXAMINATION

of Log$_e$ i vs T^{-1}

ΔE = 0·69 ev.

BIAS = 80V.

applied voltage, namely 100 volts, was investigated for a number of samples. In all these experiments samples with no history were used as a basis of comparison for the data obtained from .35 mil samples with the following diverse conditioning:

(1) Condition at 300 v. for three hours at room conditions, then apply 100 v. Fig. 3.9

(2) Condition at 50 v. for one hour at room conditions, then apply 100 v. Fig. 3.10

(3) Voltage was increased from zero to 100 v. in 10 volt steps over 50 minutes at room conditions. Fig. 3.10

(4) Same as (3) except that sample is discharged for about 10 seconds before each voltage increase.

(5) Day to day variation of i - vs - t curve for samples stored in a $CaCl_2$ desiccator. Fig. 3.11

Some of the important results are given in the indicated figures. It was found that the electrical history did not appreciably affect the current values for times greater than twenty minutes, whereas desiccation as well as temperature conditioning had marked effects. Of special significance to the reproducibility is the desiccation of the sample as is indicated by a comparison of Figs. 3.3 and 3.11

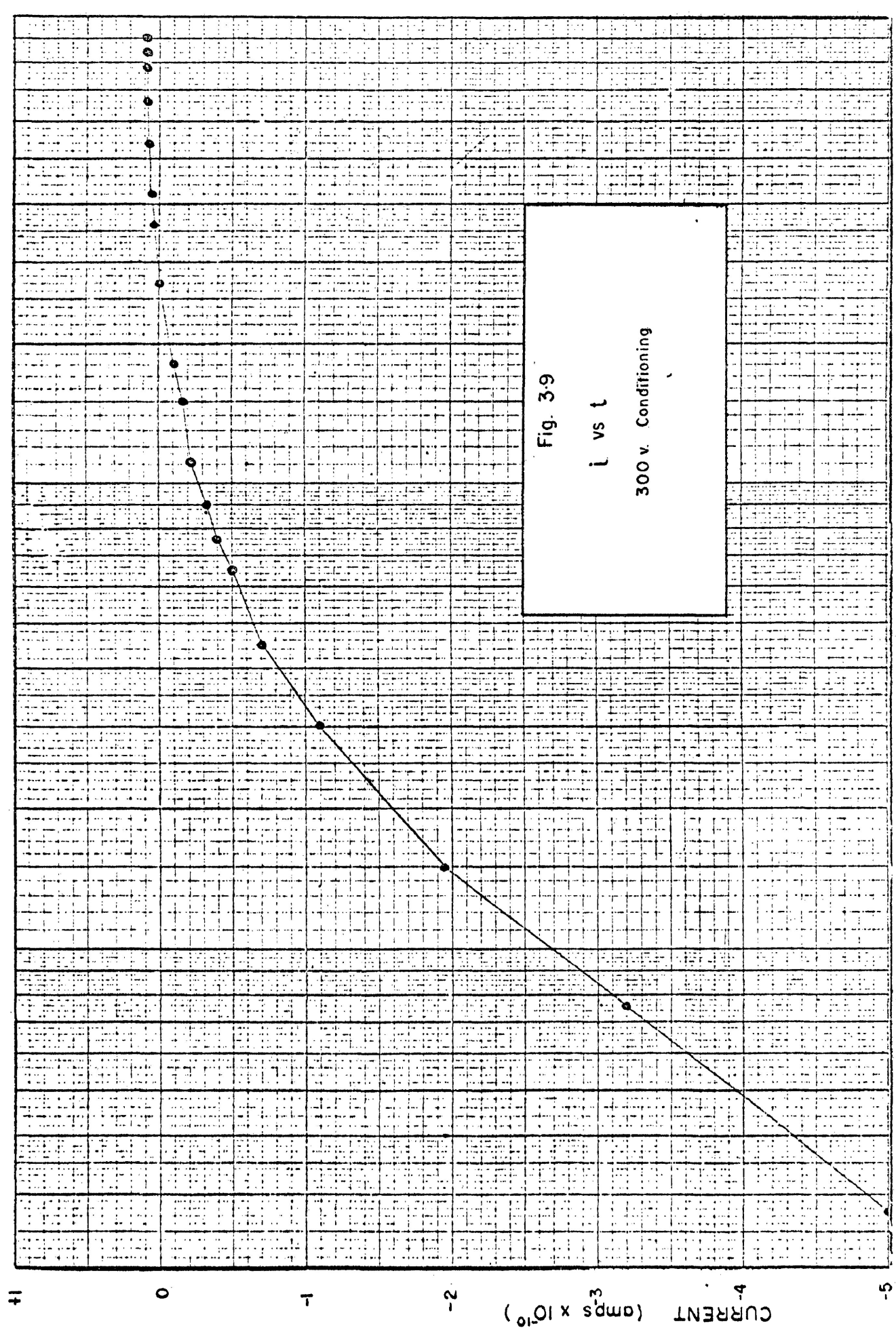
Fig. 3·9
i vs t
300 v. Conditioning
+1
0
-1
-2
-3
-4
-5
CURRENT (amps x 10⁻¹⁰)
10
10²
10³
TIME (sec.)

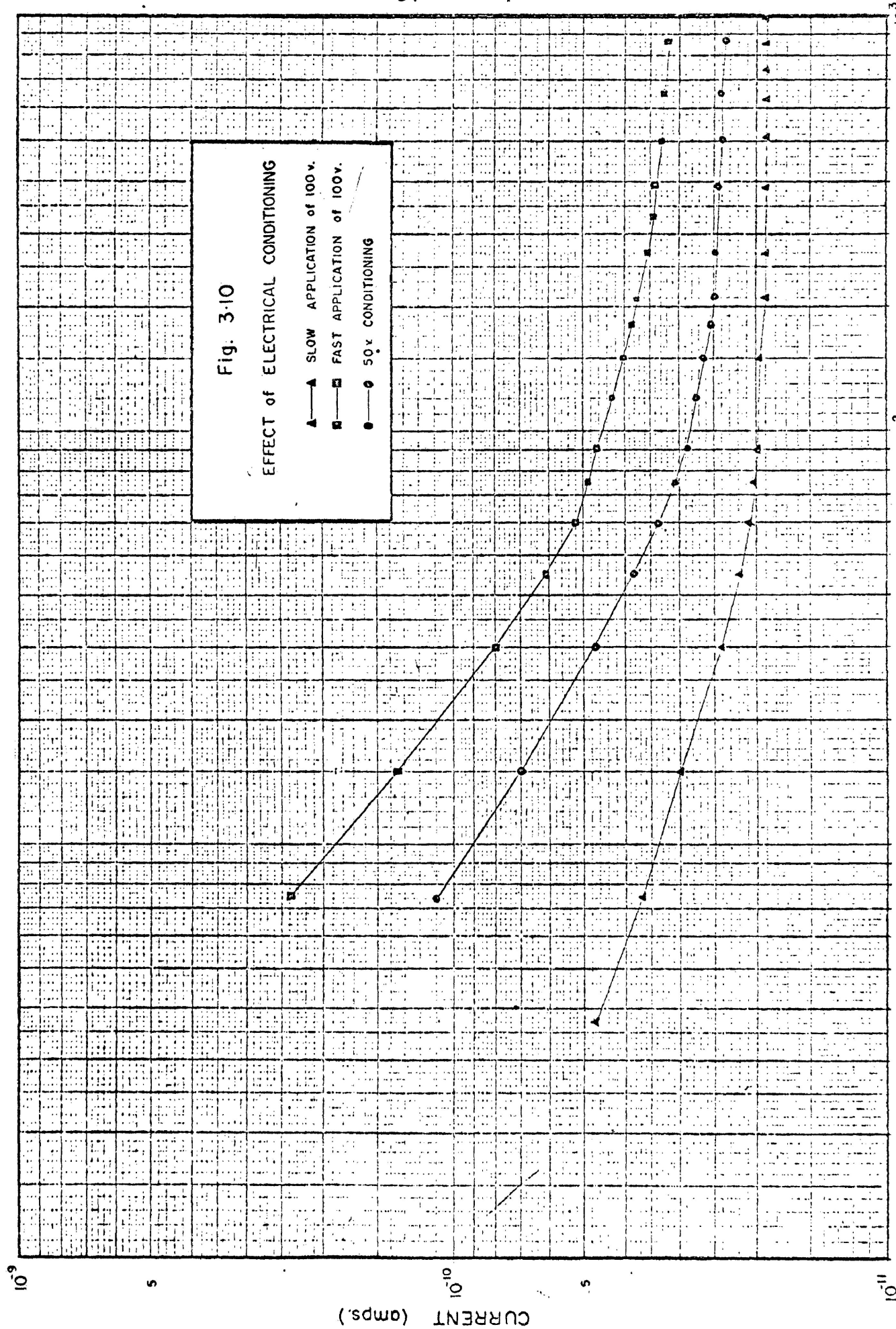
Fig. 3·10
EFFECT of ELECTRICAL CONDITIONING
SLOW APPLICATION of 100 v.
FAST APPLICATION of 100 v.
50 v CONDITIONING
CURRENT (amps.)
TIME (sec.)
10^{-9}
5
10^{-10}
5
10^{-11}
10
10^{2}
10^{3}

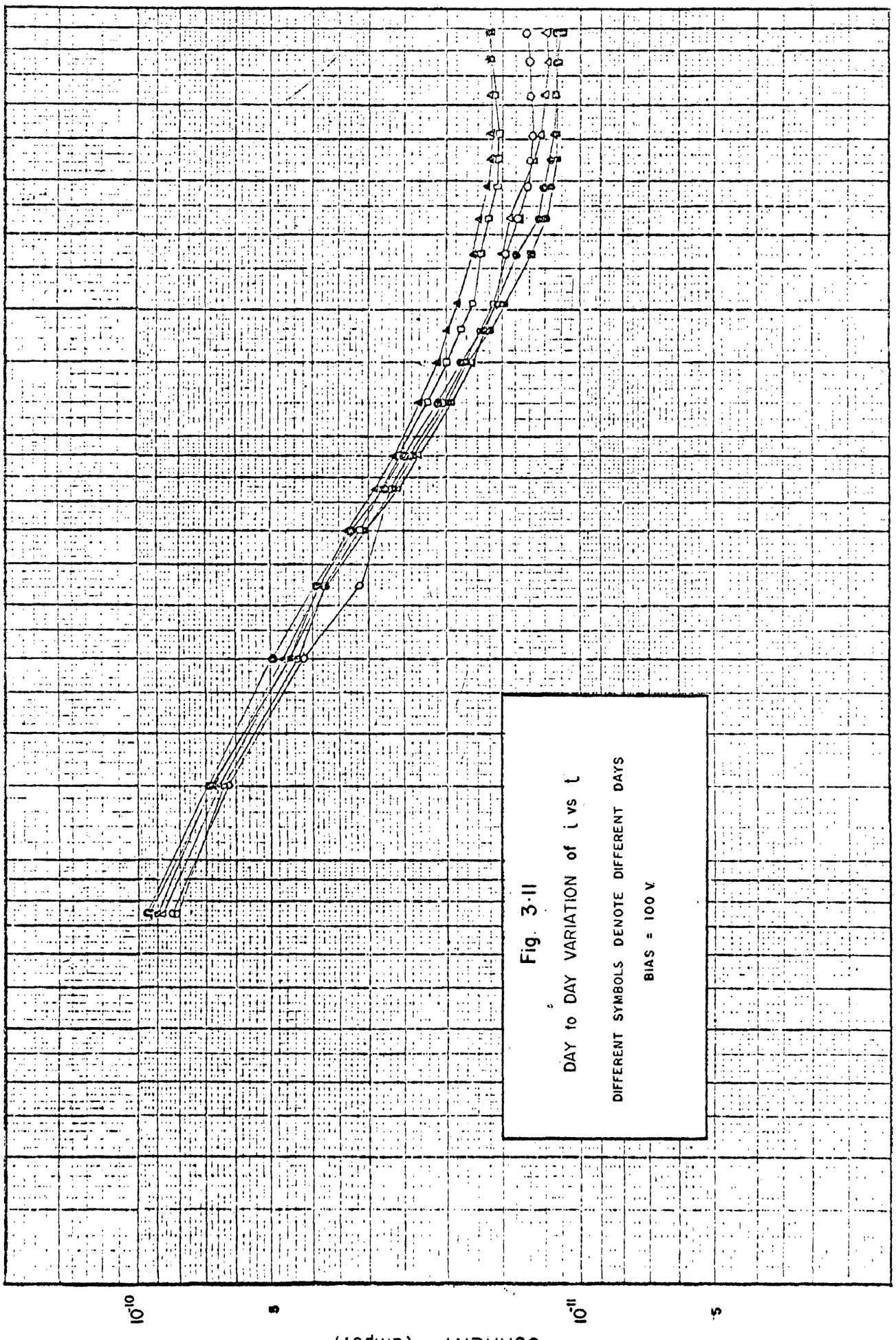

Fig. 3·11

DAY to DAY VARIATION of i vs t

DIFFERENT SYMBOLS DENOTE DIFFERENT DAYS

BIAS = 100 V.

On the basis of these experiments, the following conditioning and measuring procedure was proposed:

(1) Samples stored in desiccator.

(2) Desiccant in copper canister.

(3) Electrode pressure set arbitrarily at 325 gm. as regulated by weights No. 1 to No. 6.

(4) No thermal history

(5) Sample in canister one hour before application of voltage.

(6) Apply step potential

(7) Measure steady-state current.

In computing the steady-state values, it must be remembered that the presence of the so-called anomalous charging current which is commonly observed in insulating materials complicates the problem. The time required for the transient current to subside to a stationary value depends on the magnitude of the applied field, the temperature, and the material itself. It has been found that for capacitor tissue, the steady state is achieved most rapidly at high fields and high temperatures which is very similar to what has been observed for potassium halides[2], silicon oxide[6], and mylar[19]. However, at low voltages and low temperatures, the relaxation is a lengthy process. For

the case of mylar, Lengyel[19] observes an initial exponential decay which transforms into a hyperbolic decrease of the t^{-n} type (see Chapter I) before reaching steady-state conditions. In the present case, the initial relaxation is hyperbolic, while the onset of steady state seems to be manifested by a break from this relationship. (See for instance Fig. 3.11).

An alternate method for the computation of the steady-state current used by Lilly and McDowell[20] assumes the validity of the Superposition Principle as was discussed in Chapter I. The possibility of using this method in the present case was explored, but the method seems unsatisfactory since it is doubtful that the assumption concerning the validity of the Superposition Principle is tenable. In Figs. 3.12 to 3.16 for room temperatures, the difference between the charging and discharging currents is relatively constant for undesiccated samples in agreement with the Superposition Principle, however, for desiccated samples, the principle is definitely invalid. In spite of these difficulties, it was found that reasonable results could be obtained by taking, for the steady-state values, the current values after ten minutes. The assumption seems plausible in view of the constancy of the slopes of the ln i - vs - $V^{\frac{1}{2}}$ curves for current values beyond this time. See Figs. 3.17 to 3.20. On this basis, studies were carried out on the tissue with reference to the current-voltage, current-

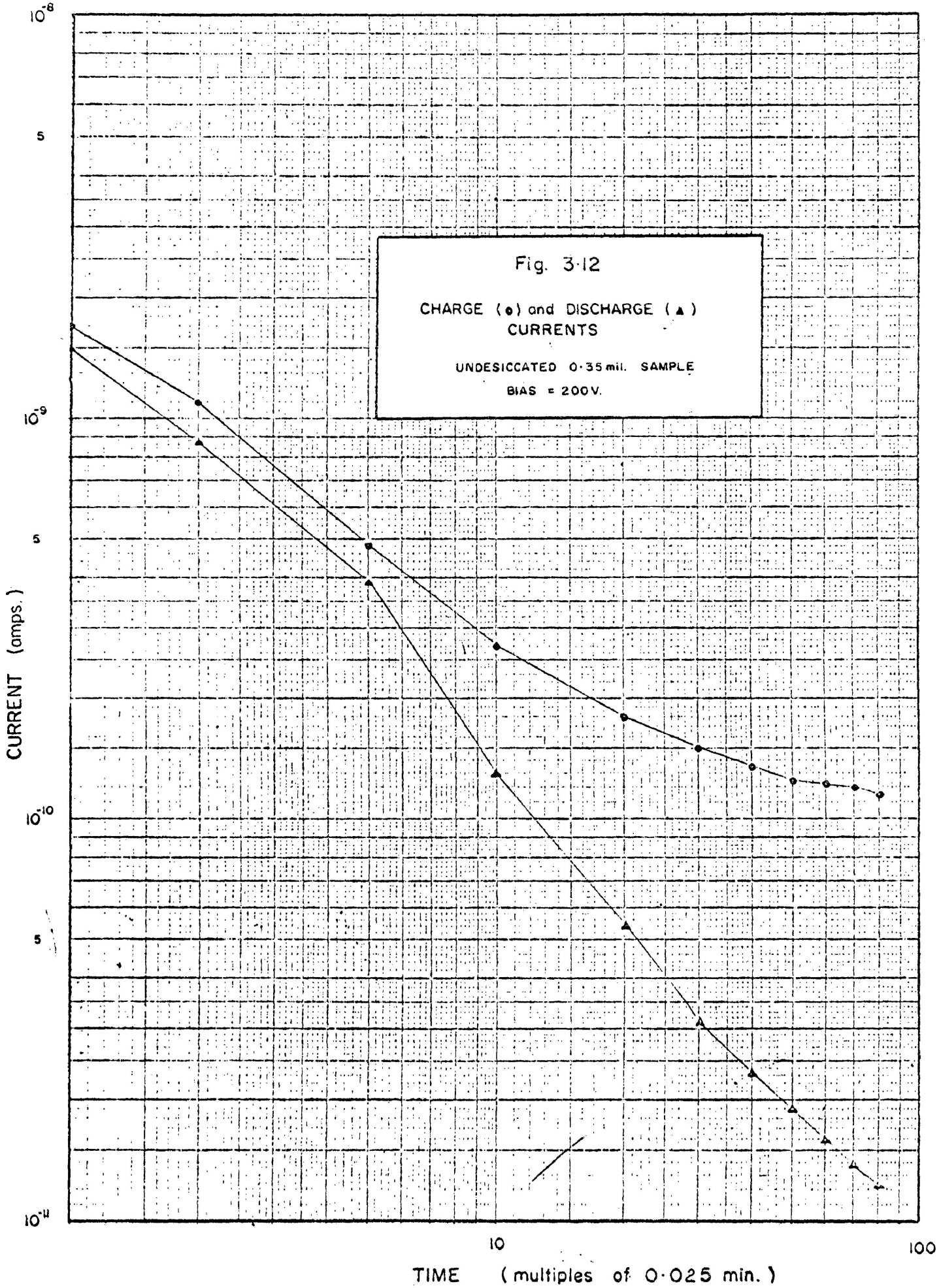
Fig. 3·12
CHARGE (●) and DISCHARGE (▲) CURRENTS
UNDESICCATED 0·35 mil. SAMPLE
BIAS = 200V.
CURRENT (amps.)
10^{-8}
5
10^{-9}
5
10^{-10}
5
10^{-11}
10
100
TIME (multiples of 0·025 min.)

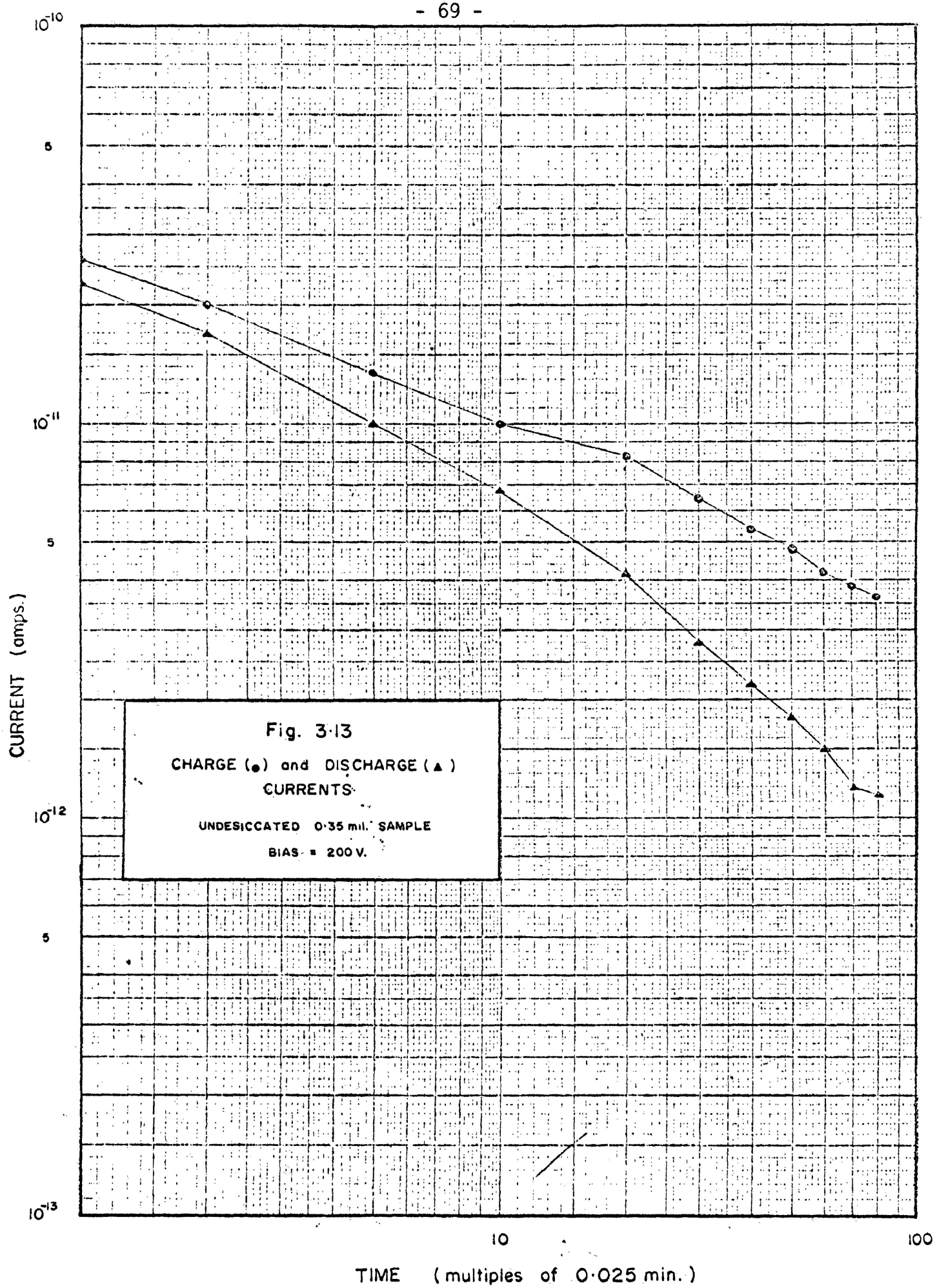

Fig. 3·13

CHARGE (●) and DISCHARGE (▲) CURRENTS

UNDESICCATED 0·35 mil. SAMPLE

BIAS = 200 V.

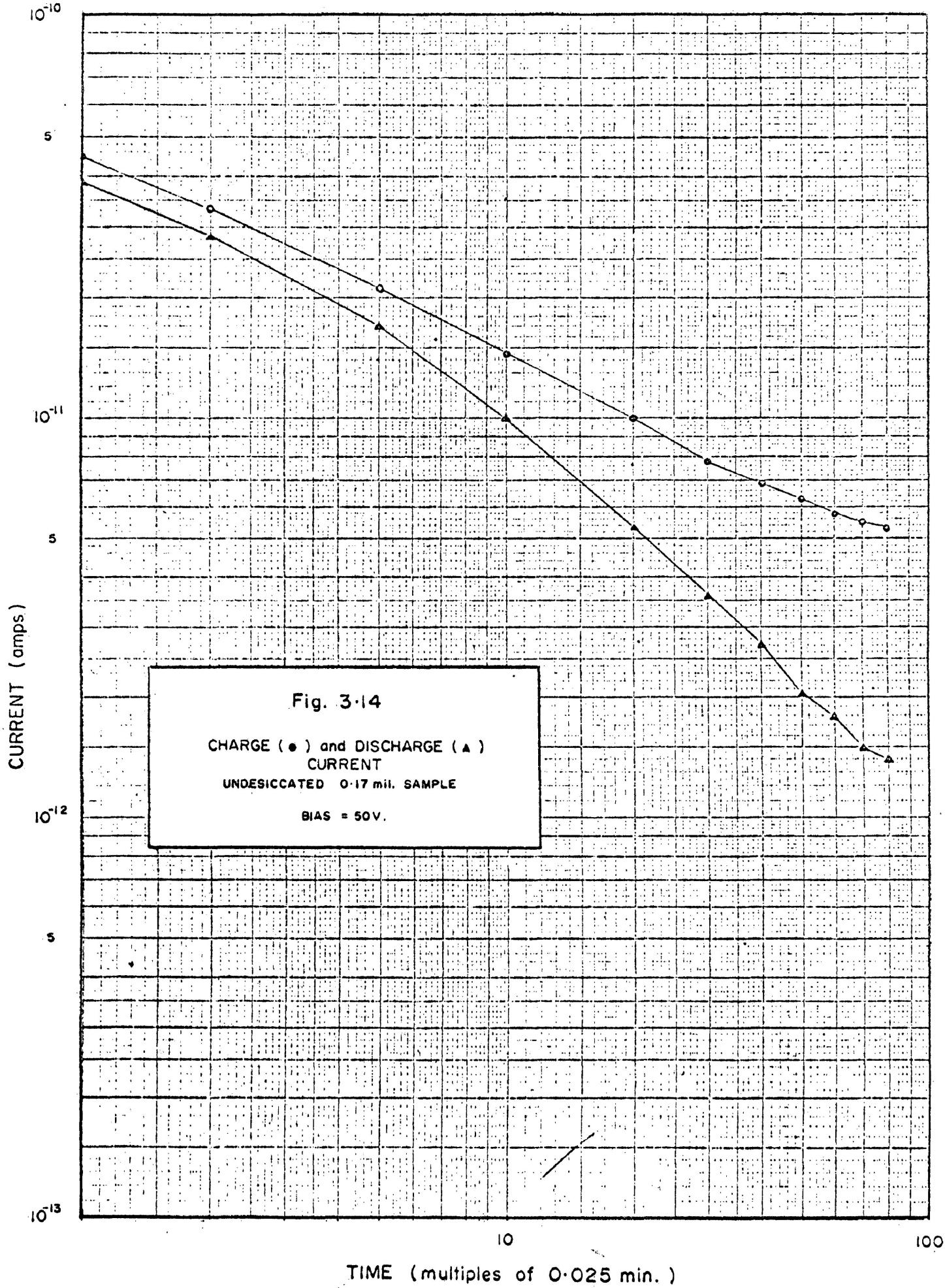

Fig. 3·14

CHARGE (●) and DISCHARGE (▲) CURRENT

UNDESICCATED 0·17 mil. SAMPLE

BIAS = 50V.

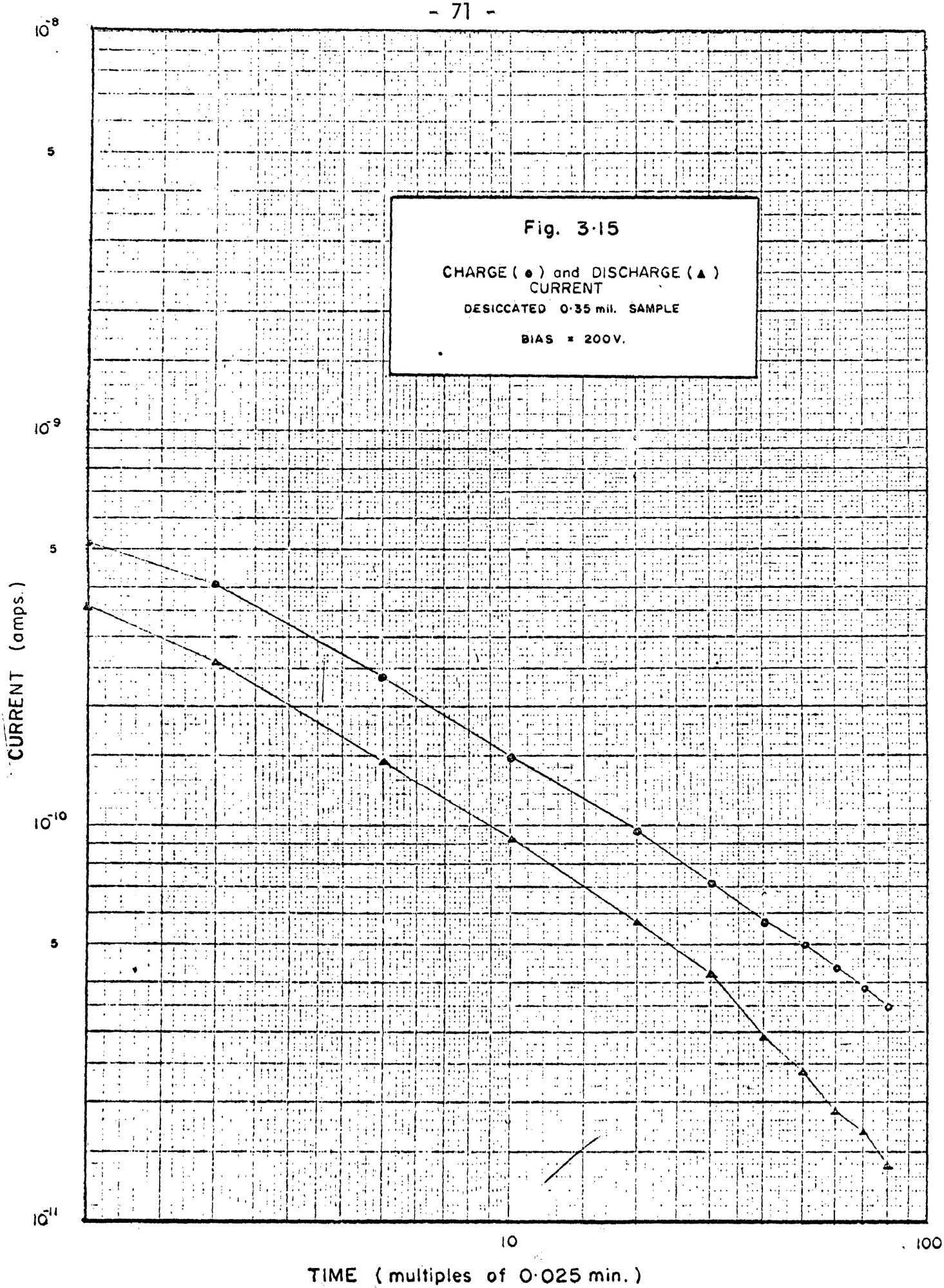
Fig. 3·15
CHARGE (●) and DISCHARGE (▲) CURRENT
DESICCATED 0·35 mil. SAMPLE
BIAS = 200V.
10^{-8}
5
10^{-9}
5
10^{-10}
5
10^{-11}
CURRENT (amps.)
10
100
TIME (multiples of 0·025 min.)

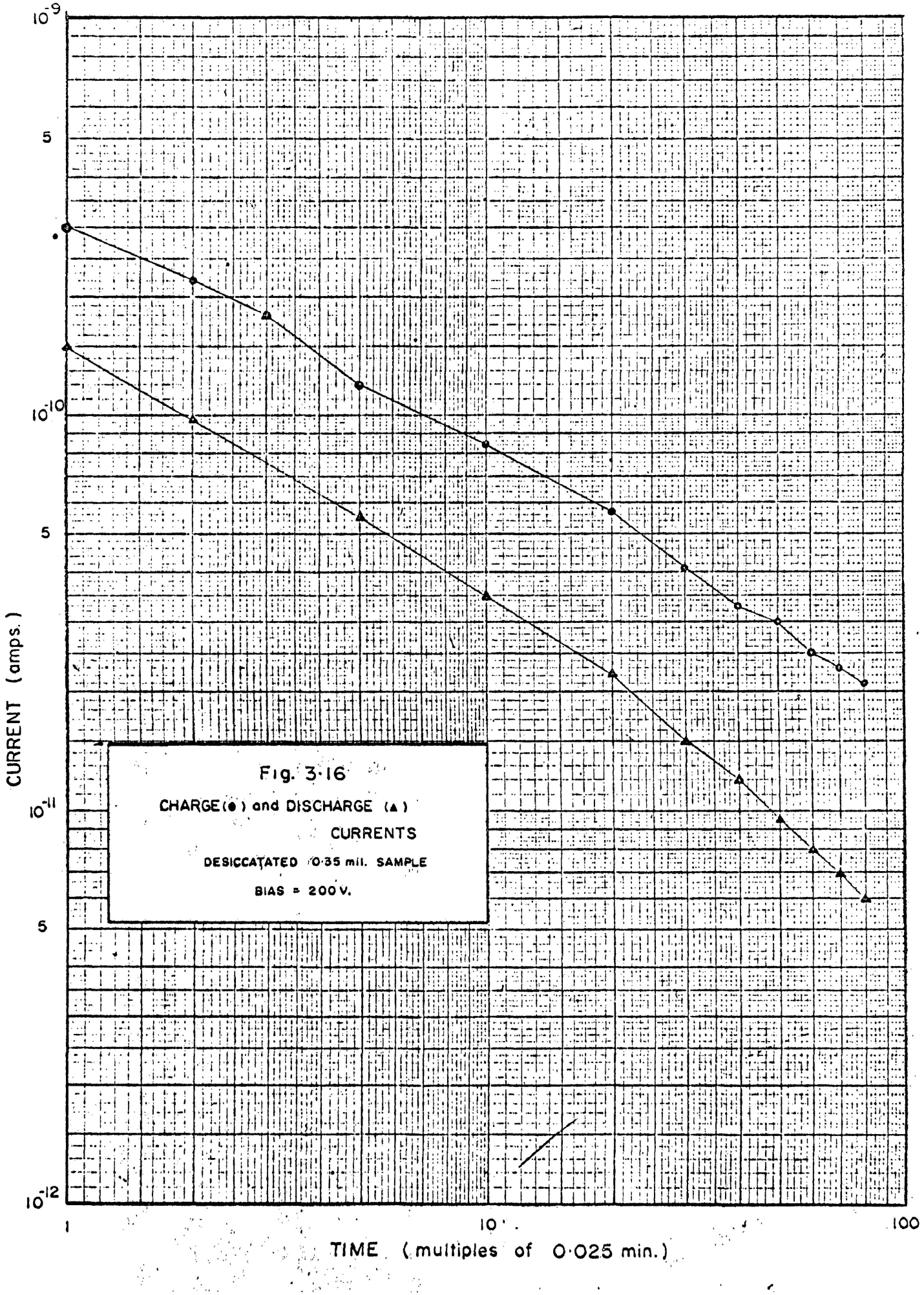

Fig. 3·16

CHARGE (●) and DISCHARGE (▲) CURRENTS

DESICCATED 0·35 mil. SAMPLE

BIAS = 200 V.

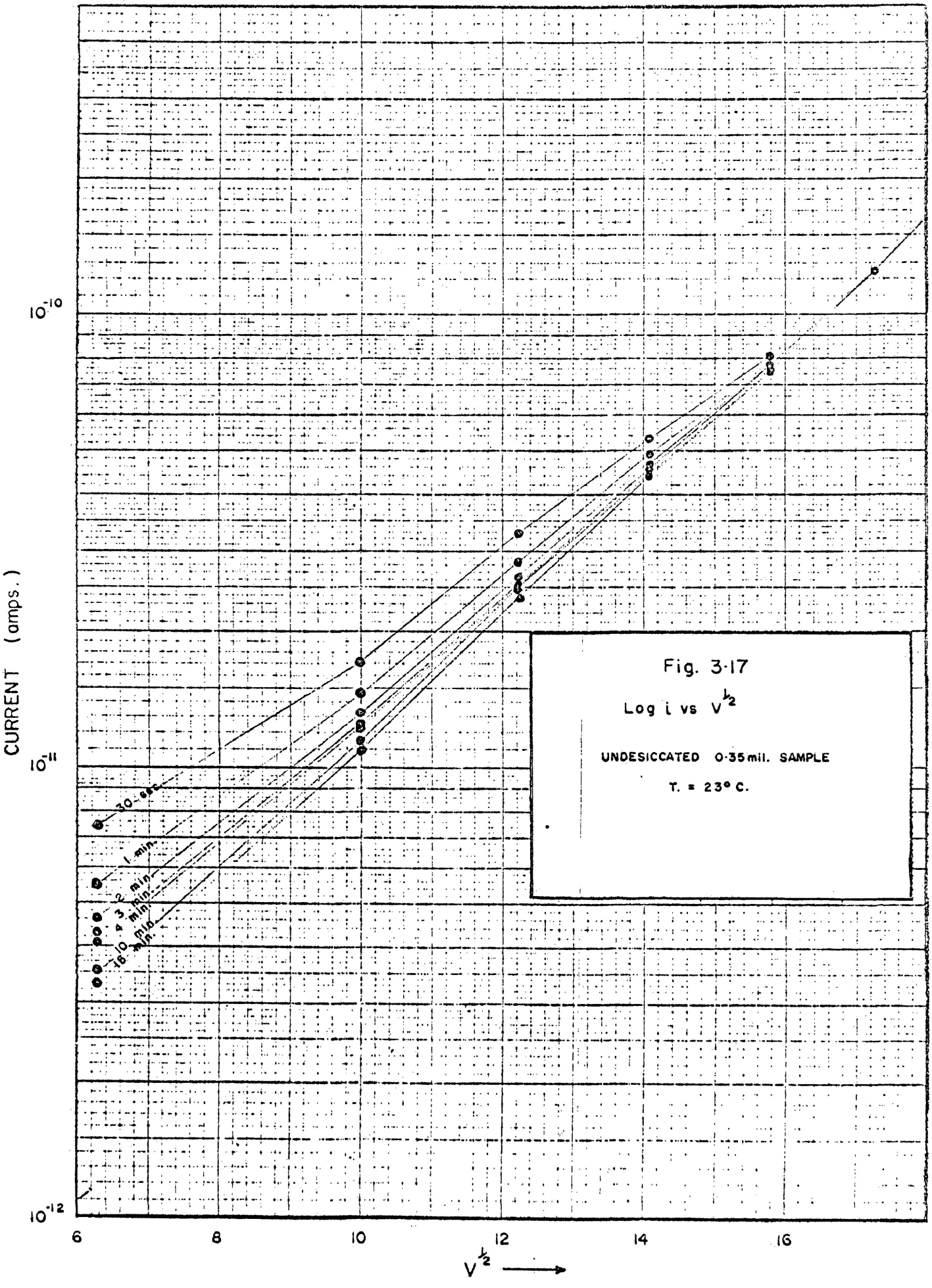

Fig. 3·17

Log i vs $V^{\frac{1}{2}}$

UNDESICCATED 0·35 mil. SAMPLE

T. = 23° C.

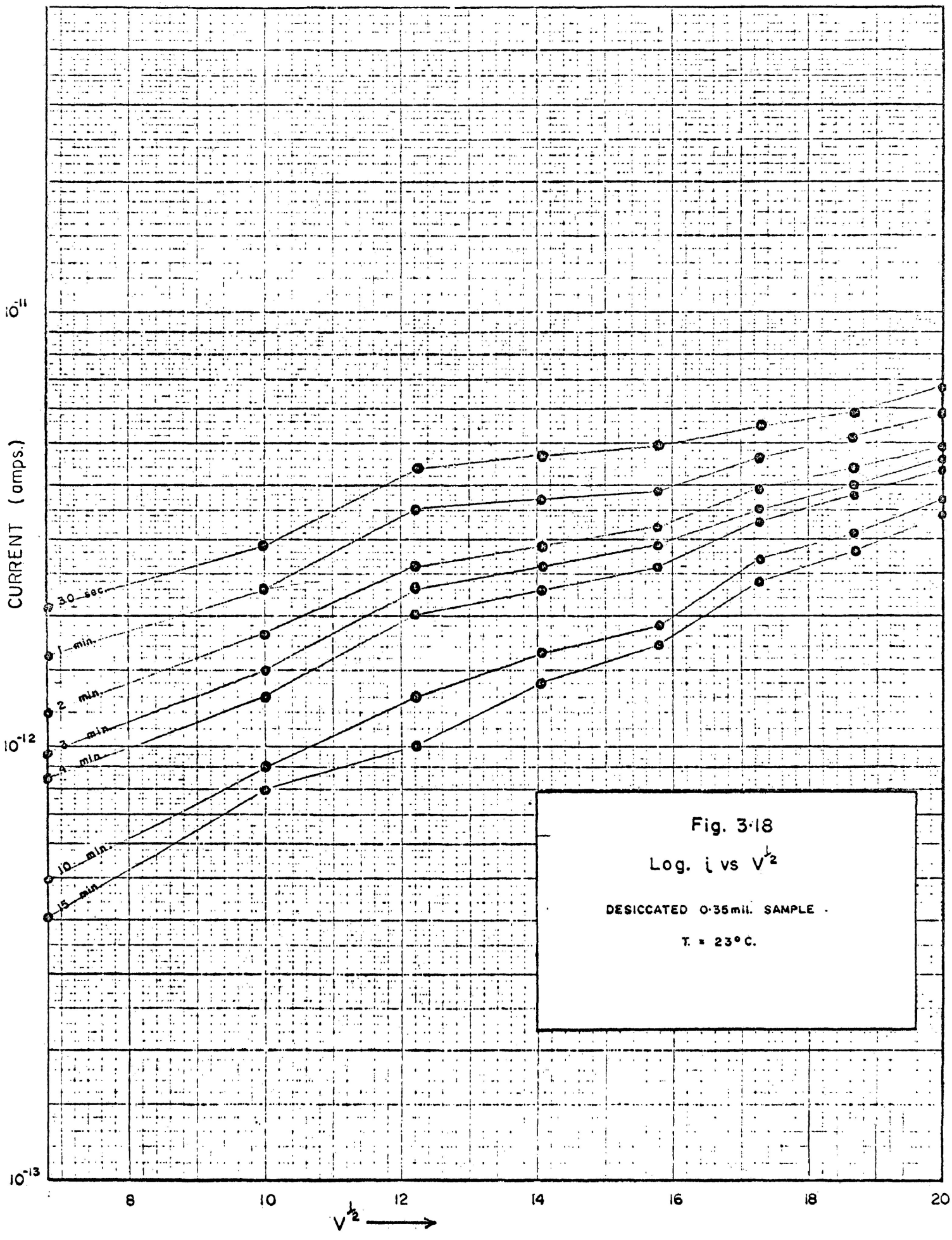

Fig. 3·18

Log. i vs $V^{\frac{1}{2}}$

DESICCATED 0·35mil. SAMPLE

T. = 23° C.

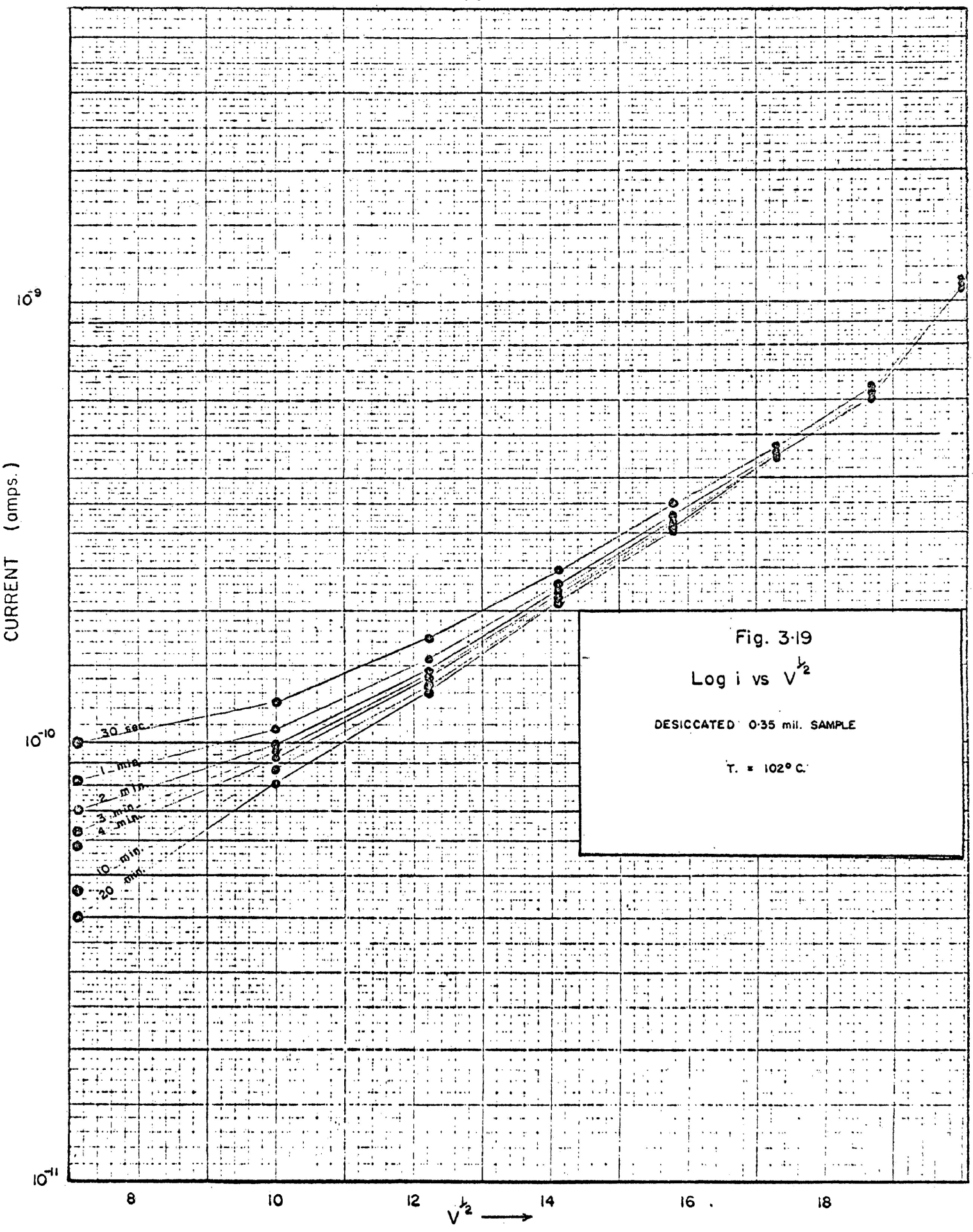

Fig. 3·19

Log i vs $V^{1/2}$

DESICCATED 0·35 mil. SAMPLE

T. = 102° C.

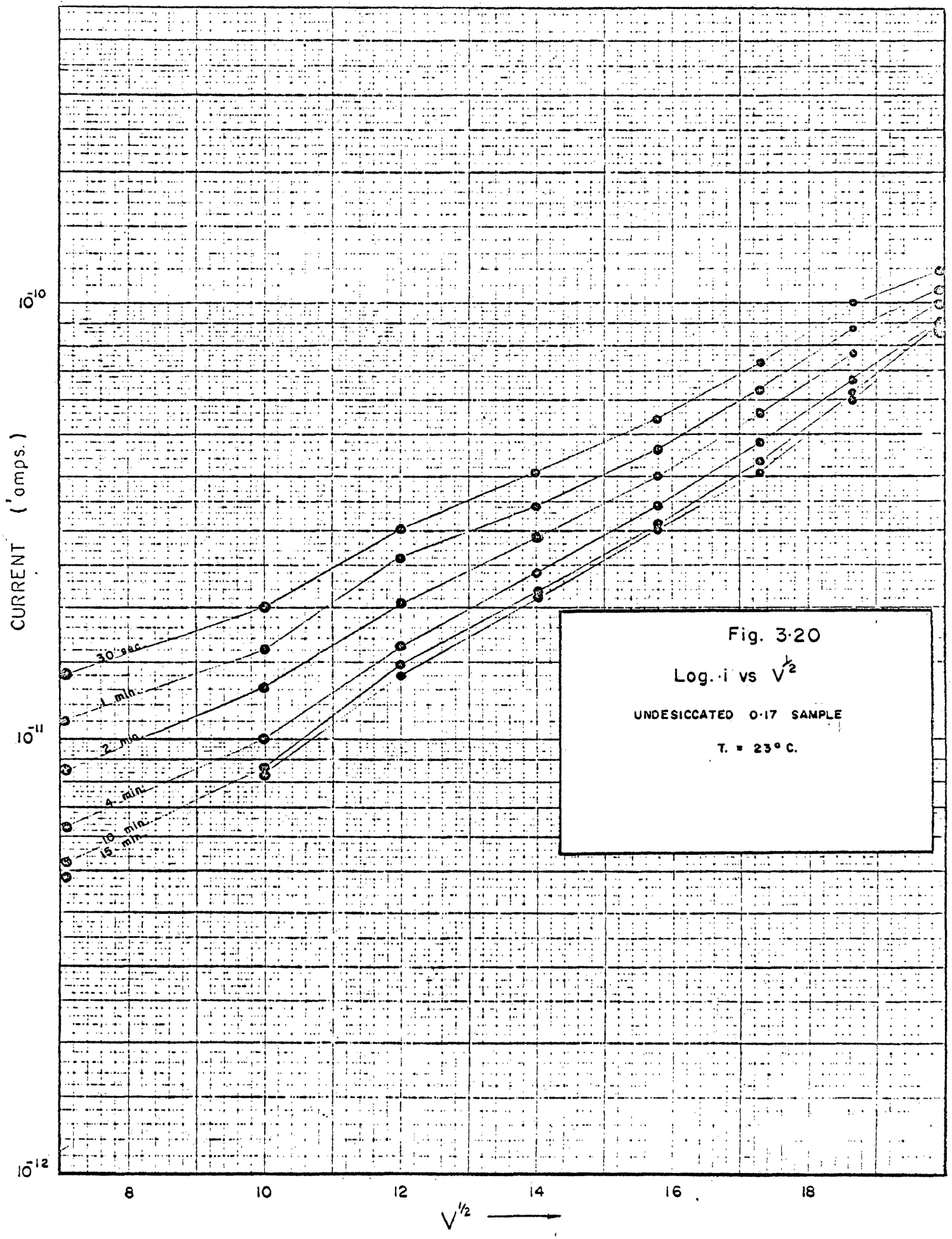

Fig. 3·20

Log. i vs $V^{1/2}$

UNDESICCATED 0·17 SAMPLE

T. = 23° C.

temperature behaviour. Before beginning this discussion, however, a brief mention should be made of experiments conducted by periodically reversing the electrode polarity. These investigations were initiated by the observance in a few samples of an unexplainable increase of current with time and more often at high temperatures and high fields. It was felt that this increase might be due to electrolysis - perhaps the formation of gases at the electrodes - and that the periodic reversal of the polarity could resolve this difficulty. With polarity reversals every two minutes, the current was still found to increase occasionally, but that the unexplained phenomenon was exclusively limited to undesiccated samples. These experiments also indicated a second abnormal behaviour of the undesiccated samples in that the current did not always increase with temperature as is normally expected. This is illustrated by Figs. 3.21 to 3.23 which give the i - vs - t dependence for elevated temperatures in comparison with the room temperature dependence before, denoted $23^{o}(1)$, and after, $23^{o}(2)$, heating. In all cases the current at any given time is the mean value observed after four polarity reversals. As Figs. 3.24 to 3.26 indicate, highly desiccated samples behave in a more predictable manner.

These experiments suggest the great relevance of moisture content to the d.c. conductivity and a supporting experiment has been conducted

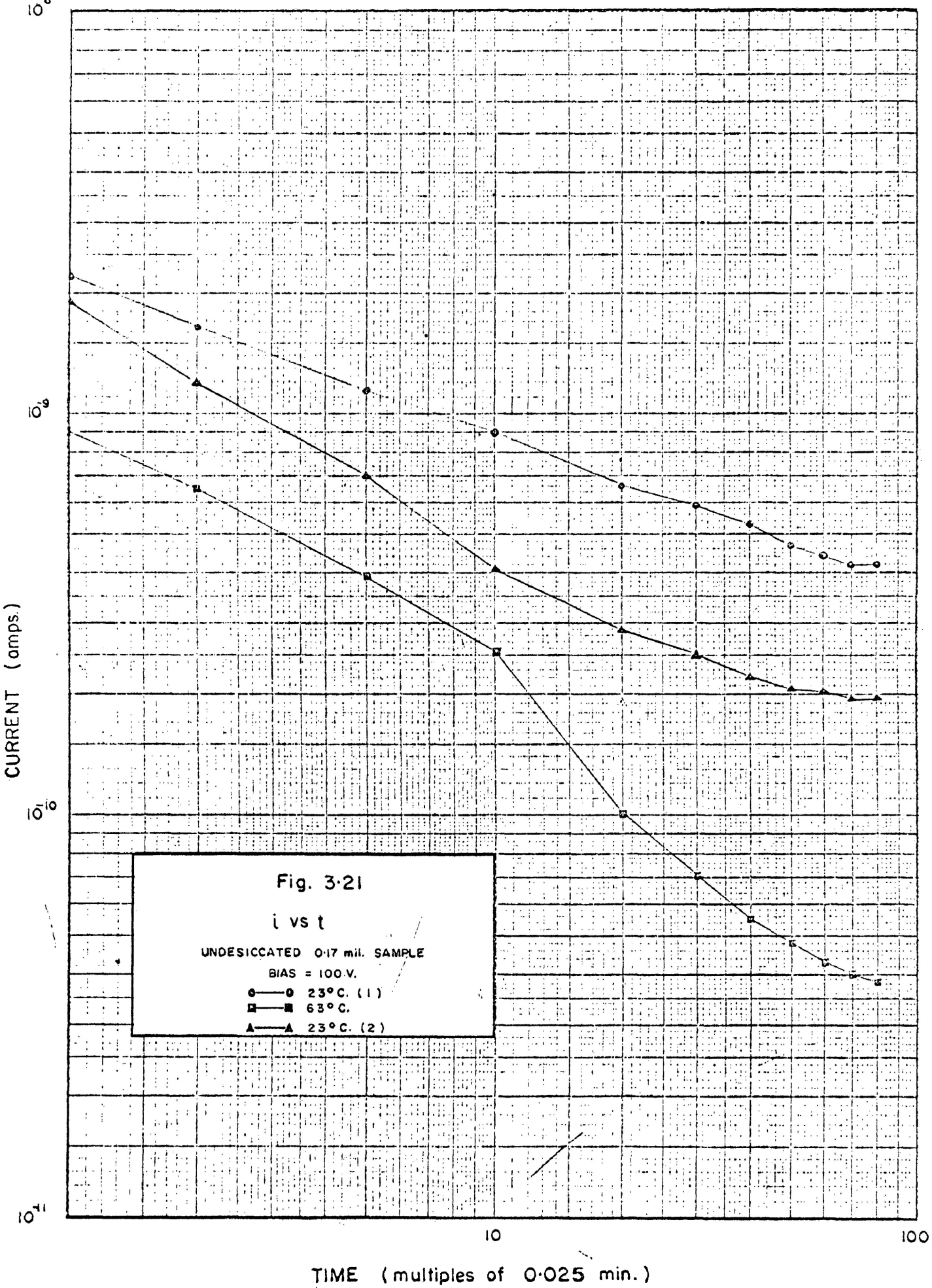
10^{-8}
10^{-9}
10^{-10}
10^{-11}
CURRENT (amps.)
10
100
TIME (multiples of 0·025 min.)
Fig. 3·21
i vs t
UNDESICCATED 0·17 mil. SAMPLE
BIAS = 100 V.
23°C. (1)
63°C.
23°C. (2)

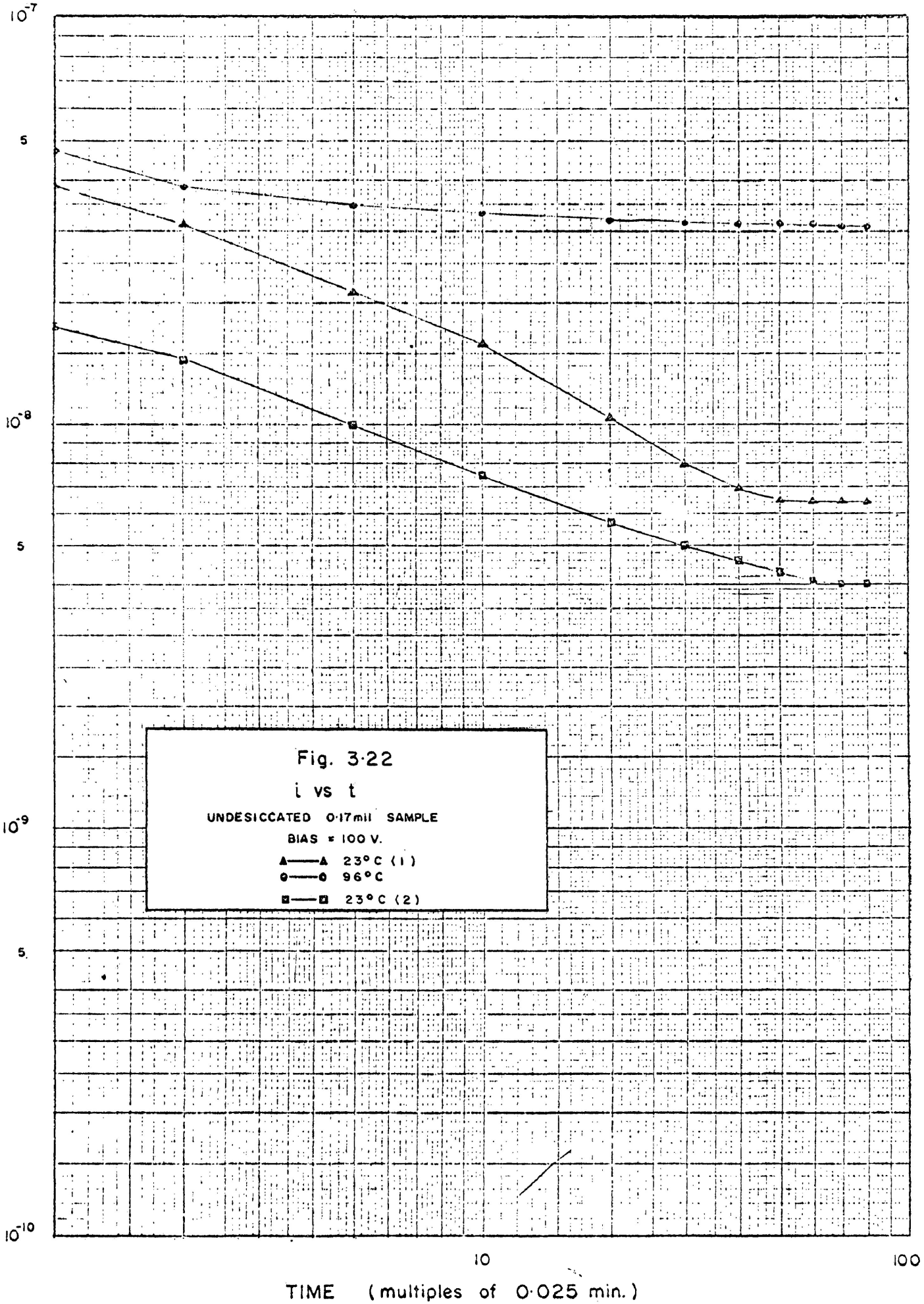
10^{-7}
5
10^{-8}
5
10^{-9}
5
10^{-10}
CURRENT (amps.)
10
100
TIME (multiples of 0·025 min.)
Fig. 3·22
i vs t
UNDESICCATED 0·17mil SAMPLE
BIAS = 100 V.
▲——▲ 23°C (1)
●——● 96°C
■——■ 23°C (2)

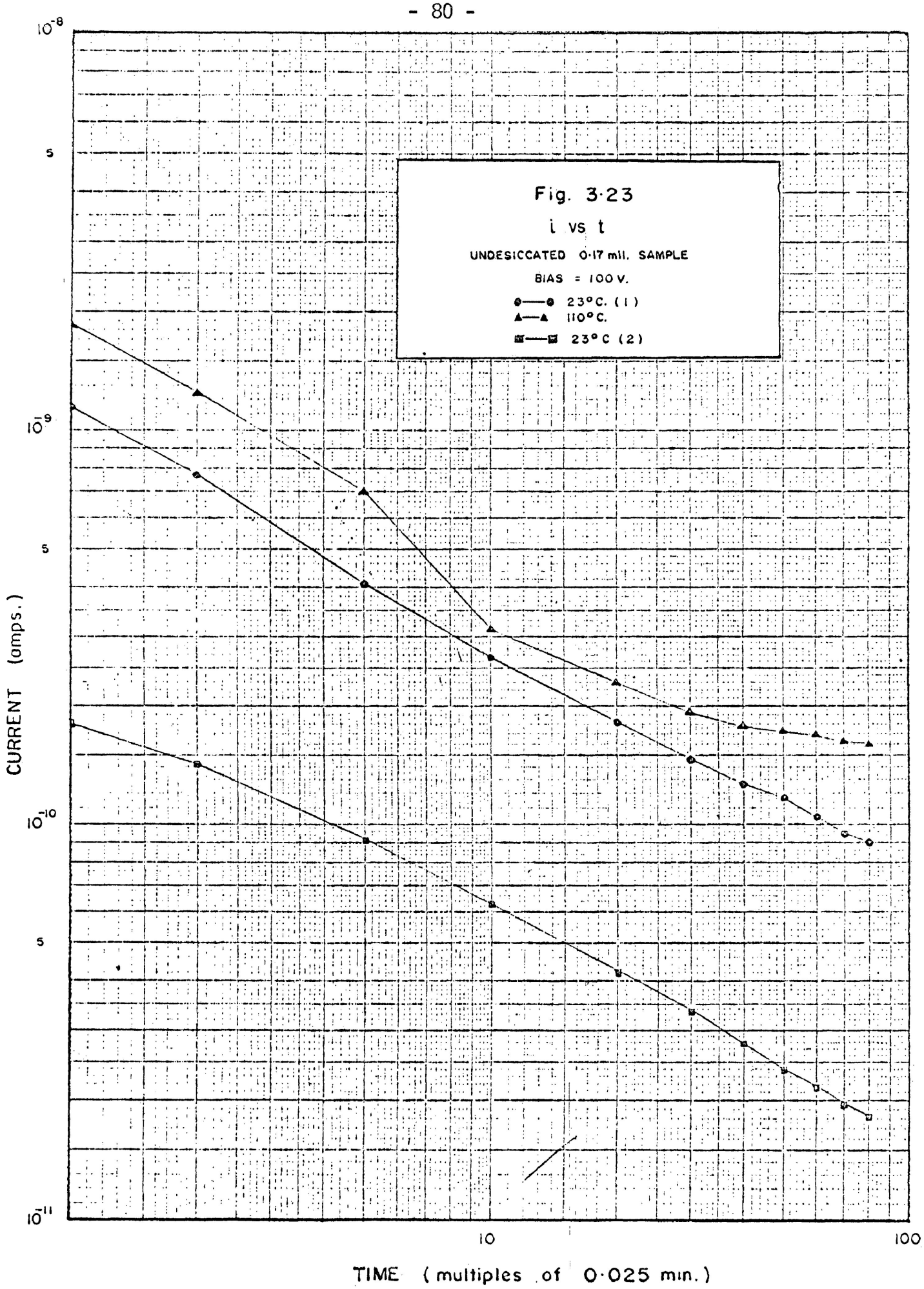
Fig. 3·23
i vs t
UNDESICCATED 0·17 mil. SAMPLE
BIAS = 100 V.
23°C. (1)
110°C.
23°C (2)
CURRENT (amps.)
10^{-8}
5
10^{-9}
5
10^{-10}
5
10^{-11}
10
100
TIME (multiples of 0·025 min.)

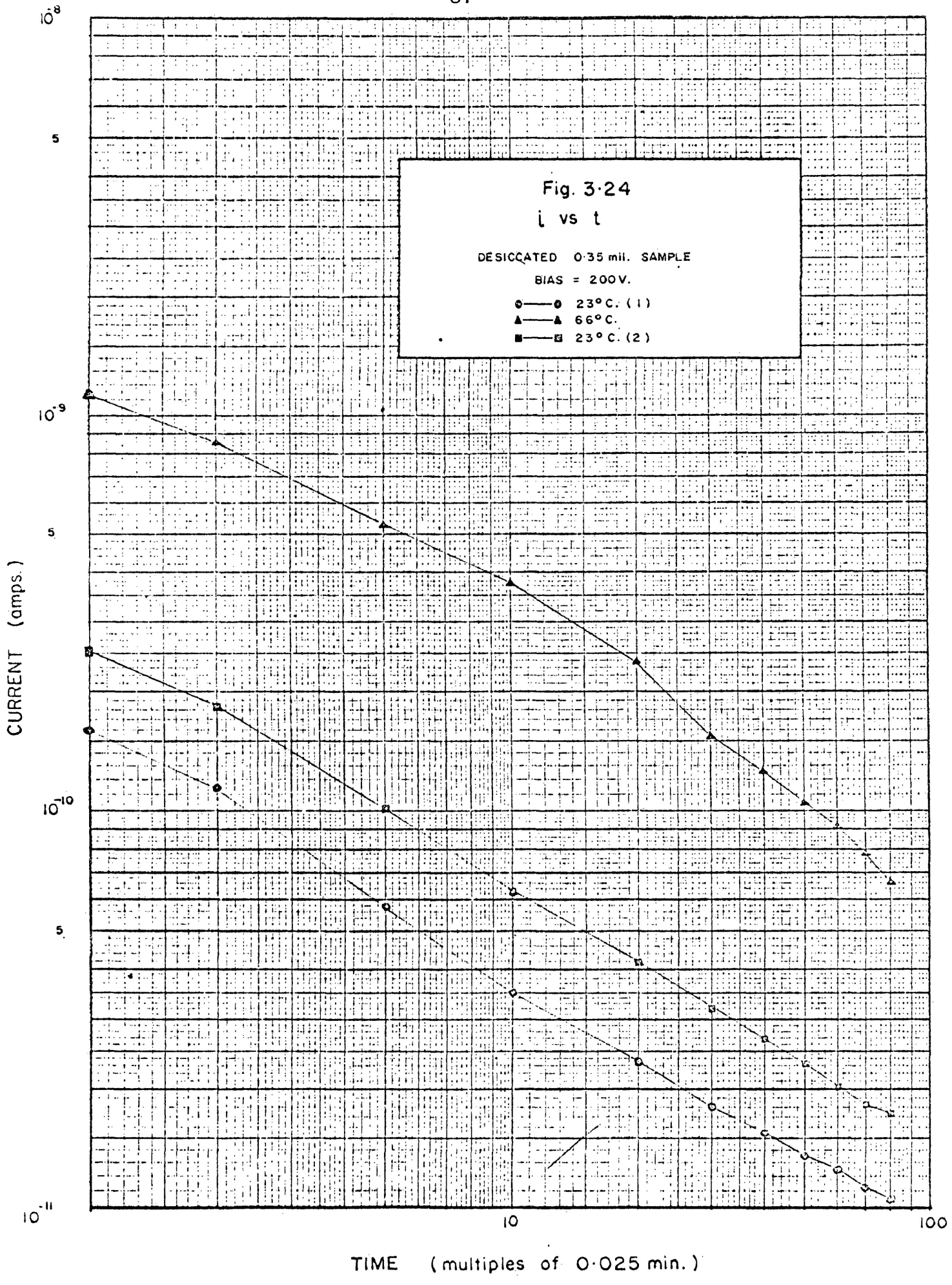
Fig. 3·24
i vs t
DESICCATED 0·35 mil. SAMPLE
BIAS = 200V.
23°C. (1)
66°C.
23°C. (2)
CURRENT (amps.)
10⁻⁸
5
10⁻⁹
5
10⁻¹⁰
5
10⁻¹¹
10
100
TIME (multiples of 0·025 min.)

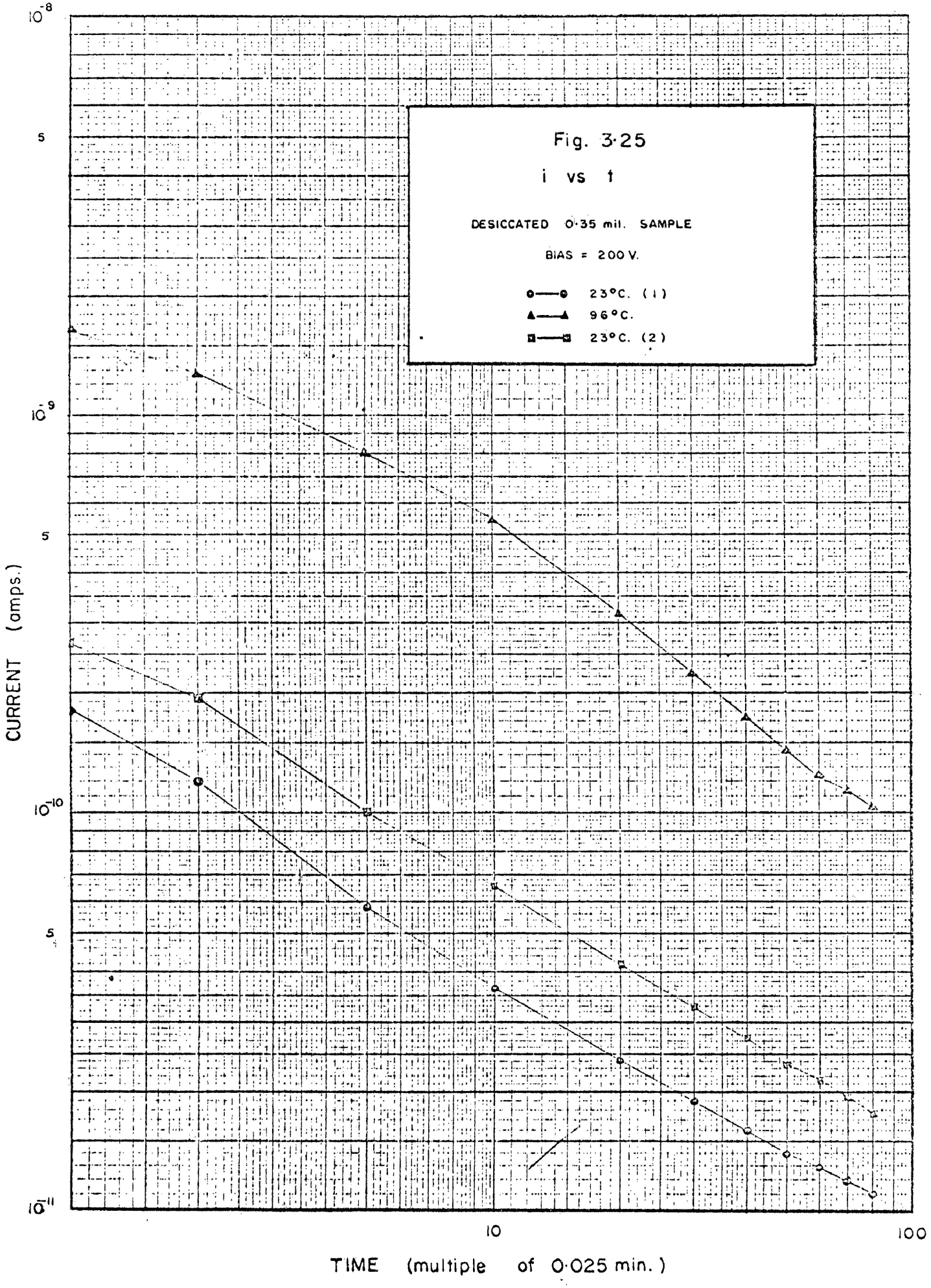
Fig. 3·25
i vs t
DESICCATED 0·35 mil. SAMPLE
BIAS = 200 V.
23°C. (1)
96°C.
23°C. (2)
CURRENT (amps.)
10⁻⁸
5
10⁻⁹
5
10⁻¹⁰
5
10⁻¹¹
10
100
TIME (multiple of 0·025 min.)

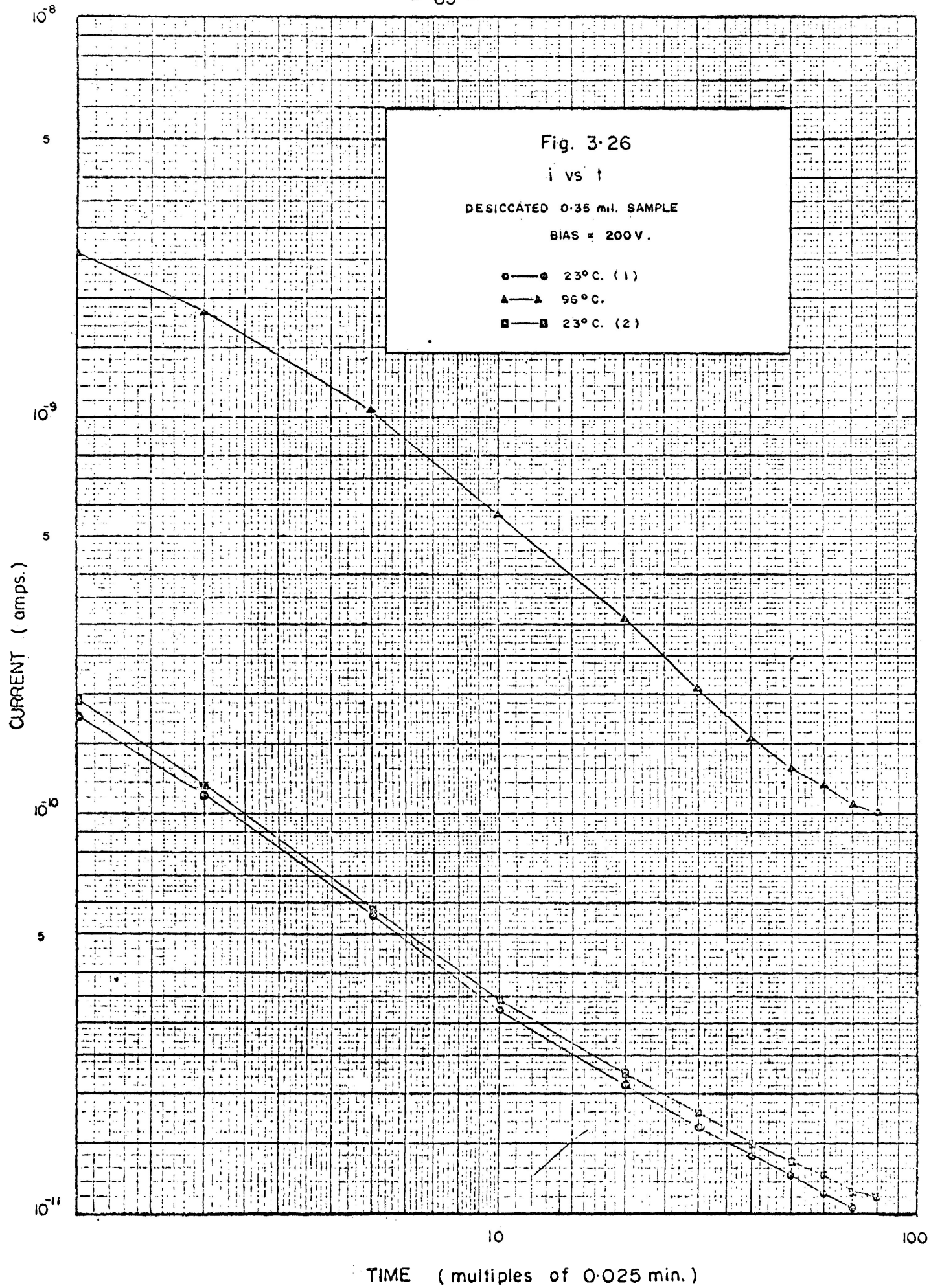
Fig. 3·26
i vs t
DESICCATED 0·35 mil. SAMPLE
BIAS = 200 V.
23° C. (1)
96° C.
23° C. (2)
CURRENT (amps.)
10^{-8}
5
10^{-9}
5
10^{-10}
5
10^{-11}
10
100
TIME (multiples of 0·025 min.)

by Dr. R. Raman with the aim of determining if the dissipation factor at 200 hz. is affected by elevated temperatures, in particular, the boiling point of water. The results are not dramatic as Fig. 3.27 indicates, although there is a slight decrease in D above 90°C. An estimation of the d.c. charging current was deduced from the value of the dielectric loss factor ε'' using Hamon's relationship[8].

$$G_o + \mathfrak{F}\left(0.63/\omega\right) = \omega C_a \varepsilon'' \qquad \text{Eq. 3.1}$$

where ω is the angular frequency, C_a is the air capacitance of the capacitor jig, G_o is the d.c. steady-state conductance and $\mathfrak{F}(t)$ is the anomalous charging (absorption) current flowing after time t. No direct comparison could be made with the conductance observed using d.c. techniques since from Eq. 3.1 the predicted value of 1.6×10^{-8}mho applies to $t = 5 \times 10^{-4}$sec. This is orders of magnitude below the response time of the electrometer, and although extrapolated plots of i - vs - t such as Fig. 3.25 indicate that this value is high, the t^{-n} law inherent in Hamon's theory is, no doubt, invalid at such short times.

(iii) MECHANISM OF CONDUCTION

With reference to the current - voltage behaviour of the capacitor tissue, it was invariably found that for high voltages, the logarithm of the current was proportional to the square-root of the voltage.

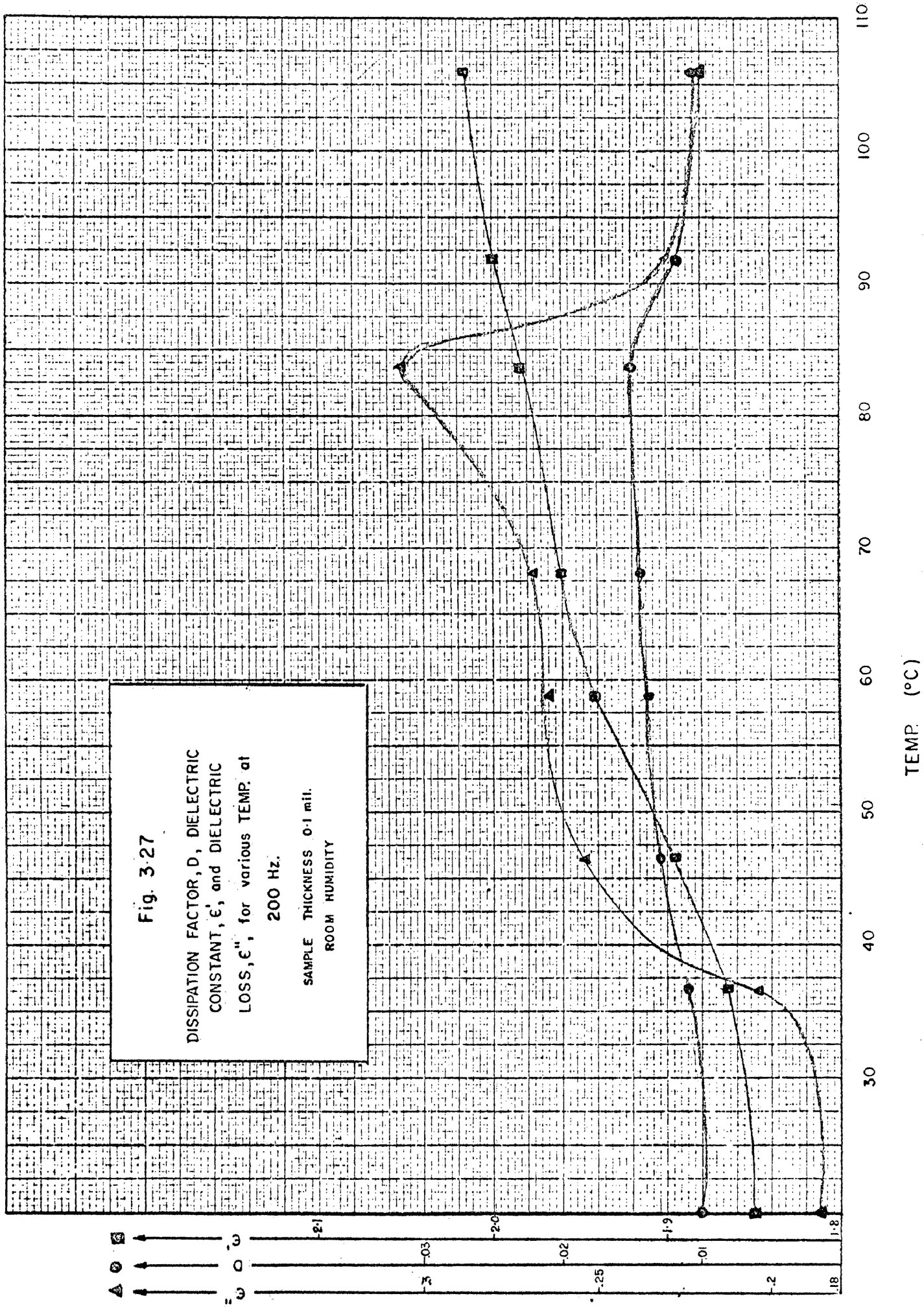
Fig. 3·27
DISSIPATION FACTOR, D, DIELECTRIC CONSTANT, ε', and DIELECTRIC LOSS, ε'', for various TEMP. at 200 Hz.
SAMPLE THICKNESS 0·1 mil.
ROOM HUMIDITY
ε'
D
ε''
2·1
2·0
1·9
1·8
·03
·02
·01
·3
·25
·2
·18
30
40
50
60
70
80
90
100
110
TEMP. (°C)

Several experiments were conducted to see how the moisture content affected the slopes of the log i - vs - $V^{\frac{1}{2}}$ curves while the amount of moisture in the sample was altered by storage in a calcium chloride desiccator for controlled periods of time. The observed slopes and the theoretical Schottky slopes are denoted in the appropriate figures as α_{exp} and α_{th} respectively. The previously mentioned standardizing procedure was rigorously adhered to except when conditioning dictated changes. The following experiments were conducted:

(1) Current - voltage curve for a sample stored in the desiccator for ten days was determined and regarded as a reference. Fig. 3.28, Curves No.1 and No. 1a.

(2) Same as (1) except for 15 - hour equilibration time from insertion of sample to first application of voltage, Fig. 3.28, Curve No. 2.

(3) Sample stored in room temperature and room humidity; readings taken with no desiccant in canister. Fig. 3.29, Curves (3), (4), (5) and (6).

(4) Sample stored in room temperature and room humidity; readings taken with desiccant in canister. Fig. 3.30.

(5) Sample stored in room temperature and desiccator; readings taken with no desiccant in canister. Fig. 3.30.

(6) Current voltage traces of desiccated samples with slight changes in electrode pressure. Fig. 3.31

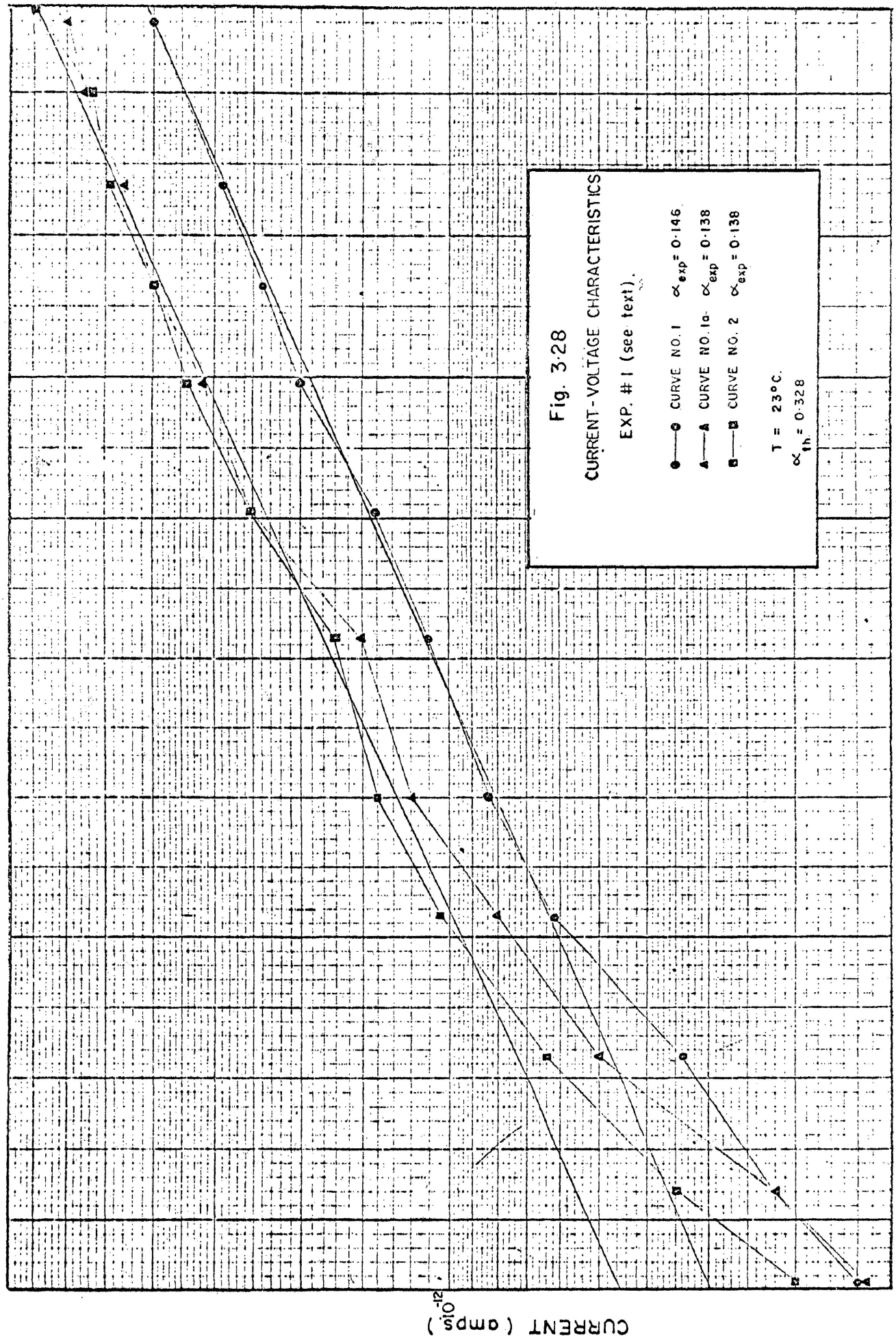
Fig. 3·28
CURRENT-VOLTAGE CHARACTERISTICS
EXP. # 1 (see text).
CURVE NO. 1 α_{exp} = 0·146
CURVE NO. 1a α_{exp} = 0·138
CURVE NO. 2 α_{exp} = 0·138
T = 23°C.
α_{th} = 0·328
CURRENT (amps $\times 10^{-12}$)
SQUARE ROOT of VOLTAGE
4
6
8
10
12
14
16
18
20

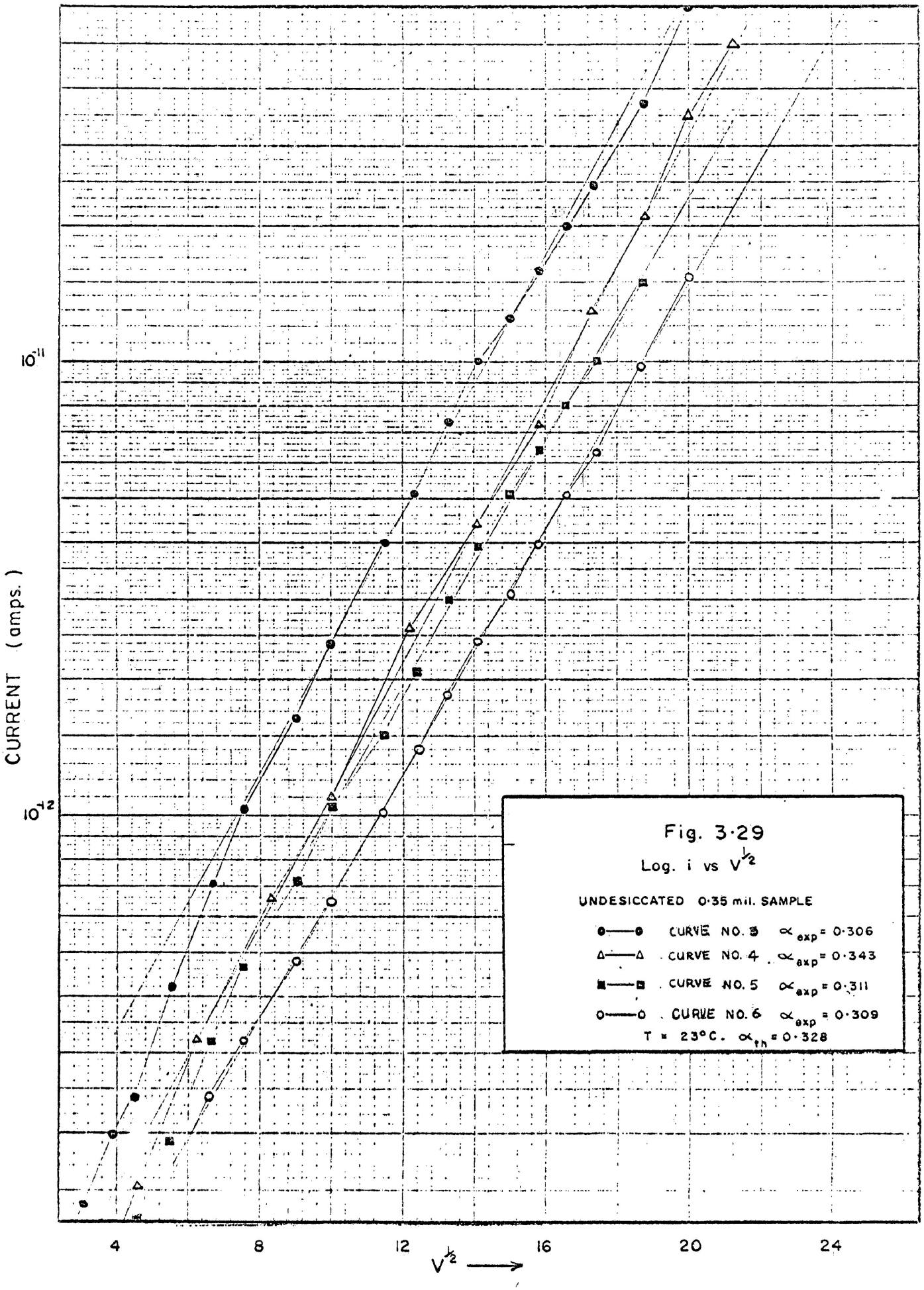
CURRENT (amps.)
10^{-11}
10^{-12}
4
8
12
16
20
24
$V^{1/2}$ ⟶
Fig. 3·29
Log. i vs $V^{1/2}$
UNDESICCATED 0·35 mil. SAMPLE
CURVE NO. 3 α_{exp} = 0·306
CURVE NO. 4 α_{exp} = 0·343
CURVE NO. 5 α_{exp} = 0·311
CURVE NO. 6 α_{exp} = 0·309
T = 23°C. α_{th} = 0·328

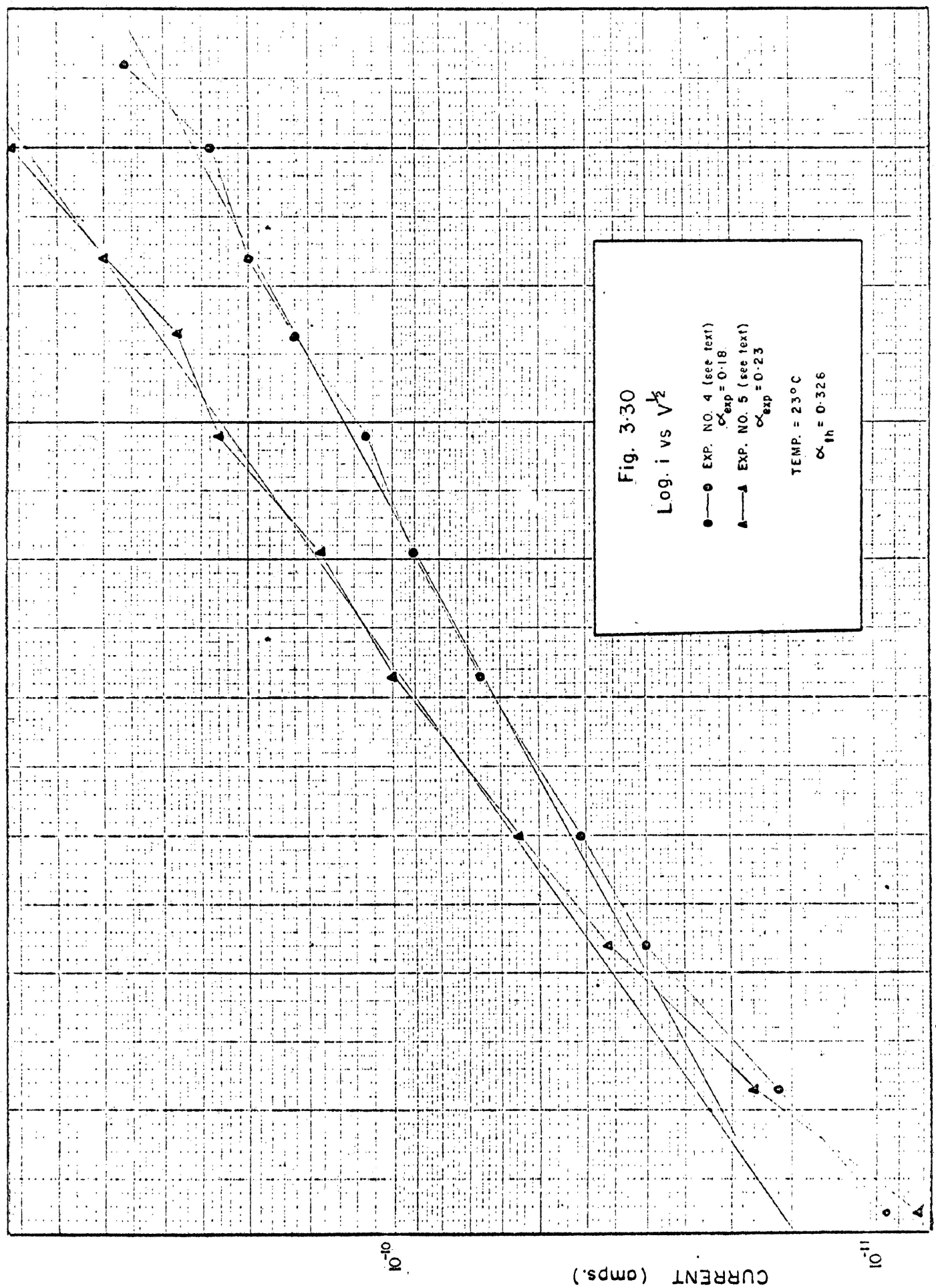
Fig. 3·30
Log. i vs $V^{\frac{1}{2}}$
EXP. NO. 4 (see text)
α_{exp} = 0·18
EXP. NO. 5 (see text)
α_{exp} = 0·23
TEMP. = 23°C
α_{th} = 0·326
CURRENT (amps.)
10^{-10}
10^{-11}
6
8
10
12
14
16
18
20
$V^{\frac{1}{2}}$

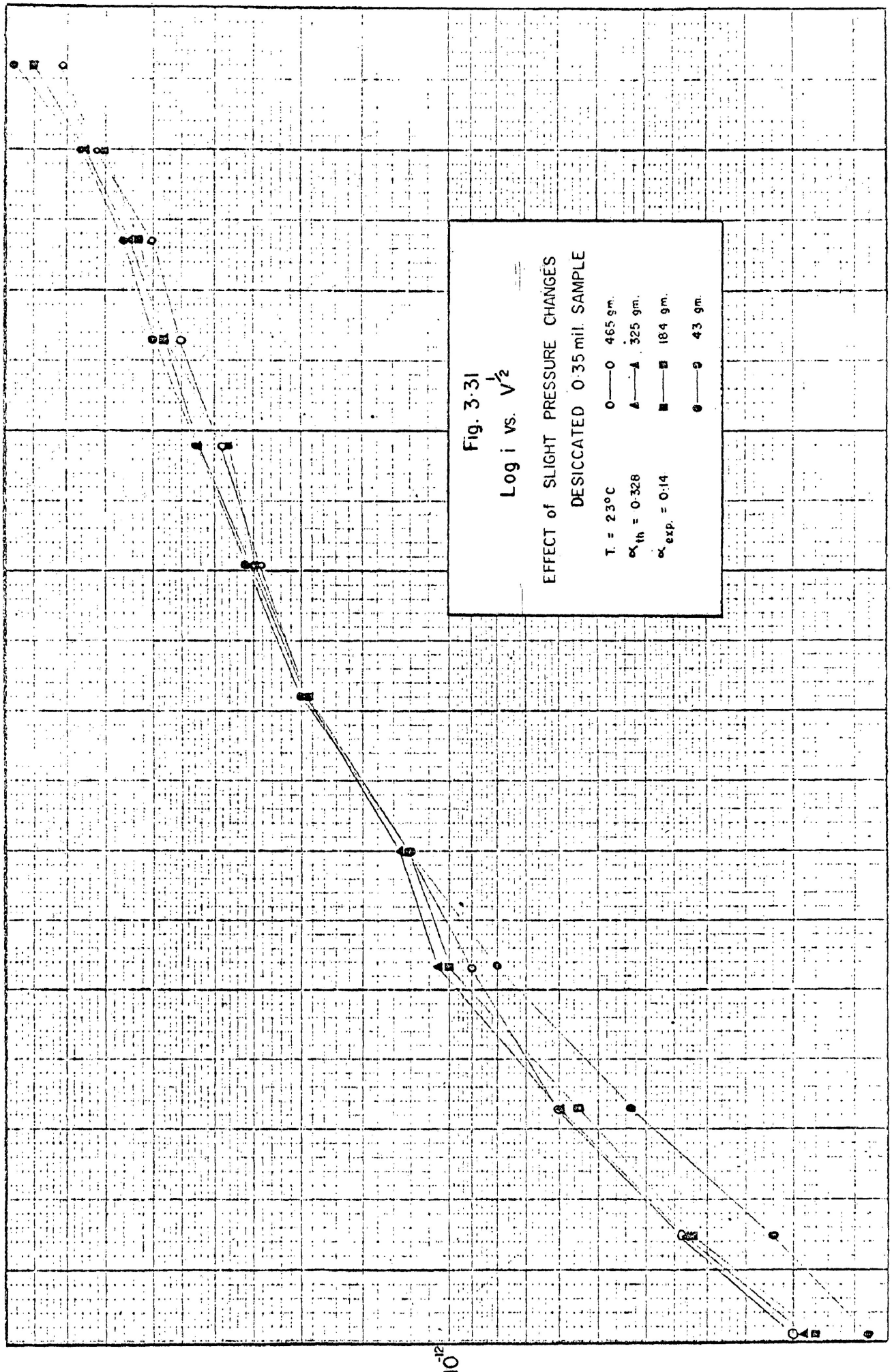
Fig. 3·31
Log i vs. $V^{\frac{1}{2}}$
EFFECT of SLIGHT PRESSURE CHANGES
DESICCATED 0·35 mil. SAMPLE
T. = 23°C
α_{th} = 0·328
$\alpha_{exp.}$ = 0·14
0—0 465 gm.
▲—▲ 325 gm.
■—■ 184 gm.
●—● 43 gm.
CURRENT 10^{-12} (amps)
$V^{\frac{1}{2}}$
6
8
10
12
14
16
18
20
22

(7) Current voltage curve for room and elevated temperatures; sample stored in room temperature and desiccator for 42 hours. Fig. 3.32

(8) As in (7) except for storage for 16 days in desiccator. Fig. 3.33.

(9) As in (7) except for storage for 71 days in desiccator. Fig. 3.34.

It is evident from the experiments just described that the removal of the moisture from the sample decreases the magnitude of the current as well as the slope of the ln i - vs - $V^{\frac{1}{2}}$ curve. However, lacking quantitative data on the moisture content, it is rather difficult to discuss this matter further. The observations on highly desiccated samples seem reasonably reproducible at room temperatures, although this is hardly true at higher temperatures.

In attemtping to determine the activation energy based on

$$i = i_o \exp \left[- \frac{\Delta E}{kT} \right]$$

the 200 v. current value from Figs. 3.32 to 3.34 were plotted against the reciprocal of the absolute temperature. Figures. 3.35 to 3.37 indicate values for ΔE, although the data is sparce and in general, not well grouped. Figs. 3.38 and 3.39 are the results of direct

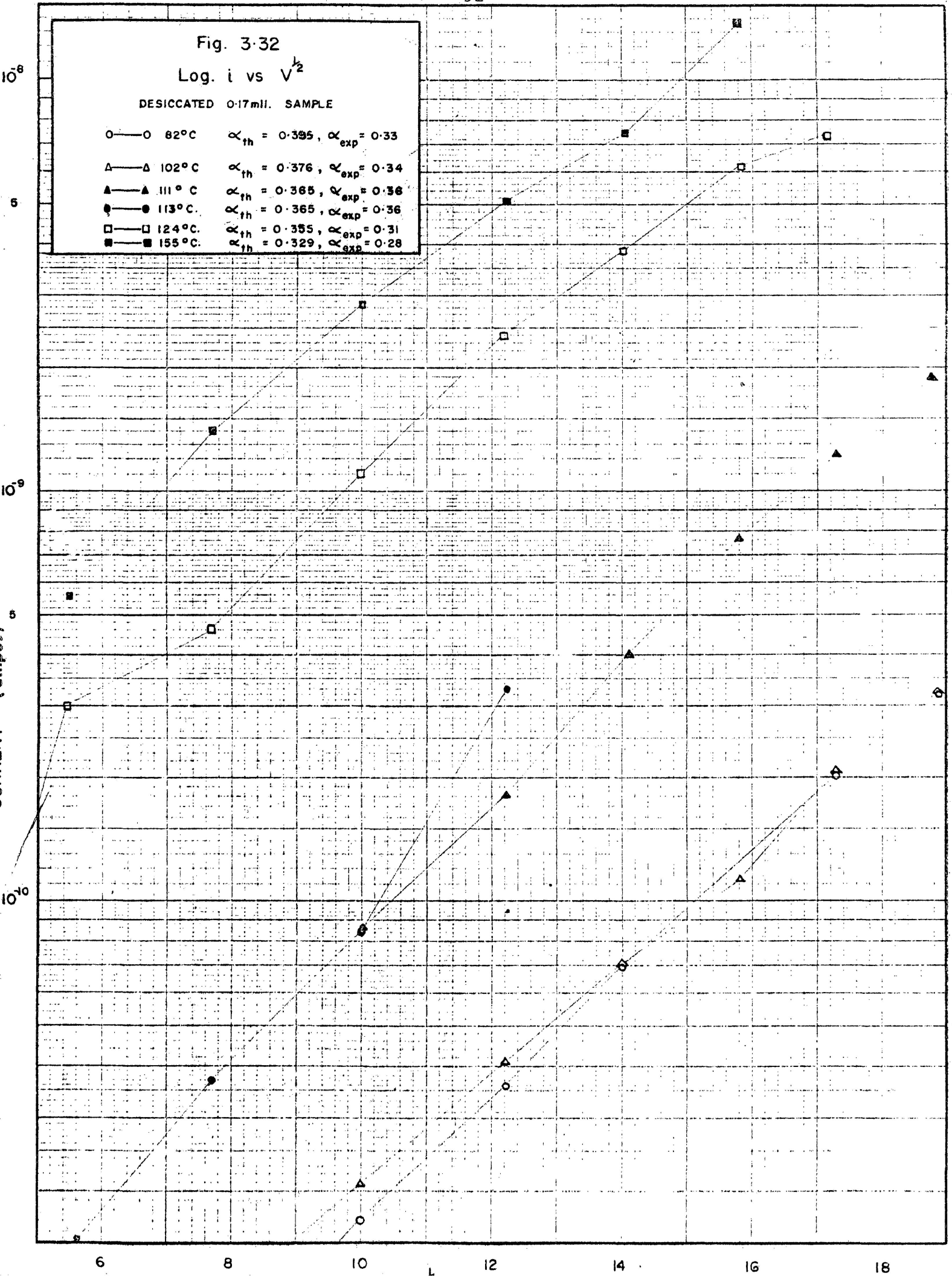
Fig. 3·32
Log. i vs $V^{1/2}$
DESICCATED 0·17mil. SAMPLE
82°C α_{th} = 0·395, α_{exp} = 0·33
102°C α_{th} = 0·376, α_{exp} = 0·34
111°C α_{th} = 0·365, α_{exp} = 0·36
113°C. α_{th} = 0·365, α_{exp} = 0·36
124°C. α_{th} = 0·355, α_{exp} = 0·31
155°C. α_{th} = 0·329, α_{exp} = 0·28
10^{-8}
5
10^{-9}
5
10^{-10}
6
8
10
12
14
16
18

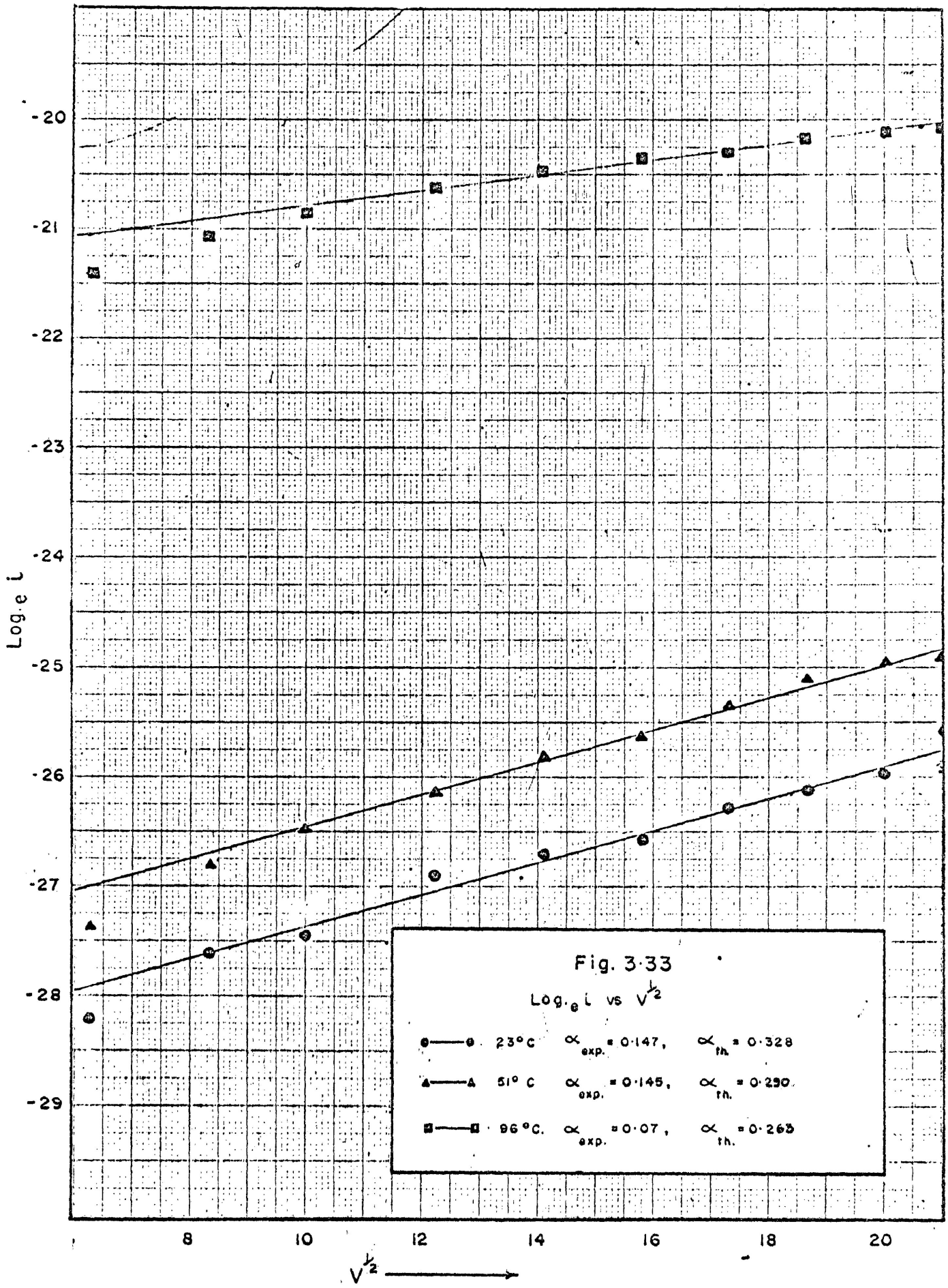
-20
-21
-22
-23
-24
-25
-26
-27
-28
-29
Log e i
8
10
12
14
16
18
20
V½
Fig. 3·33
Log e i vs V½
23°C ∝exp. = 0·147, ∝th. = 0·328
51° C ∝exp. = 0·145, ∝th. = 0·290
96 °C. ∝exp. = 0·07, ∝th. = 0·265

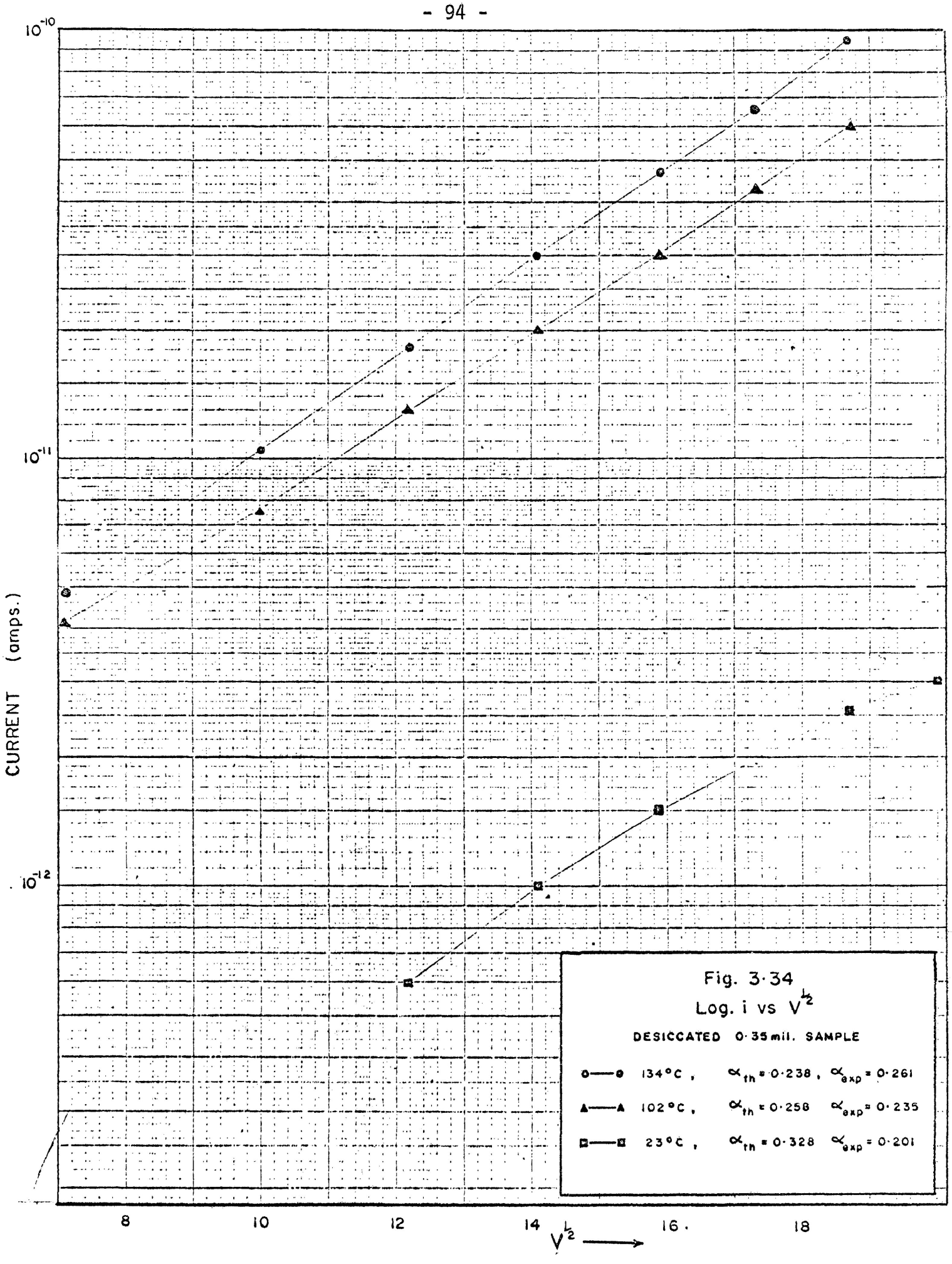

Fig. 3·34

Log. i vs $V^{\frac{1}{2}}$

DESICCATED 0·35 mil. SAMPLE

o—o 134°C , $\alpha_{th} = 0.238$, $\alpha_{exp} = 0.261$

▲—▲ 102°C , $\alpha_{th} = 0.258$ $\alpha_{exp} = 0.235$

□—□ 23°C , $\alpha_{th} = 0.328$ $\alpha_{exp} = 0.201$

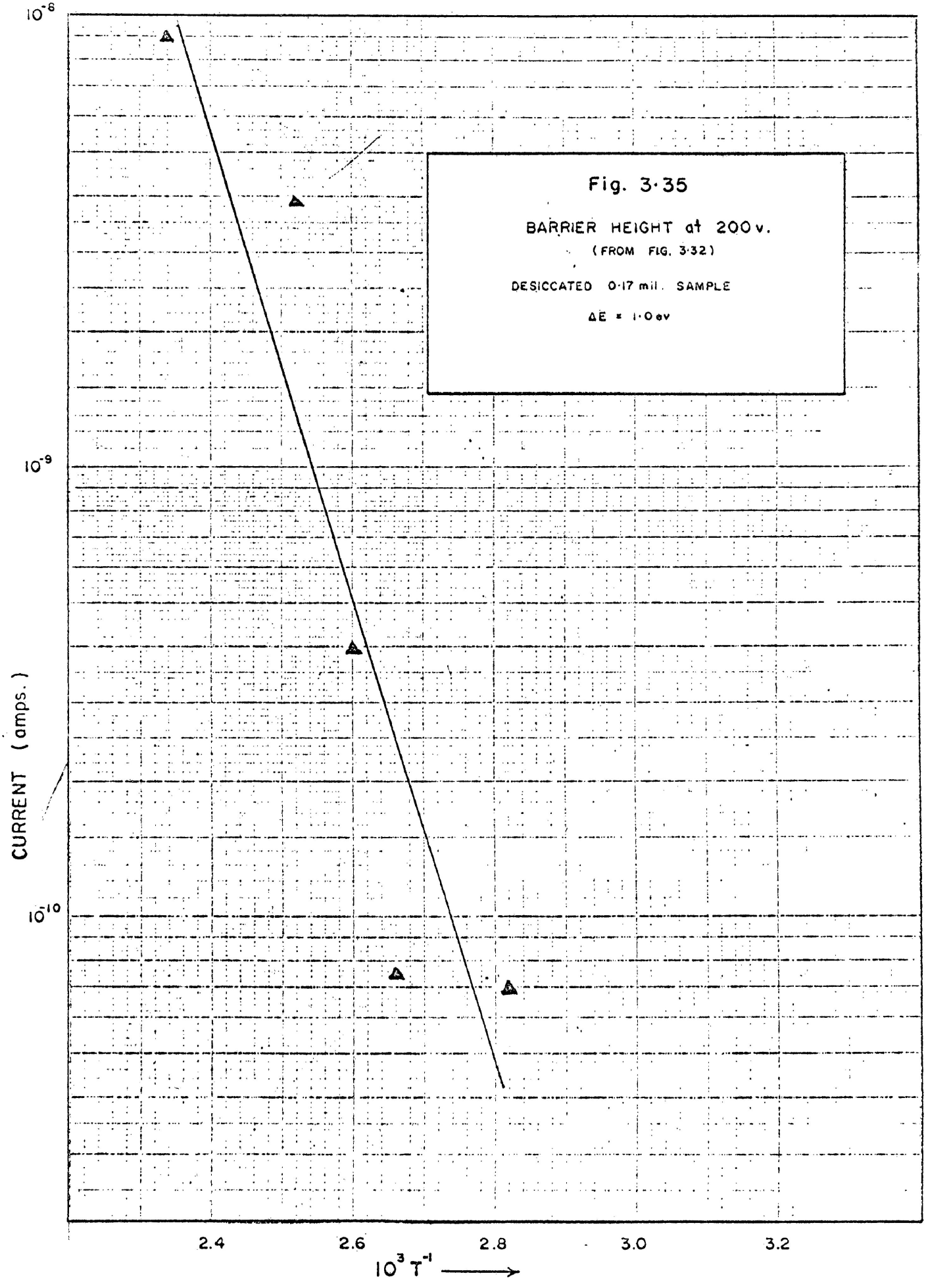

Fig. 3·35

BARRIER HEIGHT at 200 v.

(FROM FIG. 3·32)

DESICCATED 0·17 mil. SAMPLE

ΔE = 1·0 ev

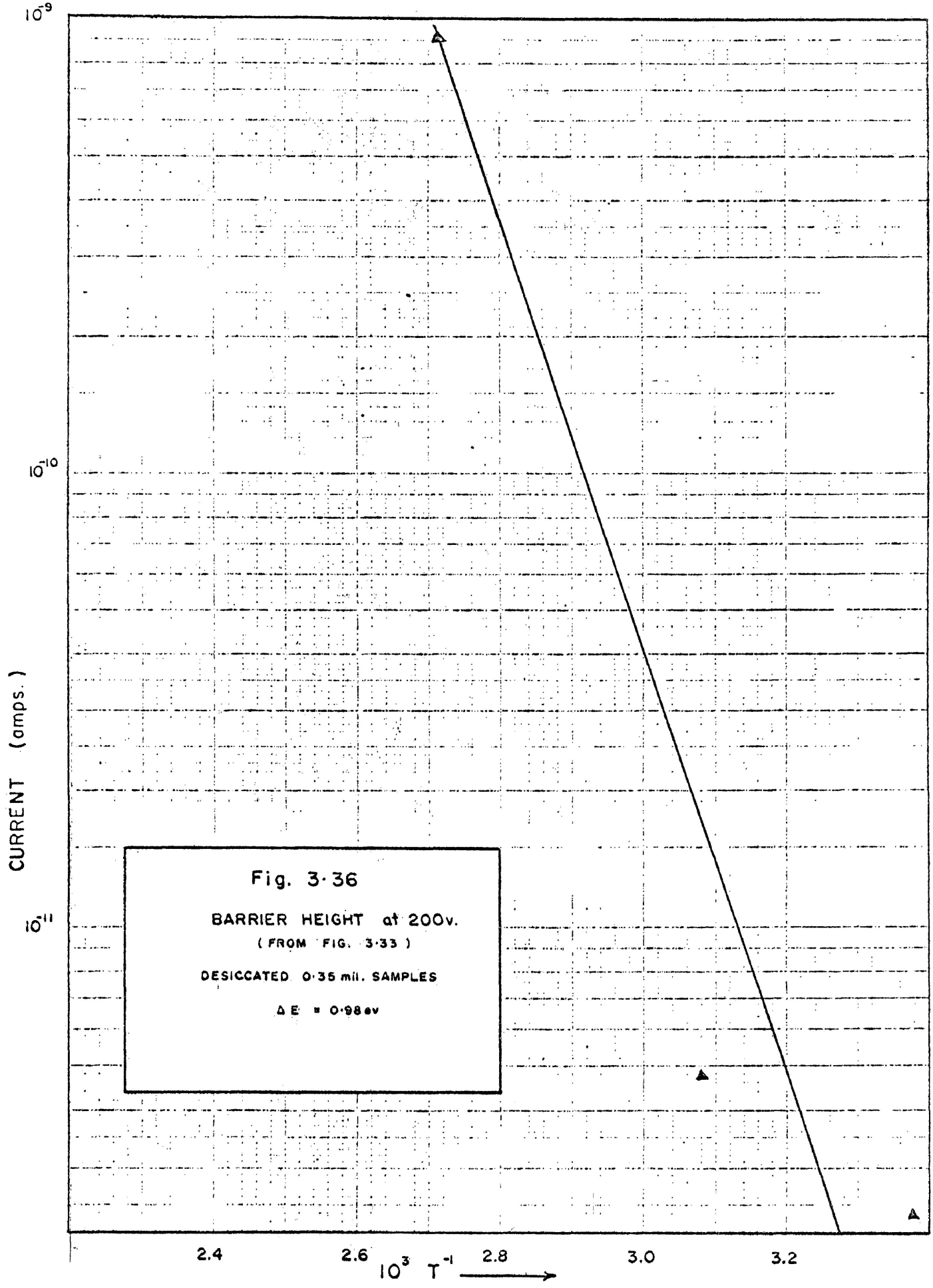

Fig. 3·36

BARRIER HEIGHT at 200v.

(FROM FIG. 3·33)

DESICCATED 0·35 mil. SAMPLES

ΔE = 0·98 ev

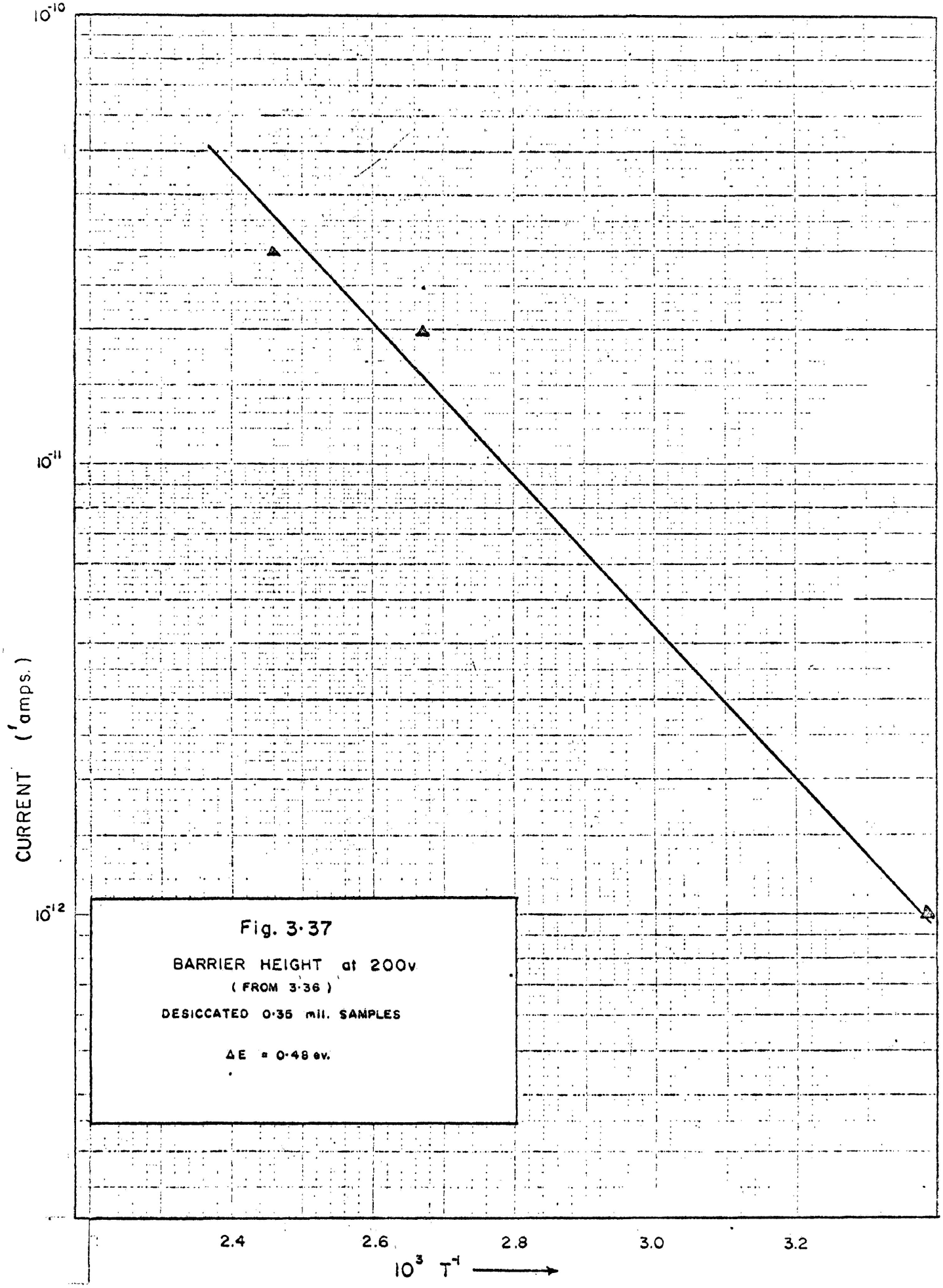

Fig. 3·37

BARRIER HEIGHT at 200v

(FROM 3·36)

DESICCATED 0·35 mil. SAMPLES

ΔE = 0·48 ev.

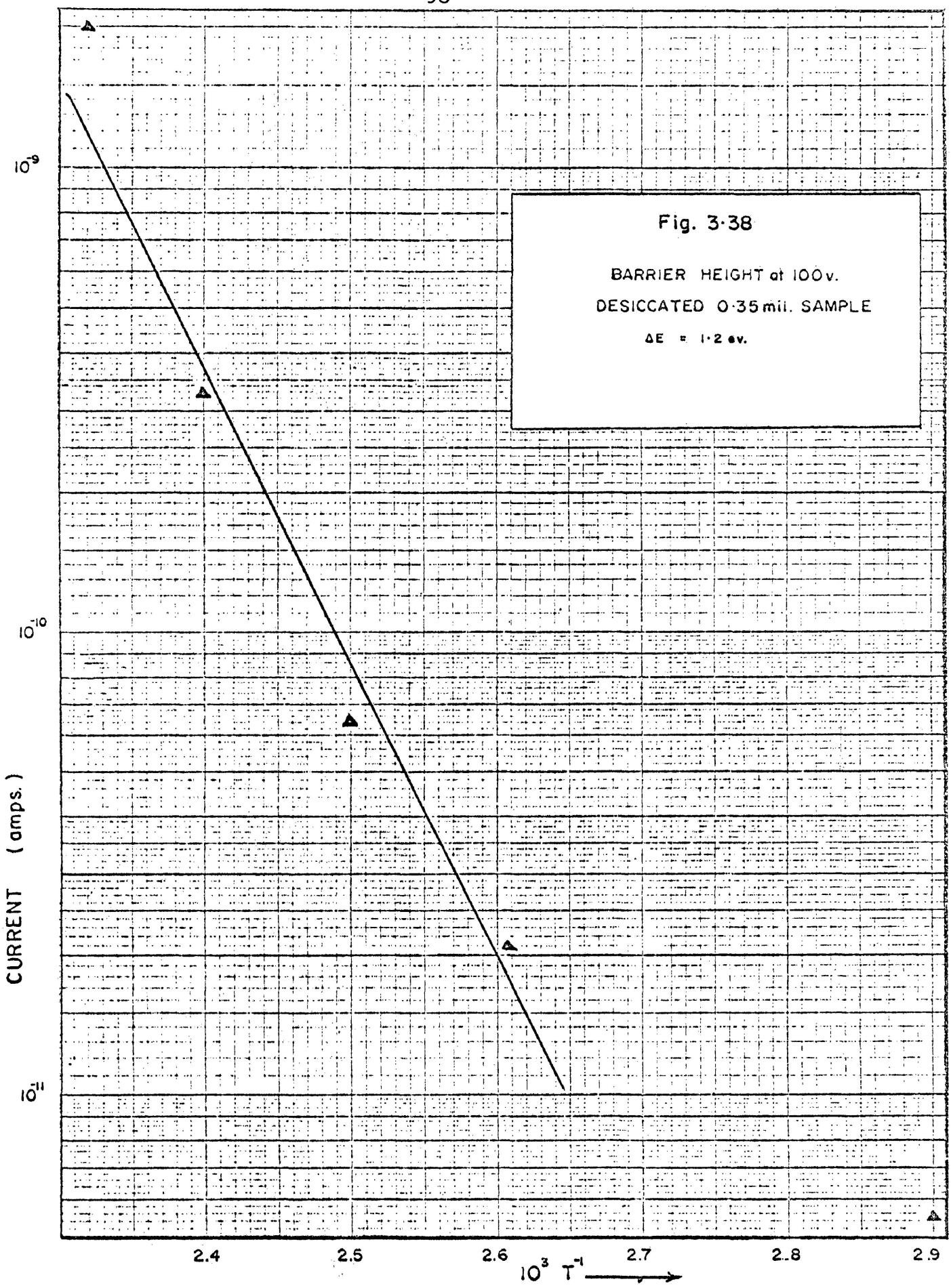
Fig. 3·38
BARRIER HEIGHT at 100v.
DESICCATED 0·35 mil. SAMPLE
ΔE = 1·2 ev.
CURRENT (amps.)
10⁻⁹
10⁻¹⁰
10⁻¹¹
2.4
2.5
2.6
2.7
2.8
2.9
10³ T⁻¹

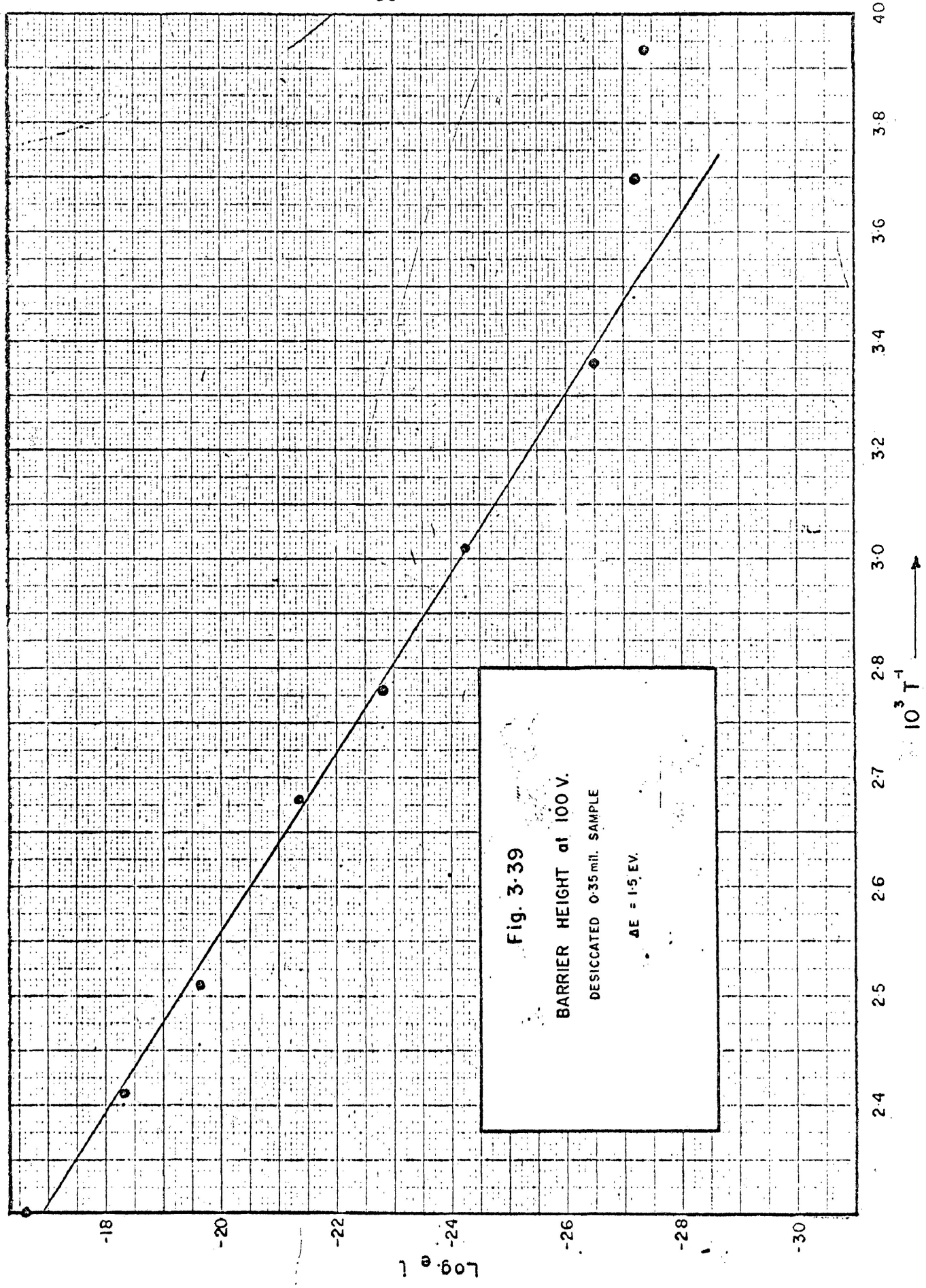
Log e I
-18
-20
-22
-24
-26
-28
-30
2·4
2·5
2·6
2·7
2·8
3·0
3·2
3·4
3·6
3·8
4·0
10³ T⁻¹
Fig. 3·39
BARRIER HEIGHT at 100 V.
DESICCATED 0·35 mil. SAMPLE
ΔE = 1·5 EV.

attempts to determine ΔE with a single sample. It appears that the activation energy is about one electron volt, with the suggestion of a second activated process around room temperatures, but in view of the theoretical discussion in Chapter I, it is difficult to say what this parameter represents. The initial values of current as predicted in Hamon's theory are given in Table 3.2 for various temperatures, but clearly it is not possible to talk of an activation energy for this set of data.

Concerning the mechanism of conduction, it would be naive on the basis of the data so far available, to make any final conclusion. There are, however, some suggestions as to what happens in the capacitor tissue when a field is impressed across it. The slow relaxation process which has been fully discussed is probably due to the build-up of ionic space charge rather than to dipole re-orientation which would be a much faster process. Supporting this conclusion are the results of an experiment to determine the voltage required to generate a given steady-state current. Based on the current density equation

$$j = e\,(n_+\mu_+ - \mu_-n_-)\frac{V}{d} \qquad \text{Eq. 3.2}$$

where these symbols have their usual meaning, we expect that if $(n_+\mu_+ - n_-\mu_-)$ is independent of position, that is no space charge, then for a given current value j, V should vary linearly with the thickness, d. As Fig. 3.40 indicates, this is not so and one supposes that ionic

i (5×10^{-4} sec.)	T
1.6×10^{-7} amps	20^{o}c
1.83	37
2.27	47
2.37	59
2.38	68
2.22	83
2.57	92
1.97	106

TABLE 3.2

INITIAL CURRENT VALUES PREDICTED BY HAMON'S THEORY.

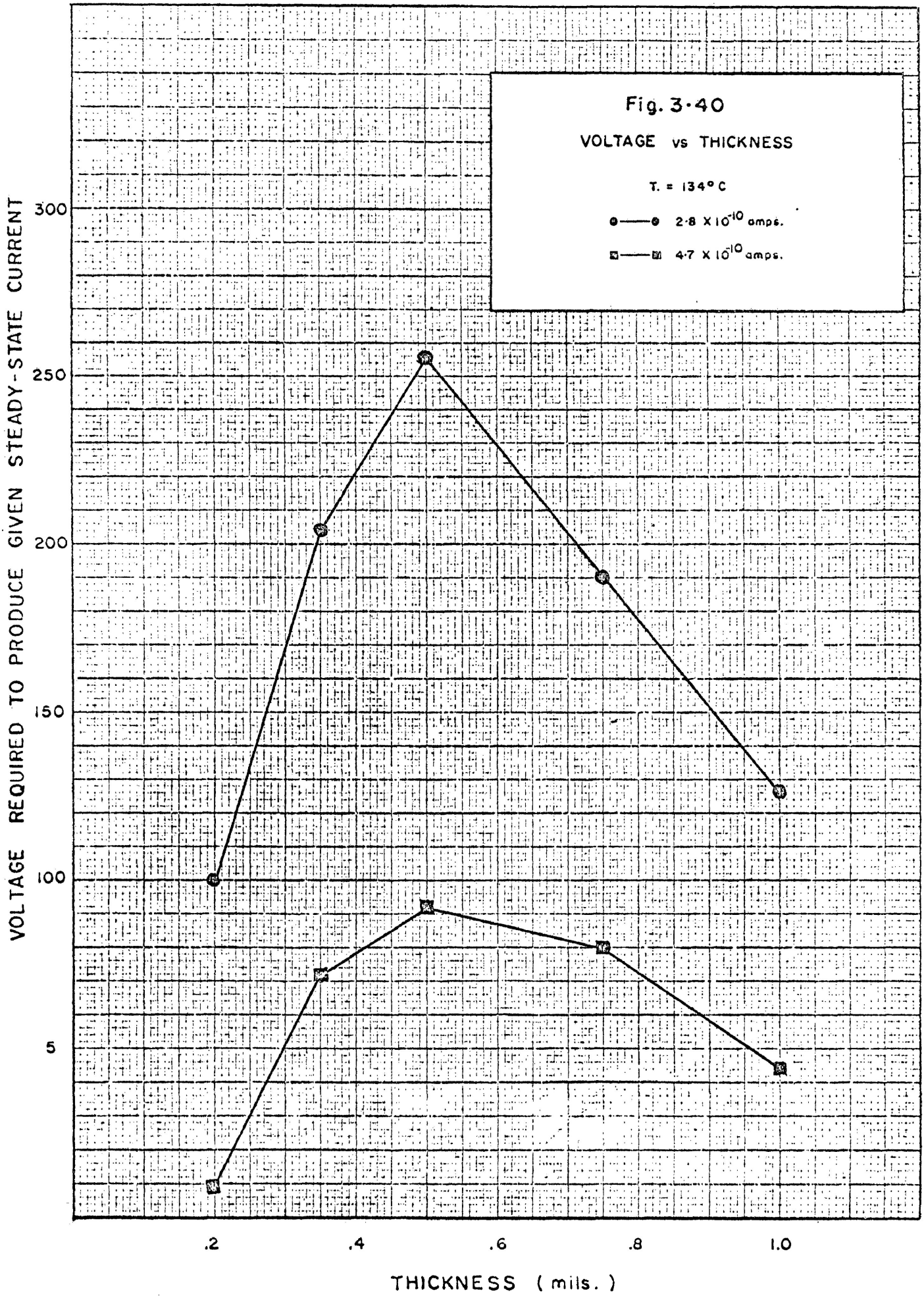
Fig. 3·40
VOLTAGE vs THICKNESS
T. = 134° C
2·8 X 10⁻¹⁰ amps.
4·7 X 10⁻¹⁰ amps.
VOLTAGE REQUIRED TO PRODUCE GIVEN STEADY-STATE CURRENT
300
250
200
150
100
5
.2
.4
.6
.8
1.0
THICKNESS (mils.)

space charge is present. It has been observed, however, that the relationship between voltage and the steady-state current is of a ln i - vs - $V^{\frac{1}{2}}$ nature which can be predicted by theory on the basis of electrode- or bulk- limited emission of electrons. This suggests that the steady-state current is electronic. Lilly and McDowell[20], whose results for polyethyleneterephthalate, are in many ways, similar to the observations described in this work, propose that mylar exhibits ionic space charge build-up (based on a slow absorption current and a non-linear voltage - thickness relationship) which increases the effective field at the electrodes. They assume in the absence of conclusive evidence, that the steady-state currents are electrode- limited so that the observed values of the j-V slopes, which invariably lie between the theoretical Schottky and Poole-Frenkel* slopes, would predict that the effective field is greater than the applied field (this explains the fact that their observed slopes are greater than the theoretical Schottky slopes). It is further assumed since limited knowledge exists as to the donor concentration, type, and contribution to the conduction mechanism, that in fact, the theory does predict different slopes (see Chapter I). They[20] believe that the resulting high fields at the electrodes permit Schottky emission of electrons from the metal into the dielectric.

---

*That is the Poole-Frenkel slopes in the presence of carrier compensation.

The present work on capacitor tissue, however, has invariably shown that the observed slopes are less than the theoretical Schottky slopes based on

$$\Delta\phi_S = \left[\frac{e^3}{4\pi\varepsilon_o\varepsilon d}\right]^{1/2} V^{1/2}$$

where ε, the relative dielectric constant, was taken as 2.3. The correct value as Frenkel[4] points out is the high frequency dielectric constant since the emission of an electron is a fast process, and would not involve the polarization of molecules or dipoles in the surrounding region. Also, the value 2.3 gives the index of refraction, n, from

$$\varepsilon_\infty = n^2 \qquad \text{Eq. 3.3}$$

as 1.5 which is not unreasonable for such a material. Furthermore, it is expected that ε varies with moisture predicting different ln i - vs - $V^{1/2}$ slopes when the moisture content varies. The γ factor discussed in the introduction can be calculated by comparison of experiment and theory using

$$\gamma = \left[\frac{\alpha\, exp}{\alpha\, th}\right]^{1/2}$$

and resulting values are given in Table 3.3. These data indicate that the effective field is almost always less than the applied field. This can be explained by the presence of ionic space charge (heterocharge) at one or both of the electrodes if the Poole-Frenkel, as opposed to Schottky, mechanism serves to limit a predominantly electronic steady-

EXPERIMENT	α EXP	αTH SCHOTTKY)	γ
Fig. 3.28 Curve No. 1	.15	.328	.20
Curve No. 1a	.14	.328	.18
Curve No. 2	.14	.328	.18
Fig. 3.29 Curve No. 3	.31	.328	.87
Curve No. 4	.34	.328	1.1
Curve No. 5	.31	.328	.91
Curve No. 6	.31	.328	.89
Fig. 3.30 Exp. No. 4	.18	.328	.30
Exp. No. 5	.23	.328	.49
Fig. 3.31 465 gm.	.14	.328	.18
325 gm.	.14	.328	.18
184 gm.	.14	.328	.18
43 gm.	.14	.328	.18
Fig. 3.32-82°C	.33	.395	.71
102°C	.34	.376	.82
111°C	.36	.365	.98
113°C	.36	.365	.98
124°C	.31	.355	.76
155°C	.28	.329	.73
Fig. 3.33-23°C	.15	.328	.20
51°C	.145	.290	.25
96°C	.07	.263	.07
Fig. 3.34-23°C	.20	.328	.37
102°C	.235	.258	.43
134°C	.26	.238	.60

TABLE 3.3

SUMMARY OF OBSERVED γ VALUES BASED ON COMPARISON OF EXPERIMENTAL DATA WITH SCHOTTKY THEORY.

state current. This would imply that deep within the bulk of the insulator, the effective field would be less than the applied field (see Fig. 1.2b and 1.2c), and would be reflected, as observed, in the slopes of the ln i - vs - $V^{1/2}$ curves. Furthermore, it is not unreasonable to think of a metal-dielectric contact which is injecting for electrons but blocking for any ions already in the bulk of the insulator. One is thus tempted to conclude on the basis of the slow decay of the absorption current and the non-linearity of the voltage-thickness curves, that the transient current is ionic and results in the build-up of ionic space charge at the electrodes. Following this, it seems that the steady-state currents, since they obey a ln i -vs - $V^{1/2}$ relationship are bulk-limited and electronic.

In spite of the fact that there is a certain quantitative agreement with the theory, it has to be remembered that it is doubtful that the band theory of solids, inherent in the development of the Poole-Frenkel equation, can be applied to an amorphous system like the present one. However, it is possible to consider the electrons as moving among shallow impurity states, and at the same time, subjected to the possibility of field-enhanced thermal excitation to a higher level corresponding to a psuedo-conduction band. This model is in keeping with the conduction observed in organic glasses[14] and physical mixtures of organic compounds in plastics[33], etc.

In view of what has been discussed in the foregoing, it can be seen that the electrical properties of capacitor tissue are extremely complex, and there is a definite need for further detailed studies.

APPENDIX A

THE SCHOTTKY EFFECT

When an electron is emitted from a metal into a vacuum it is required to overcome certain forces associated with the surface. We define the energy of an electron far from the surface as the barrier energy E_B measured from the bottom of the conduction band, so that an electron requires at least this much energy to escape the metal. Suppose however, that we approach the metal with an electron so that metal becomes polarized and exerts a force on the electron. The surface will act as an equipotential plane so that the force field will be of the form-illustrated in Fig. Ala. This field would however, be equivalent to that existing if the metal were replaced by a positive electron beyond the equipotential plane, as illustrated by Fig. Alb. This ficticious positive electron, known as the image charge[26], gives a convenient method of calculating the force on an electron outside the surface of the metal. Using Coulomb's law the force is

$$f_x = \frac{-e^2}{16\pi\varepsilon_o x^2}$$

and the potential energy will be given by

$$E_B - \frac{e^2}{16\pi\varepsilon_o x}$$

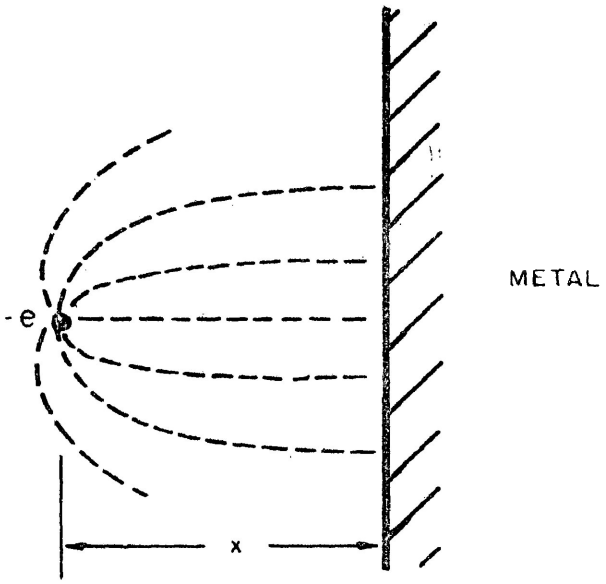

Fig. A1a

RESTORING FORCE on ESCAPING ELECTRON

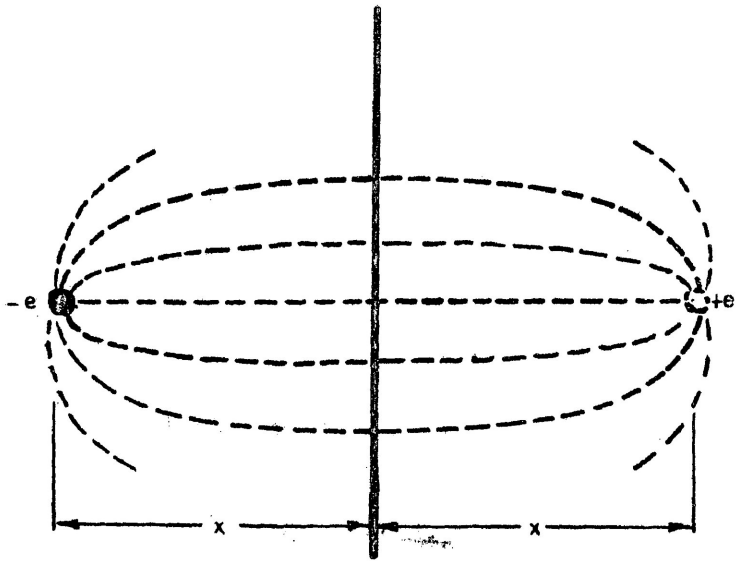

Fig. A1b

IMAGE FORCE on ELECTRON

As we will now show, the consequence of this potential due to the image charge is that it leads to a reduction in the barrier energy, E_B, when an electric field is applied; this reduction is known as the Schottky effect.

Only the most energetic electrons will leave the metal and it can be shown,[16] that within the bulk (even at absolute zero) many electrons have energies near the value E_F called the Fermi energy. Therefore, to remove an electron we need only to add an additional energy, ϕ_s, where

$$\phi_s = E_B - E_F$$

and this is known as the work function of the metal. By applying a positive potential to an electrode near the surface of the metal the emitted electrons are urged away from the surface by the accelerating forces which oppose the surface image forces. The zero-field barrier energy, ϕ_s, is thus reduced. Fig. A2 illustrates the resultant barrier energy when an external field is applied. The resultant is given by the sum of E_B and the energy imparted by the field $U_F(x)$ that the total potential energy $U(x)$ is

$$U(x) = E_B - \frac{e^2}{16\pi\varepsilon_o x} + U_F(x)$$

where $U_F(x) = -eFx$ and F is the applied field.

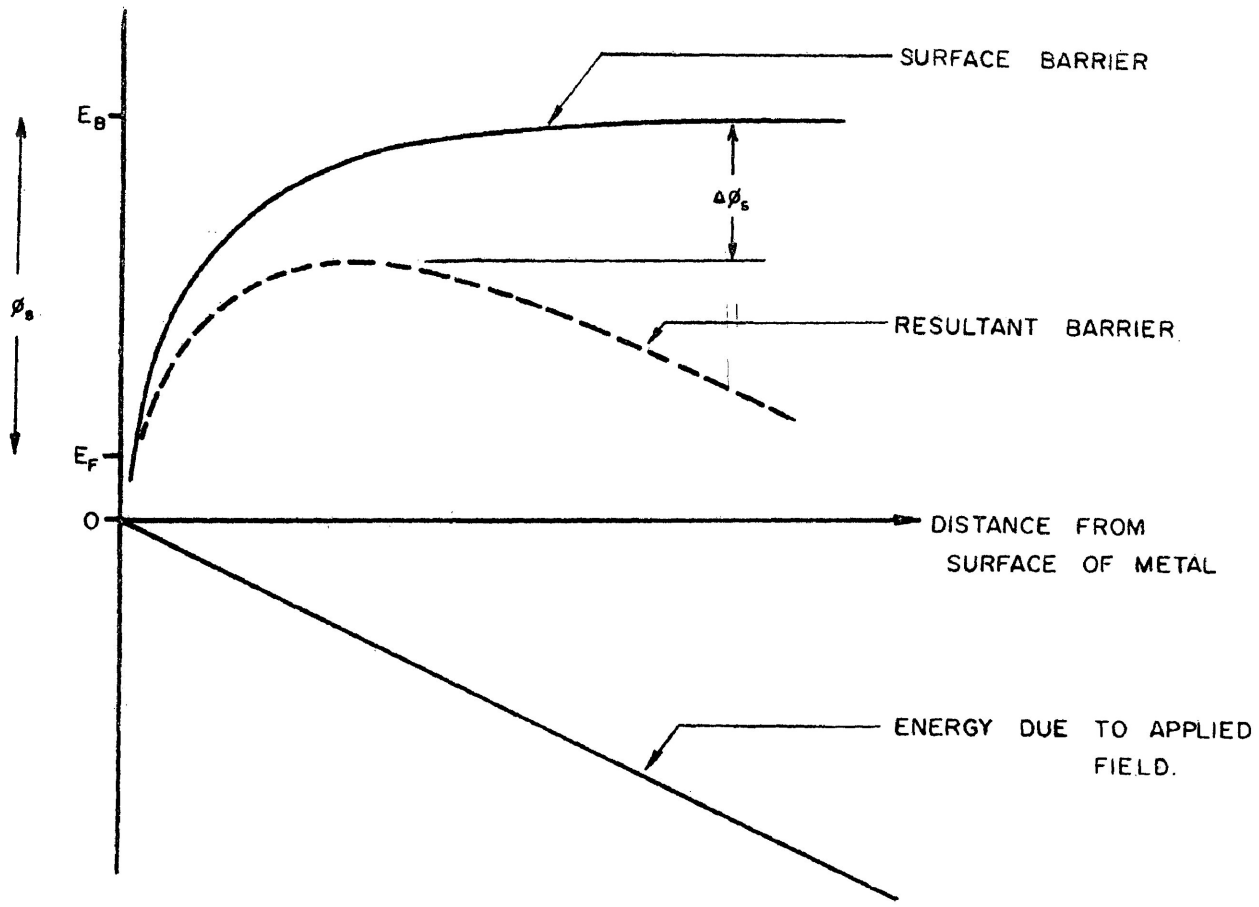

Fig. A2

BARRIER LOWERING : SCHOTTKY EFFECT

Thus

$$U(x) = E_B - \frac{e^2}{16\pi\varepsilon_o x} - eFx \qquad \text{Eq. A2}$$

We can now determine the maximum barrier height which, when we set

$$\frac{dU(x)}{dx} = 0$$

can be shown to occur at

$$x = \left[\frac{e}{16\pi\varepsilon_o F}\right]^{1/2} \equiv x_o \qquad \text{Eq. A3}$$

Substitution of Eq. A3 into Eq. A2 now gives for the maximum barrier height

$$U(x_o) = E_B - \left[\frac{e^3}{4\pi\varepsilon_o}\right]^{1/2} F^{1/2} \qquad \text{Eq. A4}$$

where E_B is seen to be the barrier height in the absence of a field and the barrier reduction is defined by

$$\Delta\phi_S \equiv \left[\frac{e^3}{4\pi\varepsilon_o}\right]^{1/2} F^{1/2} \qquad \text{Eq. A5}$$

The barrier which restricts the passage of electrons from the

metal is now seen to be field dependent and we can deduce a relationship for the current-voltage characteristics. Use is made of the Richardson-Dushman equation[16] which gives the electron current density evaporated from the metal as

$$j = AT^2 \exp\left[-\frac{\phi_s}{kT}\right] \qquad \text{Eq. A6}$$

where j is the current density, T is the absolute temperature and A is given by

$$A = \frac{4\pi m_e k^2}{h^3}$$

k is Boltzman's constant, m_e is the electronic effective mass and h is Plank's constant. We have seen that in the presence of a field the barrier energy is reduced so that Eq. A6 becomes, using Eqs. A4 and A5

$$j = AT^2 \exp\left[-\frac{\phi_s - \Delta\phi_s}{kT}\right] \qquad \text{Eq. A7}$$

This is the so called Richardson-Schottky equation for the field-enhanced current passing from a metal into a vacuum.

In the event that the metal is emitting charge into a dielectric material rather than a vacuum the image forces of Eq. A1 are reduced by a factor $1/\varepsilon$ where ε is the relative dielectric constant and similar calculations show that the barrier reduction given by Eq. A5 becomes

$$\Delta\phi_S = \left[\frac{e^3}{4\pi\varepsilon_o\varepsilon}\right]^{1/2} F^{1/2} \qquad \text{Eq. A8}$$

Using A8 in Eq. A7 gives the field-enhanced saturation current passing from the metal into the dielectric. Since the barrier in this case arises from the metal-dielectric interface we say that Eq. A7 describes an electrode-limited conduction mechanism.

APPENDIX B

THE POOLE-FRENKEL EFFECT

Consider a fixed ion with charge +e in the dielectric. The Coulombic attraction of an electron now forms the barrier to restrict the flow of current and we now show that this barrier is reduced by the application of an external field. This is the Poole-Frenkel effect. If we define ϕ_{PF} as the ionization energy of the ion in the absence of an applied field then the Coulombic potential due to the ion is

$$U_i(x) = \phi_{PF} - \frac{e^2}{4\pi\varepsilon_o\varepsilon x}$$

The energy due to the applied field F is

$$U_F(x) = -eFx$$

and the resultant barrier (see Fig. B1) is given by

$$U(x) = \phi_{PF} - \frac{e^2}{4\pi\varepsilon_o\varepsilon x} - eFx \qquad \text{Eq. B1}$$

We set

$$\frac{\partial U(x)}{\partial x} = 0$$

and determine that the maximum now occurs at

$$x = \left[\frac{e}{4\pi\varepsilon_o\varepsilon F}\right]^{1/2} \equiv x_o \qquad \text{Eq. B2}$$

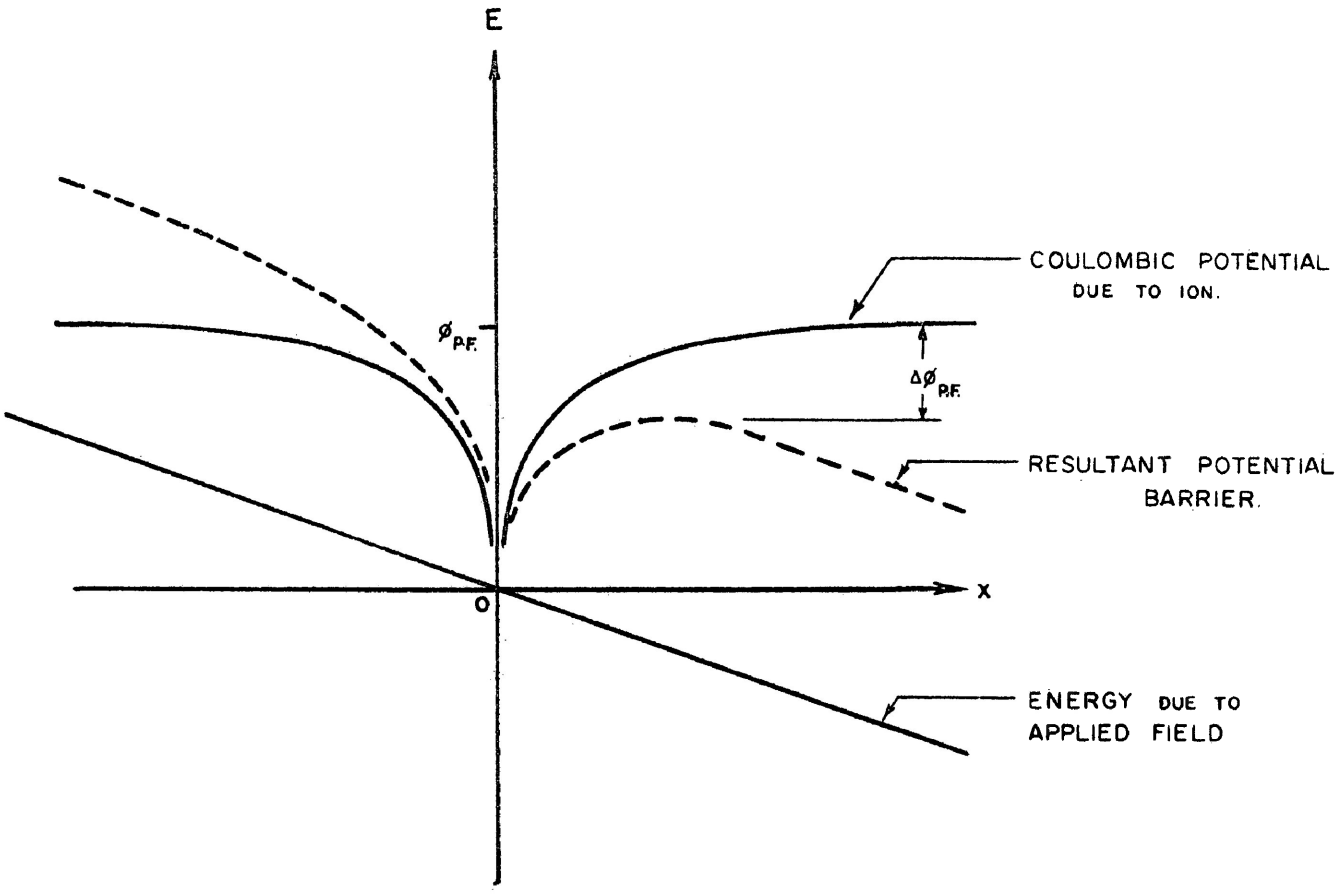

Fig. B1

BARRIER LOWERING: POOLE-FRENKEL EFFECT

Substitution of Eq. B2 in Eq. B1 determines the maximum barrier height as

$$U(x_o) = \phi_{PF} - 2\left[\frac{e^3}{4\pi\varepsilon_o\varepsilon}\right]^{1/2} F^{1/2}$$

or

$$U(x_o) = \phi_{PF} - \Delta\phi_{PF} \qquad \text{Eq. B3}$$

where we define

$$\Delta\phi_{PF} \equiv 2\left[\frac{e^3}{4\pi\varepsilon_o\varepsilon}\right]^{1/2} F^{1/2} \qquad \text{Eq. B4}$$

We observe on comparing Eqs. A8 and B4 that the barrier lowering through the Poole-Frenkel effect is twice the lowering through the Schottky effect.

We can relate the field-dependent barrier lowering to the current density by turning to the band theory of solids to determine the number of electrons in the conduction band and hence the number of free electrons able to contribute to the current flowing through the insulator. The next several pages are devoted to this purpose. Consider a substance with donor impurities near the conduction band and acceptor impurities near the valence band as shown in Fig. B2. As illustrated, the bottom of the conduction band is at E_c

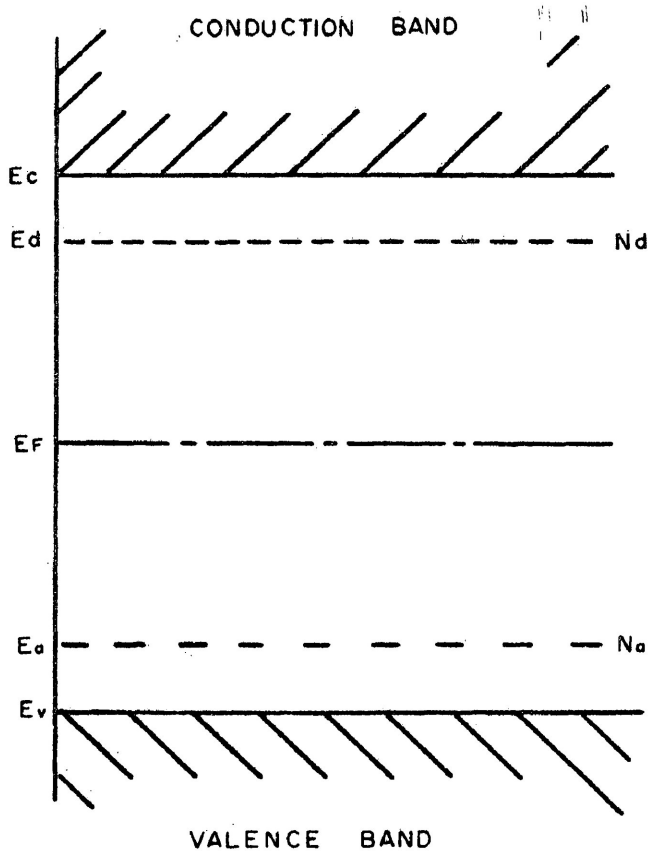

Fig. B2

ENERGY DIAGRAM SHOWING

SHALLOW DONORS and DEEP ACCEPTORS

and the top of the valence band is at E_v. The donor density is N_d and these impurities lie at energy E_d whilst N_a acceptors per unit volume lie at the energy level E_a. We can determine the number of electrons in the conduction band by integrating the product of the density of states per unit volume, g(E), given by[16]

$$g(E) = \frac{4\pi(2m)^{3/2}}{h^3} E^{1/2}$$

and the Fermi distribution function, f(E), for electron energies where

$$f(E) = \frac{1}{1+\exp[\frac{E-E_F}{kT}]}$$

E_F (which is illustrated in Fig. B2) is the Fermi energy which is that energy for which f(E) is one half. So the number of electrons in the conduction band is

$$n_c = \int_{E_c}^{\infty} f(E)\, g(E)\, dE$$
$$= N_c \exp[-\frac{E_c-E_F}{kT}] \qquad \text{Eq. B5}$$

where

$$N_c = 2[\frac{2\pi m_e kT}{h^2}]^{3/2}$$

The details of this calculation are given in most introductory texts[30] on solid state physics. The constant N_c has the dimention $(\text{Length})^{-3}$ and is usually interpreted as the number of states in the conduction band. Similarly we can derive the expression for the number of vacancies, p, in the valence band. This expression is

$$p = N_v \exp\left[-\frac{E_F - E_v}{kT}\right] \qquad \text{Eq. B6}$$

where $$N_v = 2\left[\frac{2\pi m_h kT}{h^2}\right]^3$$

and m_h is the effective mass of a vacancy in the valence band.

Since the Fermi function gives the fractional occupancy (ratio of number of occupied states to the total number of states) of energy states it can be used to calculate the density of occupied states

$$n_d = N_d\, f(E_d)$$

$$= \frac{N_d}{1 + 1/2 \exp\left[\frac{E_d - E_F}{kT}\right]} \qquad \text{Eq. B7}$$

where the pre-exponential factor of 1/2 arises from the consid-

eration of two-fold electron spin degeneracy. If N_d^+ is the number of ionized donors then

$$N_d^+ = N_d - n_d$$

$$= \frac{N_d}{1 + 2 \exp\left[-\frac{E_d - E_F}{kT}\right]} \qquad \text{Eq. B8}$$

through use of Eq. B7. Similarly the number of occupied (i.e. ionized) acceptors is

$$N_a^- = \frac{N_a}{1 + 2 \exp\left[\frac{E_a - E_F}{kT}\right]} \qquad \text{Eq. B9}$$

We are now in a position to calculate a value for the Fermi energy which, when used in Eq. B5 determines the number of electrons (in the conduction band) that are free to contribute to the current through the insulator. In determining E_F, we make use of the fact that the dielectric remains electrically neutral (electrons are merely shifted in energy and not added to or removed from the medium) and the charge neutrality equation is

$$n_c + N_a^- = p + N_d^+$$

Using Eqs. B5, B6, B8 and B9 this becomes

$$N_c \exp\left[-\frac{E_c-E_F}{kT}\right] + \frac{N_a}{1 + 2\exp\left[\frac{E_d-E_F}{kT}\right]}$$

$$N_v \exp\left[-\frac{E_F-E_V}{kT}\right] + \frac{N_d}{1 + 2\exp\left[-\frac{E_d-E_F}{kT}\right]}$$

Eq. B11

Eq. B11 is an implicit expression giving E_F in terms of the impurity concentrations and T. Solving Eq. B11 directly for E_F is not easy but approximations can be made under the following cases.

CASE 1.

First suppose that the temperature is low* and secondly that the the acceptor impurity density is negligibly small. It is evident furthermore that p is vanishingly small compared to N_d^+ since electrons are activated into the conduction band much more easily from the donor sites than from the valence band.

---

*

The capacitor tissue which initiated this discussion showed activation energies of about one electron volt for temperatures up to 150°C; at these temperatures kT is not more than 0.04 ev.

We now write the charge neutrality equation as

$$N_c \exp\left[-\frac{E_c - E_F}{kT}\right] = \frac{N_d}{1 + 2\exp\left[-\frac{E_d - E_F}{kT}\right]} \qquad \text{Eq.B12}$$

This is a quadratic in $\exp\left[-\frac{E_F}{kT}\right]$ which is more recognizable when we substitute $\lambda = \exp\left[\frac{E_F}{kT}\right]$,

$$\alpha = \exp\left[-\frac{E_d}{kT}\right], \quad \beta = \exp\left[-\frac{E_c}{kT}\right] \text{ and } b = \frac{N_d}{N_c}$$

That is

$$2\alpha\beta\lambda^2 + \beta\lambda - b = 0$$

for which the solution is

$$\lambda = \frac{1}{4a}\left[-1 + \sqrt{1 + \frac{8\alpha b}{\beta}}\right] \qquad \text{Eq. B13}$$

We have ignored the negative root term since $\alpha > 0$ and λ must be positive. If the square root term is expanded and second order terms neglected then depending on whether

$$\beta > 8b\alpha \text{ Eq. B 13} \quad \text{or} \quad \beta < 8b\alpha \qquad \text{Eq. B 14}$$

we have

$$\lambda = \frac{b}{\beta} \qquad \text{or} \qquad \lambda = \left[\frac{b}{2\alpha\beta}\right]^{\frac{1}{2}}$$

respectively.

That is

$$\exp\left[\frac{E_F}{kT}\right] = \frac{N_d}{N_c}\exp\left[\frac{E_c}{kT}\right] \qquad \text{Eq. B15}$$

or

$$\exp\left[\frac{E_F}{kT}\right] = \left[\frac{N_d}{2N_c}\right]^{\frac{1}{2}}\exp\left[\frac{E_c + E_d}{2kT}\right] \qquad \text{Eq. B16}$$

Eq. B13 can be interpreted so a temperature limitation for the validity of Eq. B14 which, after resubstituting for α, β, and b yields with slight transformation

$$T > \frac{E_c - E_d}{k \ln\left[\frac{N_c}{8N_d}\right]}$$

Eq. B14 defines a temperature range for the validity of Eq. B16. i.e.

$$T < \frac{E_c - E_d}{k \ln\left[\frac{N_c}{8N_d}\right]}$$

We now use the value of the Fermi energy which can be determined from Eq. B15 and B16 in Eq. B5 for the number of free electrons. It is readily seen that

$$n_c = N_d \qquad \text{Eq. B17}$$

when

$$T > \frac{E_c - E_d}{K \ln\left[\frac{N_c}{8N_d}\right]} \qquad \text{Eq. B18}$$

and that

$$n_c = \left[\frac{N_d N_a}{2}\right]^{\frac{1}{2}} \exp\left[-\frac{E_c - E_d}{2kT}\right] \qquad \text{Eq. B19}$$

when

$$T < \frac{E_c - E_d}{kT \ \ln\left[\frac{N_c}{8N_d}\right]} \qquad \text{Eq. B20}$$

Expression B18 describes intermediate temperatures where all donors are ionized and the extra electrons are in the conduction band. In this region, n_c is almost insensitive to temperature. Expression B20 describes low temperature where not all the donors are ionized. Before employing Eq. B19 to deduce the temperature and voltage dependence of the current, a second case must be considered which gives rise to a different expression for n_c.

CASE 2

We now wish to discuss the low temperature case where the donors are partially compensated by acceptor impurities, with $N_d > N_a$.

As before p is by far the smallest quantity in Eq. B11 which simplifies the charge netrality equation. We can approximate further by writing

$$N_a^- \simeq N_a$$

since the acceptors are located at a low energy and tend to fill first; the extra donor electrons will be shared by the acceptors and the conduction band. We now write Eq. B11 as

$$N_c \exp\left[- \frac{E_c - E_F}{kT} \right] + N_a = \frac{N_d}{1 + 2 \exp\left[- \frac{E_d - E_F}{kT} \right]} \quad \text{Eq. B21}$$

At these low temperatures not all the donors are ionized, although electrons must still be supplied to the acceptor sites. Qualitatively, it can be expected that for decreasing temperatures, the Fermi level approaches the donor level and if $E_F = E_d$ then Eq. B7 gives for the density of ionized donors

$$N_d - n_d = \frac{N_d}{3}$$

depending on whether N_a is greater or less than $N_d/3$ two different situations can exist.

If $N_d > N_a > N_d/3$ the Fermi level can never rise above the donor level since if otherwise an examination of Eq. B7 shows that

$$n_d > \frac{N_d}{1+\frac{1}{2}} = N_d - \frac{N_d}{3}$$

or

$$\frac{N_d}{3} > N_d - n_d = N_d^+$$

(If the temperature is sufficiently low $N_a \simeq N_a^-$ and $n_c \simeq 0$) and consequently

$$N_a \simeq N_a^- > N_d^+$$

This equation describes the unrealistic situation where the charge condensed in the acceptor states is greater than that available from the donors. The low temperature region is defined in this case by the condition $n_c << N_a$ which permits a further approximation for Eq. B21. This is now

$$N_a = \frac{N_d}{1+2\exp\left[-\frac{E_d - E_f}{kT}\right]}$$

The Fermi level can now be determined as

$$E_F = E_d - kT \ln\left[\frac{2N_a}{N_d - N_a}\right]$$

which, when used in Eq. B7, gives for the number of free electrons

$$n_c = \frac{N_c(N_d-N_a)}{2N_a} \exp\left[-\frac{E_c-E_d}{kT}\right]$$

Eq. B22

The condition $n_c << N_a$ now defines, through use of Eq. B22, the low temperature region in which Eq. B22 applies as

$$T < \frac{E_c - E_d}{k \ln\left[\frac{N_c(N_d-N_a)}{2N_a^2}\right]}$$

Eq. B19 is of the form

$$n_c = N_o' \exp\left[-\frac{\phi}{2kT}\right]$$

Eq. B23

and Eq. B22 has the form

$$n_c = N_o'' \exp\left[-\frac{\phi}{kT}\right]$$

Eq. B24

(n_o' & n_o'' are constants) and which of these two relations apply depend on the degree of compensation. ϕ is the energy required to move an electron from a donor site to the conduction band.

We can now determine the current density in the insulator using Eq. B23 in

$$j = n_c e\mu F \qquad \text{Eq. B25}$$

where j is the current denisty and μ is the mobility of the electrons to give

$$j = e\mu n_o' F \exp\left[-\frac{\phi}{2kT}\right] \qquad \text{Eq. B26}$$

Similarly Eqs. B24 and B25 combine to give

$$j = e\mu n_o'' F \exp\left[-\frac{\phi}{kT}\right] \qquad \text{Eq. B27.}$$

The donor ionization energy, $\phi = E_c - E_d$, is equivalent to the zero-field barrier height, ϕ_{PF}, of Eq. B3 so that in the presence of an externally applied electric field, Eqs. B26 and B27 become

$$j = e\mu n_o' F \exp\left[-\frac{\phi_{PF} - \Delta\phi_{PF}}{2kT}\right] \qquad \text{Eq. B28}$$

and

$$j = e\mu n_o'' F \exp\left[-\frac{\phi_{PF} - \Delta\phi_{PF}}{kT}\right] \qquad \text{Eq. B29}$$

SELECTED REFERENCES

1. Amborski, L. E., J. Polymer Sci., Vol. 62, p. 331, (1962)

2. Brennecke, C., J. Appl. Phys., Vol. 11, p. 202, (1940).

3. Croiteru, Z., Progress in Dielectrics, Vol. 6, Editors, J. H. Birks and J. Hart, (Temple Press Books Ltd., London, 1965), p.p. 103-146.

4. Frenkel, J., Phys. Rev., Vol. 54, p. 647, (1938).

5. Hart, J. and Mungall, A. G., J. Sci. Inst., Vol. 33, p. 411, (1956).

6. Hartman, T. E., Blair, J. C., and Bauer, R., J. Appl. Phys., Vol. 37, No. 4, p. 179, (1964).

7. Hickmott, T. W., J. Appl. Phys., Vol. 35, No. 7, p. 2118, (1964).

8. Hirose, H., and Wada, Y., Japanese J. Appl. Phys., Vol. 39, No. 12, p. 179, (1964).

9. Hu, S. M., Kerr, D. R., and Gregor, L. V., Appl. Phys. Letters, Vol. 10, No. 3, p. 97, (1967).

10. Inokuchi, H., and Akamatu, H., Solid State Physics, Vol. 12, Academic Press Inc., London, 1961) p. 115.

11. Inuishi, Y., and Powers, D. A., J. Appl. Phys., Vol. 28, p. 1017, (1957).

12. Joffe, A., The Physics of Crystals, (McGraw-Hill Book Co., Inc., New York, 1928) Ch. VII.

13. Johansen, I. T., J. Appl. Phys., Vol. 37, p. 499, (1966).

14. Johnson, G. E., and Albrecht, A. C., J. Chem. Phys., Vol. 44, No. 9, p. 3162, (1966).

15. Kendall, E. J. M., Can. J. Physics, Vol. 46, p. 2509, (1968).

16. Kittel, C., Introduction to Solid State Physics, Third Edition, (John Wiley and Sons, New York, 1966). p. 246.

17. Lamb, D. R., Electrical Conduction Mechanisms in Thin Insulating Films, (Methune and Co., Ltd., London), p. 8.

18. Lampert, M. A., Phys. Rev., Vol. 103, No. 6, p. 1648, (1956).

19. Lengyel, G., J. Appl. Phys., Vol. 37, No. 2, p. 807, (1966).

20. Lilly, A. C., and McDowell, J. R., J. Appl. Phys., Vol. 39, No. 1, p. 141, (1968).

21. McCall, P. M., and Anderson, E. W., J. Chem. Phys. Vol. 32, p. 237, (1960).

22. Mead, C. A., Phys. Rev., Vol. 128, No. 5, p. 2088, (1962).

23. Muller, R. S., J. Appl. Phys., Vol. 34, No. 8, p. 2401, (1963).

24. Poole, H. H., Phil. Mag., Vol. 32, p. 112, (1916), and Vol. 34, p. 195, (1917).

25. Rose, A., Phys. Rev., Vol. 97, No. 6, p. 1538, (1955).

26. Ryder, J., Electronic Fundamentals and Applications, Third Edition, (Prentice-Hall, Inc., Englewood Cliffs, N.J., 1965) p. 100.

27. Stewart, M., Phys. Stat. Sol., Vol. 23, p. 595, (1967).

28. Sutter, P. H., and Nowick, A. S., J. Appl. Phys., Vol. 34, No. 4, p. 734, (1963).

29. Sze, S. M., J. Appl. Phys., Vol. 38, No. 7, p. 2951, (1967).

30. Wang, S., Solid State Electronics, (McGraw-Hill Book Co. Inc., New York, 1966).

31. Yeargan, J. R., and Taylor, H. L., J. Appl. Phys., Vol. 39, No. 12, p. 5600, (1968).

32. Yeargan, J. R., and Taylor, H. L., J. Electrochem. Soc.: Solid State Science, Vol. 115, No. 3, p. 273, (1968).

33. Raman, R., Ph.D. Thesis, University of Nottingham, 1967.